Charles University
Faculty of Science

Study programme: Chemistry
Study branch: Physical Chemistry

Jakub Kocák

Nová metoda řešení Schrödingerovy rovnice
A new method for the solution of the Schrödinger equation

MASTER THESIS

Supervisor: doc. RNDr. Filip Uhlík, Ph.D.

Prague, 2017

Prohlášení:
Prohlašuji, že jsem závěrečnou práci zpracoval samostatně a že jsem uvedl všechny použité informační zdroje a literaturu. Tato práce ani její podstatná část nebyla předložena k získání jiného nebo stejného akademického titulu.

V Praze dne ..... Podpis

Název práce: Nová metoda řešení Schrödingerovy rovnice

Autor: Jakub Kocák

Katedra: Katedra fyzikální a makromolekulární chemie

Vedoucí bakalářské práce: doc. RNDr. Filip Uhlík, Ph.D.

Abstrakt: Tato práce se věnuje metodě řešení časově nezávislé Schrödingerovy rovnice pro základní stav. Vlnová funkce interpretována jako hustota pravděpodobnosti je reprezentovaná vzorky. V každé iteraci je aplikován aproximant propagátoru podél imaginárního času. Působení operátora je implementováno Monte Carlo simulací. Nemalá část práce se věnuje metodám výpočtu energie vlnové funkce reprezentované vzorky. Je rozebrána metoda na základě odhadu hodnoty vlnové funkce, metoda konvoluce s tepelným jádrem, metoda průměrné energie vážené vlnovou funkcí a metoda exponenciálního poklesu. Metoda řešení byla použita k nalezení základního stavu a enegie 6-dimenzionálního harmonického oscilátoru, anharmonického 3-dimenzionální oktického oscilátoru a atomu vodíku.

Klíčová slova: propagace v imaginárním čase, Monte Carlo metoda, variační princip, základní stav

Title: A new method for the solution of the Schrödinger equation

Author: Jakub Kocák

Department: Department of Physical and Macromolecular Chemistry

Supervisor: doc. RNDr. Filip Uhlík, Ph.D.

Abstract: In this thesis we study method for the solution of time-independent Schrödinger equation for ground state. The wave function, interpreted as probability density, is represented by samples. In each iteration we applied approximant of imaginary time propagator. Acting of the operator is implemented by Monte Carlo simulation. Part of the thesis is dedicated to methods of energy calculation from samples of wave function: method based on estimation of value of wave function, method of convolution with heat kernel, method of averaged energy weighed by wave function and exponential decay method. The method for the solution was used to find ground state and energy for 6-dimensional harmonic oscillator, anharmonic 3-dimensional octic oscillator and hydrogen atom.

Keywords: imaginary time propagation, Monte Carlo method, variational principle, ground state

I would like to express my deep gratitude and appreciation to my supervisor doc. RNDr. Filip Uhlík, Ph.D. for his helpful and witty comments, useful discussions, his assistance with overcoming many obstacles and infinite patience.

Special thanks to my family and friends, I would not be able to finish the work without their support.

Contents

Introduction

Chemistry on the scale of atoms and molecules can be successfully described by *quantum mechanics*. The evolution of quantum systems is determined by *time-dependent Schrödinger equation*. An important role in microworld is played by *stationary states*, which remain stationary in sense of any observable variable. However according to *quantum field theory* they are not stationary and spontaneously decay into *ground state*, the stationary state with the lowest energy. Stationary states can be found as solution of *time-independent Schrödinger equation*.[1] In general it is difficult (if not impossible) to find analytical solution and we have to rely on computing methods. From the time of formulation of the quantum mechanics there have been developed wide spectrum of methods, each with its own limitation. A large portion of the methods is dependent on the choice of basis and can obtain accurate results using huge set of basis functions and sufficiently large computational time. In some sense the choice of basis brings a certain degree of arbitrariness. Therefore our attention was focused on methods, where choice of basis is not necessary and they are independent of basis. One example of another approach are methods based on the simulations of samples.

In this thesis we have studied methods, where wave function is represented by samples. Even though the similar methods are well-studied, to our knowledge this specific approach is rare and we could not find any related literature. With *Monte Carlo* implementation of *imaginary time propagation* (ITP) methods we simulated propagation of initial wave function to the ground state. Inevitable part of the study is development of methods for calculation of energy of wave function represented by samples. Developed methods have been applied on systems with different difficulties: dimensionality and singular potential.

The first chapter is dedicated to short introduction to key elements of the quantum mechanics and in more detail to ITP methods. We summarised results in this field and reconfirmed some of them. We compared various methods based on different order approximants in one dimension.

The second chapter contains development of computational algorithms for calculation of energy, implementation of ITP methods for wave function represented by samples and brief insight into one-dimensional optimization.

The third chapter summarises results of ITP method for 4 systems: 6-dimensional harmonic oscillator, anharmonic oscillator and hydrogen atom. We compared convergence for different systems and precision of energy calculation methods.

Note to the reader: To achieve more fluent reading of main text the extensive derivations of formulas and mathematically rigorous justifications have been moved into Appendices and footnotes depending on the range of text. The variables in text are dimensionless and correspond to transformation of units to characteristic units for given system.[2]

[1] This holds for explicitly time-independent Hamiltonian.

[2] For example, the characteristic units of atoms and molecules are atomic units.

1. Theoretical Background

At the beginning it is instructive to provide a brief recapitulation of concepts and principles of the quantum mechanics [1], which will be useful subsequently.

1.1 Quantum Mechanics

In formalism of non-relativistic quantum theory the state of a system is completely described by *the state vector* $|\psi\rangle$ from the Hilbert space $\mathscr{H}$. The state at instant t is denoted as $|\psi(t)\rangle$. The evolution of the state in the quantum mechanics is described by *the time-dependent Schrödinger equation* with the formal solution[1]

$$i\frac{\partial}{\partial t}|\psi(t)\rangle = \widehat{H}(t)|\psi(t)\rangle \implies |\psi(t)\rangle = \underbrace{\mathrm{e}^{-i\int_0^t \mathrm{d}\tau\, \widehat{H}(\tau)}}_{=:\widehat{U}(t)}|\psi(0)\rangle\,, \tag{1.1}$$

where $\widehat{H}(t)$ is Hamiltonian of the system (in general time-dependent) and $\widehat{U}(t)$ the time evolution operator.

We assume non-relativistic time-independent Hamiltonian $\widehat{H}$ on the Hilbert space $\mathscr{H} = L^2(\mathbb{R}^N)$, which is separable to the kinetic $\widehat{T}$ and potential energy $\widehat{V}$

$$\begin{aligned} \widehat{H}(t) = \widehat{H} &= \widehat{T} + \widehat{V}\,, \\ \widehat{T} = -\frac{1}{2}\Delta_N\,, &\qquad \widehat{V} = V(\boldsymbol{x})\,, \end{aligned} \tag{1.2}$$

where $\Delta_N = \sum_{i=1}^{N} \dfrac{\partial^2}{\partial x_i^2}$ is the Laplace operator in N-dimensional space[2] and $\boldsymbol{x} \in \mathbb{R}^N$ is N-dimensional position vector[3].

We denote the momentum eigenvectors $|\boldsymbol{p}\rangle$ by N-dimensional momentum vector $\boldsymbol{p} \in \mathbb{R}^N$. In position representation they can expressed as

$$\langle \boldsymbol{x}|\boldsymbol{p}\rangle = \frac{1}{(2\pi)^{N/2}}\mathrm{e}^{i\boldsymbol{p}\cdot\boldsymbol{x}}\,. \tag{1.3}$$

For explicitly time-independent Hamiltonian $\widehat{H}$ there are important states $|E,\alpha\rangle$ called *the stationary states*[4], which are eigenvectors of the Hamiltonian $\widehat{H}$ (solution of *the time-independent Schrödinger equation*)

$$\widehat{H}|E,\alpha\rangle = E|E,\alpha\rangle\,. \tag{1.4}$$

In formalism of spectral decomposition the eigenvectors $|E,\alpha\rangle$ of Hermitian operator $\widehat{H}$ (or set of operators called *complete set of commuting observables* (CSCO))[5] form

[1] In suitable units we can assume $\hbar = 1$.

[2] The kinetic energy of particles with different masses m_i can be linearly transformed into desired form as

$$\widehat{T} = \sum_{i=1} -\frac{1}{2m_i}\frac{\partial^2}{\partial x_i^2} \xrightarrow{\sqrt{m_i}x_i \to x_i} \sum_{i=1} -\frac{1}{2}\frac{\partial^2}{\partial x_i^2}\,.$$

One has to bear in mind the change of coordinates also in the potential energy.

[3] The position of M particles in 3D space can be denoted by $3M$-dimensional position vector.

[4] The symbol α denotes other necessary labels of different degenerate stationary states from same subspace.

[5] For instance, in the Hilbert space $\mathscr{H} = L^2(\mathbb{R}^3)$ the CSCO $\{\widehat{T}, \widehat{L}^2, \widehat{L}_z\}$ forms an orthonormal basis $|E,l,m\rangle$.

orthonormal basis[6]

$$\langle E', \alpha' | E, \alpha \rangle = \delta(E - E')\delta_{\alpha'\alpha}\,, \qquad \widehat{I} = \sum\!\!\!\!\!\!\int_{E,\alpha} \mathrm{d}E\, |E, \alpha\rangle\langle E, \alpha|\,. \tag{1.5}$$

The orthonormal basis (1.5) guarantees unique decomposition of any state $|\psi\rangle$ into the eigenvectors $|E, \alpha\rangle$

$$|\psi\rangle = \sum\!\!\!\!\!\!\int_{E,\alpha} \mathrm{d}E\, \langle E, \alpha|\psi\rangle |E, \alpha\rangle \tag{1.6}$$

and the evolution of the state $|\psi\rangle$ for time-independent Hamiltonian $\widehat{H}$ can be described as

$$\widehat{U}(t)|\psi\rangle = \mathrm{e}^{-it\widehat{H}}|\psi\rangle \overset{(1.6)}{=} \sum\!\!\!\!\!\!\int_{E,\alpha} \mathrm{d}E\, \langle E, \alpha|\psi\rangle \mathrm{e}^{-itE}|E, \alpha\rangle\,.$$

The *variational principle* in the quantum mechanics ensures that energy of any state $|\psi\rangle$ is greater or equal to the ground state energy E_0. Using decomposition (1.6) we can write

$$\begin{aligned}
\frac{\langle\psi|\widehat{H}|\psi\rangle}{\langle\psi|\psi\rangle} &\overset{(1.6)}{=} \frac{1}{\langle\psi|\psi\rangle} \sum\!\!\!\!\!\!\int_{E',\alpha'} \mathrm{d}E' \sum\!\!\!\!\!\!\int_{E,\alpha} \mathrm{d}E\, \langle\psi|E', \alpha'\rangle \underbrace{\langle E', \alpha'|\widehat{H}|E, \alpha\rangle}_{E\,\delta(E-E')\delta_{\alpha'\alpha}} \langle E, \alpha|\psi\rangle \\
&\geq \frac{1}{\langle\psi|\psi\rangle} \sum\!\!\!\!\!\!\int_{E',\alpha'} \mathrm{d}E' \sum\!\!\!\!\!\!\int_{E,\alpha} \mathrm{d}E\, \langle\psi|E', \alpha'\rangle E_0\, \delta(E - E')\delta_{\alpha'\alpha}\langle E, \alpha|\psi\rangle \\
&= \frac{E_0}{\langle\psi|\psi\rangle} \sum\!\!\!\!\!\!\int_{E,\alpha} \mathrm{d}E\, \langle\psi|E, \alpha\rangle\langle E, \alpha|\psi\rangle \overset{(1.5)}{=} E_0\,.
\end{aligned} \tag{1.7}$$

Let $\widehat{A}$ be time-independent operator, then the expectation value of its commutator with time-independent Hamiltonian $\widehat{H}$ for any eigenstate $|E, \alpha\rangle$ is zero (the *hypervirial theorem*)[7]

$$\langle[\widehat{A}, \widehat{H}]\rangle = 0\,.$$

For the operator $\widehat{A} = \widehat{\boldsymbol{p}} \cdot \widehat{\boldsymbol{x}}$ the commutator reads

$$[\widehat{\boldsymbol{p}} \cdot \widehat{\boldsymbol{x}}, \widehat{H}] = \widehat{\boldsymbol{p}} \cdot \underbrace{[\widehat{\boldsymbol{x}}, \widehat{H}]}_{i\widehat{\boldsymbol{p}}/m} + \underbrace{[\widehat{\boldsymbol{p}}, \widehat{H}]}_{-i\boldsymbol{\nabla}V} \cdot \widehat{\boldsymbol{x}} = i(2\widehat{T} - \boldsymbol{\nabla}V \cdot \widehat{\boldsymbol{x}})\,,$$

and we obtain special case of the hypervirial theorem – *virial theorem*

$$\langle \boldsymbol{\nabla}V \cdot \widehat{\boldsymbol{x}}\rangle = 2\langle\widehat{T}\rangle\,.$$

For *homogeneous potential*[8] with degree of homogeneity n the relation becomes

$$n\langle V\rangle = 2\langle\widehat{T}\rangle\,.$$

[6] The symbol $\sum\!\!\!\!\!\!\int_{E,\alpha} \mathrm{d}E$ denotes summation over *bound states* and integration over *scattering states*.

[7] On eigenstates the Hamiltonian behaves like multiplicative constant, which is always commutative with anything.

[8] Examples of homogeneous potentials: *N-dimensional harmonic oscillator* ($n = 2$) and *Coulomb potential* ($n = -1$). In case of Coulomb potential the number of particles or different charges does not matter.

1.2 The Imaginary Time Propagation Methods

The formal substitution $it \to \tau$ in time-dependent Schrödinger equation (1.1) for time-independent Hamiltonian $\widehat{H}$ leads to heat or diffusion type equation with analogous formal solution

$$-\frac{\partial}{\partial\tau}|\psi(\tau)\rangle = \widehat{H}|\psi(\tau)\rangle \implies |\psi(\tau)\rangle = \mathrm{e}^{-\tau\widehat{H}}|\psi\rangle\,.$$

The unique decomposition (1.6) into the orthonormal basis (1.5) is still valid and we can write for imaginary time evolution of the state $|\psi\rangle$

$$\mathrm{e}^{-\tau\widehat{H}}|\psi\rangle \overset{(1.6)}{=} \sum\!\!\!\!\!\!\int_{E,\alpha} \mathrm{d}E\,\langle E,\alpha|\psi\rangle \mathrm{e}^{-\tau E}|E,\alpha\rangle\,.$$

We can see, that with increasing parameter τ the coefficients of the excited states are exponentially decreasing relatively to the coefficient of the ground state $|E_0\rangle$

$$\frac{\langle E_i,\alpha|\psi\rangle \mathrm{e}^{-\tau E_i}}{\langle E_0|\psi\rangle \mathrm{e}^{-\tau E_0}} = \frac{\langle E_i,\alpha|\psi\rangle}{\langle E_0|\psi\rangle}\mathrm{e}^{-\tau(E_i-E_0)}\,.$$

The basic idea of the *imaginary time propagation* (ITP) methods is to apply (repetitively) the operator (or its approximation) $\mathrm{e}^{-\tau\widehat{H}}$ on the initial wave function $|\psi_0\rangle$ with non-zero overlap with the ground state $\langle E_0|\psi_0\rangle \neq 0$. In each iteration the ground state component in wave function is relatively to other components amplified. Repeating this process the wave function converges to the ground state.

Similarly formulated problems arise in many fields of mathematics and physics, *e.g.* already mentioned *quantum mechanics* [2–5], *classical mechanics* [6–10] or *statistical mechanics* [11, 12]. The common element is the evolution operator $\mathrm{e}^{-\tau(\widehat{T}+\widehat{V})}$, where $\widehat{T}$ and $\widehat{V}$ are non-commuting operators.[9] Thus the development of the ITP methods is beneficial for several areas.

There have been attempts to use the imaginary time evolution operator $\mathrm{e}^{-\tau\widehat{H}}$ directly, *e.g.* [13]. But generally the eigenvectors and eigenvalues of the operator $\widehat{H}$ are not known, therefore the direct formalism of spectral decomposition cannot be applied. Instead we are forced to use approximations of the imaginary time propagator.

1.2.1 Approximations of the Imaginary Time Propagator

In position representation, the operator $\mathrm{e}^{-\tau\widehat{V}}$ can be computed exactly. The operator $\mathrm{e}^{-\tau\widehat{T}}$ is exactly known in momentum representation, but can be easily transformed into position representation, more in Appendix A.1. Hence it is convenient to build approximations using operators $\mathrm{e}^{-\tau\widehat{T}}$ and $\mathrm{e}^{-\tau\widehat{V}}$. But there is restriction $\mathrm{Re}(\tau) \geq 0$, because otherwise the operator $\mathrm{e}^{-\tau\widehat{T}}$ is ill-defined. Also, the condition $\mathrm{Re}(\tau) \geq 0$ for the operator $\mathrm{e}^{-\tau\widehat{V}}$ is often necessary, otherwise the operator $\mathrm{e}^{-\tau\widehat{V}}$ causes infinities and instabilities[10].

[9] The meaning of terms τ, $\widehat{T}$ and $\widehat{V}$ can differ from field to field. For instance, in quantum statistical mechanics the variable $\tau = \beta = 1/(k_\mathrm{B}T)$ has meaning of the inverse temperature.

[10] For instance, the operator $\mathrm{e}^{-\tau\widehat{V}}$ for LHO potential $V(x) = \frac{1}{2}x^2$ and $\mathrm{Re}(\tau) < 0$ goes rapidly to infinity for $x \to \pm\infty$ and produces vector outside of the Hilbert space.

Approximations without Gradient

The general form of the approximants is a linear combination of products of operators $\mathrm{e}^{-\tau\widehat{T}}$ and $\mathrm{e}^{-\tau\widehat{V}}$ (sometimes denotes as *multi-product expansion* [14])

$$\mathrm{e}^{-\tau\widehat{H}} = \sum_i c_i \prod_j \mathrm{e}^{-\tau a_{i,j}\widehat{T}} \mathrm{e}^{-\tau b_{i,j}\widehat{V}} + o(\tau^n)\,, \tag{1.8}$$

where c_i, $a_{i,j}$ and $b_{i,j}$ are fixed constants and n is the order of approximation in terms of parameter τ. However the most common approximants have form of a single product of operators $\mathrm{e}^{-\tau\widehat{T}}$ and $\mathrm{e}^{-\tau\widehat{V}}$ (sometimes denoted as *factorization* [6], *decomposition scheme* [9], or *splitting* [5])

$$\mathrm{e}^{-\tau\widehat{H}} = \prod_i \mathrm{e}^{-\tau a_i\widehat{T}} \mathrm{e}^{-\tau b_i\widehat{V}} + o(\tau^n)\,. \tag{1.9}$$

We tried to systematically find for given decomposition form the highest order approximants. We used program *Mathematica* [15] with extra packages: *VEST* [16] (Einstein summation convention, simplification of complex operator products), and *NCAlgebra, Version 4.0.6* [17] (non-commutative algebra, expansion and simplification of non-commutative terms). Our process of finding coefficient a_i and b_i can be described as follows:

1. We expressed operator products in terms of Einstein notation operators. For instance $\widehat{T}\widehat{V}\psi = -V_{,i}\psi_{,i} - \frac{1}{2}V\psi_{,ii}$.
2. We expanded the approximant (1.9) in terms of τ (the n-th order) and operator products. For instance $\mathrm{e}^{-\tau a_1\widehat{T}}\mathrm{e}^{-\tau b_1\widehat{V}} = \widehat{1} - a_1\tau\widehat{T} - b_1\tau\widehat{V} + o(\tau^1)$.
3. We substituted operator products with Einstein notation operators, compared both sides term by term and obtained equations for coefficients a_i and b_i.
4. We solved equations. If there were left some free variables, we returned to the 2nd step for the $(n+1)$-th order.

For simple schemes[11] VT and TV we obtain the simplest straightforward the 1st order approximation (called the *Trotter decomposition* or the *Lie splitting*)

$$\mathrm{e}^{-\tau\widehat{H}} = \mathrm{e}^{-\tau\widehat{T}}\mathrm{e}^{-\tau\widehat{V}} + o(\tau^1) = \mathrm{e}^{-\tau\widehat{V}}\mathrm{e}^{-\tau\widehat{T}} + o(\tau^1)\,.$$

The schemes VTV and TVT lead to the 2nd order approximation (called *Strang splitting*)

$$\mathrm{e}^{-\tau\widehat{H}} = \mathrm{e}^{-\frac{\tau}{2}\widehat{T}}\mathrm{e}^{-\tau\widehat{V}}\mathrm{e}^{-\frac{\tau}{2}\widehat{T}} + o(\tau^2) = \mathrm{e}^{-\frac{\tau}{2}\widehat{V}}\mathrm{e}^{-\tau\widehat{T}}\mathrm{e}^{-\frac{\tau}{2}\widehat{V}} + o(\tau^2)\,.$$

If we restrict ourselves to real positive coefficients $a_i > 0$ and $b_i > 0$ (to avoid ill-definedness and infinities), it have been shown, that the product can be at most the 2nd order approximation (*non-existence theorem of positive decomposition*) [18–20]. This is in agreement with our results. The higher schemes $VTV\ldots$ and $TVT\ldots$ produce negative or complex coefficients. For instance for the scheme $VTVTV$ we obtained the 3rd order approximation with complex coefficients (agrees with [21])

$$\mathrm{e}^{-\tau\widehat{H}} = \mathrm{e}^{-\tau b_1\widehat{V}}\mathrm{e}^{-\tau a_1\widehat{T}}\mathrm{e}^{-\tau b_2\widehat{V}}\mathrm{e}^{-\tau a_2\widehat{T}}\mathrm{e}^{-\tau b_3\widehat{V}} + o(\tau^3)$$

$$b_1 = \frac{1}{12}\left(3 \pm \sqrt{3}i\right), a_1 = \frac{1}{6}\left(3 \pm \sqrt{3}i\right), b_2 = \frac{1}{2}, a_2 = \frac{1}{6}\left(3 \mp \sqrt{3}i\right), b_3 = \frac{1}{12}\left(3 \mp \sqrt{3}i\right).$$

[11] For convenience we denote particular decomposition schemes by the order of operators in exponents, e.g. $\mathrm{e}^{-\tau a_1\widehat{T}}\mathrm{e}^{-\tau b_1\widehat{V}}\mathrm{e}^{-\tau a_2\widehat{T}} \to TVT$.

It has been shown how to construct approximations with real coefficients (also negative) of any order (*fractal decomposition*, *jump composition*) [22,23]. As mentioned above, negative imaginary time propagation is not well-defined and cannot be used. Similarly there have been studied complex coefficients schemes for $\mathrm{Re}(a_i) \geq 0$ [5,21,24, 25].

Even though the single-product expansions are generally more common, there are studies of multi-product expansions [14, 26]. But Sheng showed that sum (1.8) for positive coefficients $a_{i,j} > 0$, $b_{i,j} > 0$ and $c_i > 0$ can be maximally the 2nd order approximation [18].

Approximations with Gradient

When the kinetic $\widehat{T}$ and potential $\widehat{V}$ operators have form of the Laplace operator and multiplication with function $V(\boldsymbol{x})$ (equation (1.2)), one may observe[12] that the operator $[\widehat{V},[\widehat{T},\widehat{V}]]$ is also multiplication with a function

$$[\widehat{V},[\widehat{T},\widehat{V}]] = \boldsymbol{\nabla} V \cdot \boldsymbol{\nabla} V \,.$$

This also implies 2 useful corollaries:

- Some commutators in expansion of the operator $\mathrm{e}^{-\tau(\widehat{T}+\widehat{V})}$ are zero. For instance
$$[\widehat{V},[\widehat{V},[\widehat{T},\widehat{V}]]] = 0 \,.$$
- Besides operators $\mathrm{e}^{-\tau\widehat{T}}$ and $\mathrm{e}^{-\tau\widehat{V}}$ we can construct the operator $\mathrm{e}^{-\tau^3[\widehat{V},[\widehat{T},\widehat{V}]]}$.

To find any other useful operators we studied which linear combinations (LC) of products of operators $\widehat{T}$ and $\widehat{V}$ lead to operator with similar behaviour (multiplication with a function). Again we used program *Mathematica* [15] with package *VEST* [16].

For the LC of a single operators and products of 2 operators we obtain only trivial cases

$$\widehat{V} = V \,, \qquad \widehat{V}^2 = V^2 \,.$$

For the LC of products of 3 operators we get the already known LC

$$[\widehat{V},[\widehat{T},\widehat{V}]] = V_{,i} V_{,i} \,.$$

The LC of products of 4 operators leads to 2 obvious LCs

$$\widehat{V}[\widehat{V},[\widehat{T},\widehat{V}]] = V V_{,i} V_{,i} \,, \qquad [\widehat{V},[\widehat{T},\widehat{V}]]\widehat{V} = V V_{,i} V_{,i} \,.$$

The LC of products of 5 operators produces 7 obvious LCs

$$\widehat{V}^2[\widehat{V},[\widehat{T},\widehat{V}]] = V^2 V_{,i} V_{,i} \,, \qquad \widehat{V}[\widehat{V},[\widehat{T},\widehat{V}]]\widehat{V} = V^2 V_{,i} V_{,i} \,, \qquad [\widehat{V},[\widehat{T},\widehat{V}]]\widehat{V}^2 = V^2 V_{,i} V_{,i} \,,$$
$$\widehat{T}[\widehat{V}[\widehat{V},[\widehat{T},\widehat{V}]]] = 0 \,, \qquad [\widehat{V}[\widehat{V},[\widehat{T},\widehat{V}]]]\widehat{T} = 0 \,,$$
$$\widehat{V}[\widehat{V}[\widehat{V},[\widehat{T},\widehat{V}]]] = 0 \,, \qquad [\widehat{V}[\widehat{V},[\widehat{T},\widehat{V}]]]\widehat{V} = 0 \,,$$

and one new useful operator

$$[\widehat{V},[\widehat{T},[\widehat{V},[\widehat{T},\widehat{V}]]]] = 2 V_{,i} V_{,j} V_{,ij} \,.$$

We can see simple pattern and generate other operators by recursive definition[13]

$$\widehat{C}_0 := \widehat{V} \,, \qquad \widehat{C}_{i+1} := [\widehat{V},[\widehat{T},\widehat{C}_i]] = \boldsymbol{\nabla} V \cdot \boldsymbol{\nabla} C_i \,.$$

[12] Or not.

[13] In fact we can generate more operators by formula $[\widehat{C}_i,[\widehat{T},\widehat{C}_j]]$ and plugging in any already generated operator.

We may ask, how to define operators $\widehat{C}_i$ for negative i? We will start with operator $\widehat{C}_{-1}$. The straightforward condition on operator $\widehat{C}_{-1}$ is equation

$$C_0 = \boldsymbol{\nabla} V \cdot \boldsymbol{\nabla} C_{-1}\,. \tag{1.10}$$

Let C_{-1} be a solution to equation (1.10). But this solution is not unique. Let W be function with gradient $\boldsymbol{\nabla} W$ orthogonal to the gradient of potential $\boldsymbol{\nabla} V$ everywhere

$$\boldsymbol{\nabla} V \cdot \boldsymbol{\nabla} W = 0\,.$$

Then the function $C_{-1} + \alpha W$ for any coefficient $\alpha \in \mathbb{R}$ is also a solution to equation (1.10). One may notice a property of operators $\widehat{C}_i$, which is common for all operators with non-negative i and can help to define functions C_{-i} uniquely. Gradients $\boldsymbol{\nabla} C_i$ are collinear with gradient of potential $\boldsymbol{\nabla} V$. This implies, that any tangent gradient (like the gradient $\boldsymbol{\nabla} W$) should be zero.

$$\boldsymbol{\nabla} C_{i-1} \sim \boldsymbol{\nabla} V \quad \wedge \quad C_i = \boldsymbol{\nabla} V \cdot \boldsymbol{\nabla} C_{i-1} \quad \Longrightarrow \quad \boldsymbol{\nabla} C_{i-1} = \frac{C_i}{\boldsymbol{\nabla} V \cdot \boldsymbol{\nabla} V} \boldsymbol{\nabla} V\,. \tag{1.11}$$

The equation (1.11) can be integrated back and the function C_{i-1} is determined up to a constant.

It is instructive to calculate a few functions $\widehat{C}_i$ for some potential. For Coulomb potential $V = -1/r$ in 3D space we get the following sequence (Table 1.1). For Coulomb potential we have problem with operator $\mathrm{e}^{-\tau\widehat{V}}$ because it produces divergent state vector at origin $r = 0$, which cannot be normalised and thus is outside of the Hilbert space $\mathscr{H}$.[14]

$\dots$	C_{-3}	C_{-2}	C_{-1}	C_0	C_1	C_2	C_3	C_4	$\dots$
$\dots$	$-r^8/80$	$-r^5/10$	$-r^2/2$	$-1/r$	$1/r^4$	$-4/r^7$	$28/r^{10}$	$-280/r^{13}$	$\dots$

Table 1.1: Functions C_i.

As before, the general form of approximation consists of products of operators $\mathrm{e}^{-\tau\widehat{T}}$, $\mathrm{e}^{-\tau\widehat{V}}$ and $\mathrm{e}^{-\tau^{2i+1}\widehat{C}_i}$. However, the nature of the operators $\mathrm{e}^{-\tau^{2i+1}\widehat{C}_i}$ implies that they can improve only approximations of the $(2i+1)$-th order or higher. It is important to remark, that for Coulomb potential the combination of operators $\mathrm{e}^{-\tau\widehat{V}}$ and $\mathrm{e}^{-\tau^3\widehat{C}_1}$ (see Table 1.1) will avoid the infinity at origin and we obtain a normalisable state vector.

Same as before, the most common approximants are single products. We use the same process to find the coefficients of different schemes. We get the following approx-

[14] Let $\langle \boldsymbol{x}|\psi\rangle$ be spherically symmetric initial wavefunction with Taylor expansion at origin

$$\langle \boldsymbol{x}|\psi\rangle = \sum_{i=0}^{+\infty} \frac{a_i}{i!} r^i\,.$$

Then the integral of $|\mathrm{e}^{-\tau\widehat{V}}\psi|^2$ over ball $B_R(0)$ with radius R and center at origin is convergent only if $a_i = 0$ for all $i \in \mathbb{N}$. This is not in general possible to ensure.

imations

$$
\begin{aligned}
\mathrm{e}^{-\tau\widehat{H}} &= \mathrm{e}^{-\frac{1}{6}\tau\widehat{V}}\mathrm{e}^{-\frac{1}{2}\tau\widehat{T}}\mathrm{e}^{-\frac{2}{3}\tau\widehat{V}}\mathrm{e}^{-\frac{1}{2}\tau\widehat{T}}\mathrm{e}^{-\frac{1}{6}\tau\widehat{V}}\mathrm{e}^{-\frac{1}{72}\tau^3\widehat{C}_1} + o(\tau^3)\,,\\
\mathrm{e}^{-\tau\widehat{H}} &= \mathrm{e}^{-\frac{1}{48}\tau^3\widehat{C}_1}\mathrm{e}^{-\frac{1}{3}\tau\widehat{T}}\mathrm{e}^{-\frac{3}{4}\tau\widehat{V}}\mathrm{e}^{-\frac{2}{3}\tau\widehat{T}}\mathrm{e}^{-\frac{1}{4}\tau\widehat{V}} + o(\tau^3)\,,\\
\mathrm{e}^{-\tau\widehat{H}} &= \mathrm{e}^{-\frac{1}{6}\tau\widehat{V}}\mathrm{e}^{-\frac{1}{2}\tau\widehat{T}}\mathrm{e}^{-\frac{2}{3}\tau\widehat{V}}\mathrm{e}^{-\frac{1}{72}\tau^3\widehat{C}_1}\mathrm{e}^{-\frac{1}{2}\tau\widehat{T}}\mathrm{e}^{-\frac{1}{6}\tau\widehat{V}} + o(\tau^4)\,,\\
\mathrm{e}^{-\tau\widehat{H}} &= \mathrm{e}^{-\frac{1}{6}\tau\widehat{V}}\mathrm{e}^{-\frac{1}{144}\tau^3\widehat{C}_1}\mathrm{e}^{-\frac{1}{2}\tau\widehat{T}}\mathrm{e}^{-\frac{2}{3}\tau\widehat{V}}\mathrm{e}^{-\frac{1}{2}\tau\widehat{T}}\mathrm{e}^{-\frac{1}{6}\tau\widehat{V}}\mathrm{e}^{-\frac{1}{144}\tau^3\widehat{C}_1} + o(\tau^4)\,,\\
\mathrm{e}^{-\tau\widehat{H}} &= \mathrm{e}^{-\frac{1}{6}\tau\widehat{V}}\mathrm{e}^{-c_1\tau^3\widehat{C}_1}\mathrm{e}^{-\frac{1}{2}\tau\widehat{T}}\mathrm{e}^{-\frac{2}{3}\tau\widehat{V}}\mathrm{e}^{-c_2\tau^3\widehat{C}_1}\mathrm{e}^{-\frac{1}{2}\tau\widehat{T}}\mathrm{e}^{-\frac{1}{6}\tau\widehat{V}}\mathrm{e}^{-c_1\tau^3\widehat{C}_1} + o(\tau^4)\,,\\
\mathrm{e}^{-\tau\widehat{H}} &= \mathrm{e}^{-\frac{3-\sqrt{3}}{6}\tau\widehat{T}}\mathrm{e}^{-\frac{1}{2}\tau\widehat{V}}\mathrm{e}^{-\frac{2-\sqrt{3}}{48}\tau^3\widehat{C}_1}\mathrm{e}^{-\frac{1}{\sqrt{3}}\tau\widehat{T}}\mathrm{e}^{-\frac{1}{2}\tau\widehat{V}}\mathrm{e}^{-\frac{2-\sqrt{3}}{48}\tau^3\widehat{C}_1}\mathrm{e}^{-\frac{3-\sqrt{3}}{6}\tau\widehat{T}} + o(\tau^4)\,,
\end{aligned}
$$

where $c_1 = \frac{1}{16}\left(\frac{1}{9} - 8c_2\right)$ and $c_2 \in \left\langle 0, \frac{1}{72}\right\rangle$. To have one pseudopotential $V + 6c_1\tau^2 C_1$ we can choose $c_1 = \frac{1}{432}$ and $c_2 = \frac{1}{108}$. The 4th order approximations are in agreement with literature [9].

Chin showed that using the operators $\widehat{C}_i$ and positive coefficients it is not possible to get higher than the 4th order approximation [27]. Combination of complex coefficients $\mathrm{Re}(a_i) > 0$ and operators $\widehat{C}_i$ was also studied [5].

1.2.2 Related Methods

Besides the ITP methods there are other similar methods based on application of operators which amplify the ground state. One of the methods is the *inverse iteration method* applying operator $(\widehat{H} - \lambda)^{-1}$. Repeated application of the operator converges to eigenvector with energy E_i nearest to the parameter λ. Its convergence depends on how accurately we know the energy E_i. Good estimation of E_i ensures quicker convergence than ITP methods [28].

Other methods are based on application of operator $\mathrm{e}^{-\tau^n\widehat{H}^n}$, where $n \geq 2$. We can carefully choose the origin of potential to shift energy spectrum so that energy of any state is positive ($E_0 \geq 0$). In the limit $\tau \to +\infty$ the wave function converges to the ground state

$$|\psi\rangle \to \langle E_0|\psi\rangle \mathrm{e}^{-\tau^n E_0^n}|E_0\rangle\,.$$

The approximation of the operator $\mathrm{e}^{-\tau^n\widehat{H}^n}$ has to be a linear combination of products of operators $\mathrm{e}^{-\tau\widehat{T}}$ and $\mathrm{e}^{-\tau\widehat{V}}$.[15] We found an approximant of the 2nd order for operator $\mathrm{e}^{-\tau^2\widehat{H}^2}$

$$\mathrm{e}^{-\tau^2\widehat{H}^2} = 2\mathrm{e}^{-\frac{1}{2}\tau\widehat{T}}\mathrm{e}^{-\tau\widehat{V}}\mathrm{e}^{-\frac{1}{2}\tau\widehat{T}} - \mathrm{e}^{-\tau\widehat{T}}\mathrm{e}^{-2\tau\widehat{V}}\mathrm{e}^{-\tau\widehat{T}} + o(\tau^2)\,.$$

1.2.3 Comparison of Different Approximants

To show how the order of approximants affects the convergence, we simulated numerically the ITP method on 1D grid. We used 2 model potentials: *linear harmonic oscilator* (LHO) and *double-well potential* (2WP). The ground state and its energy for these models are known.

As the initial wave function $\phi_0(x)$ we chose

$$\phi_0(x) = \max\left\{0, 1 - (x-1)^2\right\}\,.$$

In the Table (1.2) we list the used approximants.

[15] In the linear order of τ the expansion has to cancel out. In case of one product, this would lead to negative coefficients, which are not desirable.

$$V_{\mathrm{LHO}}(x) = \frac{1}{2}x^2 - \frac{1}{2}$$
$$\psi_{0,\mathrm{LHO}}(x) = \frac{1}{(\pi)^{1/4}}\mathrm{e}^{-\frac{x^2}{2}}$$
$$E_{0,\mathrm{LHO}} = 0$$

$$V_{\mathrm{2WP}}(x) = \frac{1}{2}\left(x^6 - 3x^3\right)$$
$$\psi_{0,\mathrm{2WP}}(x) = N\mathrm{e}^{-\frac{x^4}{4}}$$
$$E_{0,\mathrm{2WP}} = 0$$

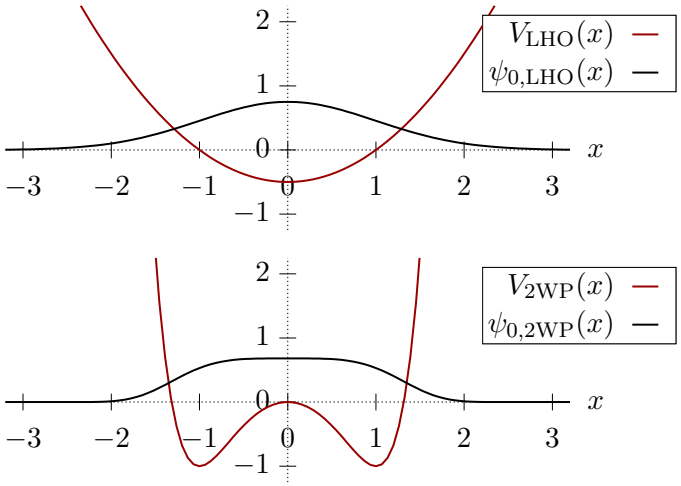

Figure 1.1: Potential $V_{\mathrm{LHO/2WP}}(x)$, ground state $\psi_{0,\mathrm{LHO/2WP}}(x)$ and the ground state energy $E_{0,\mathrm{LHO/2WP}}$. The normalizing constant is $N \approx 0.6811$.

i	n	scheme	$G_i(\tau)$
1	1	TV	$\mathrm{e}^{-\tau\widehat{T}}\mathrm{e}^{-\tau\widehat{V}}$
2	1	VT	$\mathrm{e}^{-\tau\widehat{V}}\mathrm{e}^{-\tau\widehat{T}}$
3	2	TVT	$\mathrm{e}^{-\frac{1}{2}\tau\widehat{T}}\mathrm{e}^{-\tau\widehat{V}}\mathrm{e}^{-\frac{1}{2}\tau\widehat{T}}$
4	2	VTV	$\mathrm{e}^{-\frac{1}{2}\tau\widehat{V}}\mathrm{e}^{-\tau\widehat{T}}\mathrm{e}^{-\frac{1}{2}\tau\widehat{V}}$
5	4	$VTVCTV$	$\mathrm{e}^{-\frac{1}{6}\tau\widehat{V}}\mathrm{e}^{-\frac{1}{2}\tau\widehat{T}}\mathrm{e}^{-\frac{2}{3}\tau\widehat{V}}\mathrm{e}^{-\frac{1}{72}\tau^3\widehat{C}_1}\mathrm{e}^{-\frac{1}{2}\tau\widehat{T}}\mathrm{e}^{-\frac{1}{6}\tau\widehat{V}}$
6	4	$VCTVTVC$	$\mathrm{e}^{-\frac{1}{6}\tau\widehat{V}}\mathrm{e}^{-\frac{1}{144}\tau^3\widehat{C}_1}\mathrm{e}^{-\frac{1}{2}\tau\widehat{T}}\mathrm{e}^{-\frac{2}{3}\tau\widehat{V}}\mathrm{e}^{-\frac{1}{2}\tau\widehat{T}}\mathrm{e}^{-\frac{1}{6}\tau\widehat{V}}\mathrm{e}^{-\frac{1}{144}\tau^3\widehat{C}_1}$
7	4	$VCTVCTVC$	$\mathrm{e}^{-\frac{1}{6}\tau\widehat{V}}\mathrm{e}^{-\frac{1}{432}\tau^3\widehat{C}_1}\mathrm{e}^{-\frac{1}{2}\tau\widehat{T}}\mathrm{e}^{-\frac{2}{3}\tau\widehat{V}}\mathrm{e}^{-\frac{1}{108}\tau^3\widehat{C}_1}\mathrm{e}^{-\frac{1}{2}\tau\widehat{T}}\mathrm{e}^{-\frac{1}{6}\tau\widehat{V}}\mathrm{e}^{-\frac{1}{432}\tau^3\widehat{C}_1}$
8	4	$TVCTVCT$	$\mathrm{e}^{-\frac{3-\sqrt{3}}{6}\tau\widehat{T}}\mathrm{e}^{-\frac{1}{2}\tau\widehat{V}}\mathrm{e}^{-\frac{2-\sqrt{3}}{48}\tau^3\widehat{C}_1}\mathrm{e}^{-\frac{1}{\sqrt{3}}\tau\widehat{T}}\mathrm{e}^{-\frac{1}{2}\tau\widehat{V}}\mathrm{e}^{-\frac{2-\sqrt{3}}{48}\tau^3\widehat{C}_1}\mathrm{e}^{-\frac{3-\sqrt{3}}{6}\tau\widehat{T}}$

Table 1.2: Reference number i, order n, scheme of approximant $G_i(\tau)$.

We used grid with 1000 equidistant points on the interval $\langle -6, 6\rangle$. The operators have been applied numerically: operators $\mathrm{e}^{-\tau\widehat{V}}$ and $\mathrm{e}^{-\tau^3\widehat{C}_i}$ by multiplying in each point, operator $\mathrm{e}^{-\tau\widehat{T}}$ using the formula

$$\langle x|\mathrm{e}^{-\tau\widehat{T}}|\phi_i\rangle = \int_{-\infty}^{+\infty}\mathrm{d}x'\langle x|\mathrm{e}^{-\tau\widehat{T}}|x'\rangle\langle x'|\phi_i\rangle \overset{(A.8)}{=} \int_{-\infty}^{+\infty}\mathrm{d}x'\frac{1}{(2\pi\tau)^{1/2}}\mathrm{e}^{-\frac{(x-x')^2}{2\tau}}\phi_i(x')\,.$$

In each iteration we varied τ to find the minimal energy, which is according to *vari-*

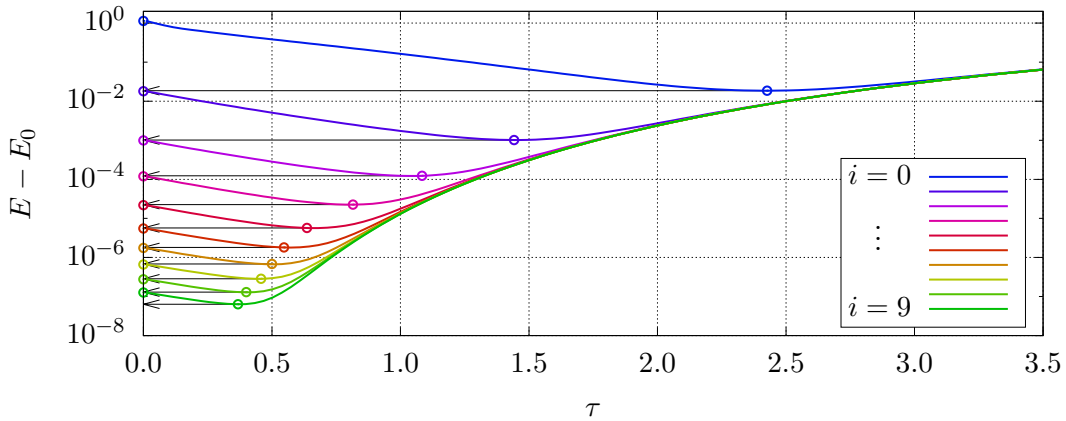

Figure 1.2: Energy difference $E - E_0$ of state $\phi_{i+1}(x) = \widehat{G}_6(\tau)\phi_i(x)$ for LHO (i-th iteration).

ational principle (1.7) an upper bound for the ground state energy E_0. The principle of the method can be seen in Figure 1.2. In each iteration the wave function is normalised.

The evolution of the wave function $\phi_i(x)$ after each iteration can be seen in Figure 1.5 (LHO) and 1.6 (2WP). We can clearly distinguish between approximants of different order. The 4th order operators $\widehat{G}_5(\tau)$ to $\widehat{G}_8(\tau)$ are better than the 2nd order operators $\widehat{G}_3(\tau)$ and $\widehat{G}_4(\tau)$, which are better than the 1st order operators $\widehat{G}_1(\tau)$ and $\widehat{G}_2(\tau)$. This property is visible for both potentials.

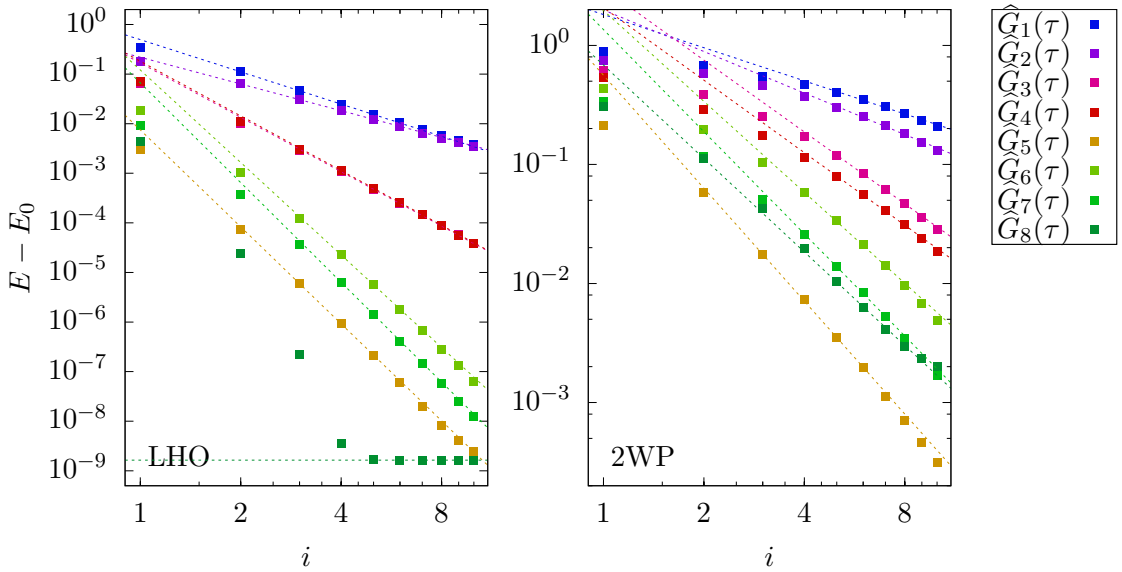

Figure 1.3: Conv. ($\log - \log$ plot) of the energy difference $E - E_0$ depending on i number of iterations for operators $\widehat{G}_j(\tau)$ (LHO – left, 2WP – right). The lines serve as a visual aid to compare convergence of different operators.

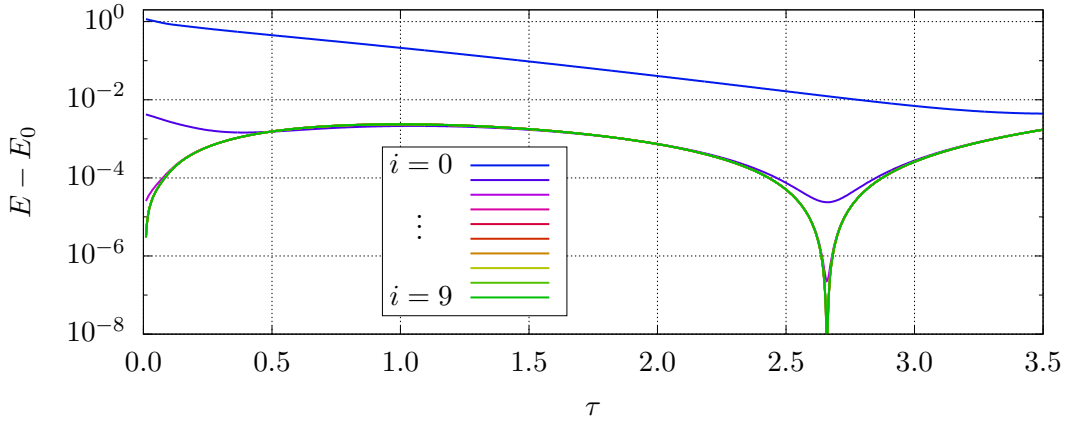

Figure 1.4: Energy difference $E - E_0$ of state $\phi_{i+1}(x) = \widehat{G}_8(\tau)\phi_i(x)$ for LHO (i-th iteration).

To visualise the rate of convergence we plotted dependence of the energy difference $E - E_0$ on the number of iterations i into $\log - \log$ plot (Figure 1.3). We can see different convergence rate for different order operators. We can see unusual behaviour for operator $\widehat{G}_8(\tau)$ in LHO potential. To understand this behaviour we replotted Figure 1.2 for our case in Figure 1.4. We can see different trend of lines in Figures 1.2 and 1.4. This is special case of LHO. The ground state wave function is Gaussian function, the the operators $\mathrm{e}^{-\tau\widehat{V}}$ and $\mathrm{e}^{-\tau\widehat{C}_1}$ are Gaussian functions. Also the operator $\mathrm{e}^{-\tau\widehat{T}}$ produces from Gaussian functions Gaussian functions of different width. Therefore it is possible for same bigger τ to obtain ground state Gaussian function. But this problem occurs only for purely quadratic potentials. This explains the first rapid convergence. The second constant trend can be explained as effect of the rounding error at level $\approx 10^{-9}$.

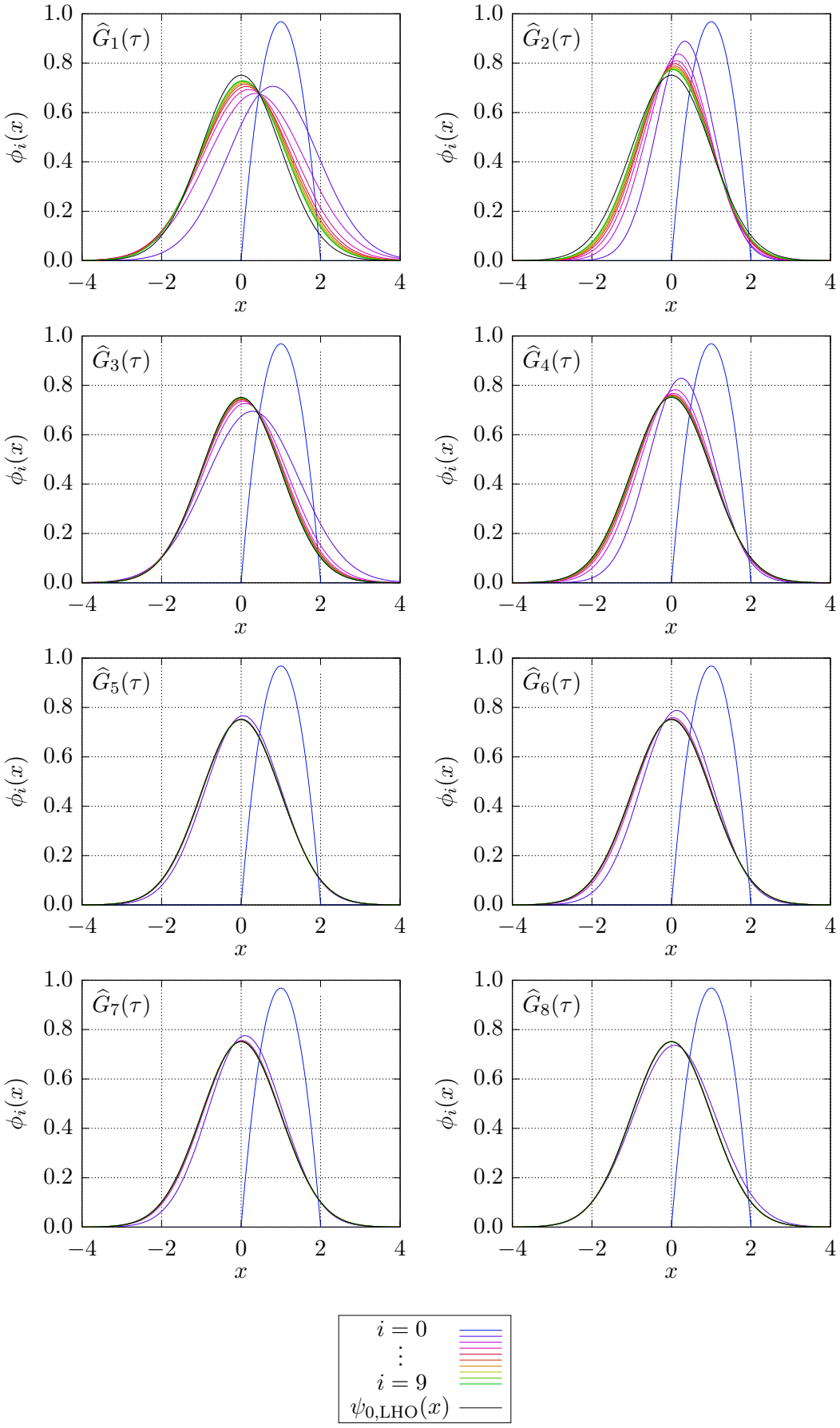

Figure 1.5: Progress of states $\phi_{i+1}(x) = \widehat{G}_j(\tau)\phi_i(x)$ for different operators $\widehat{G}_j(\tau)$ for LHO.

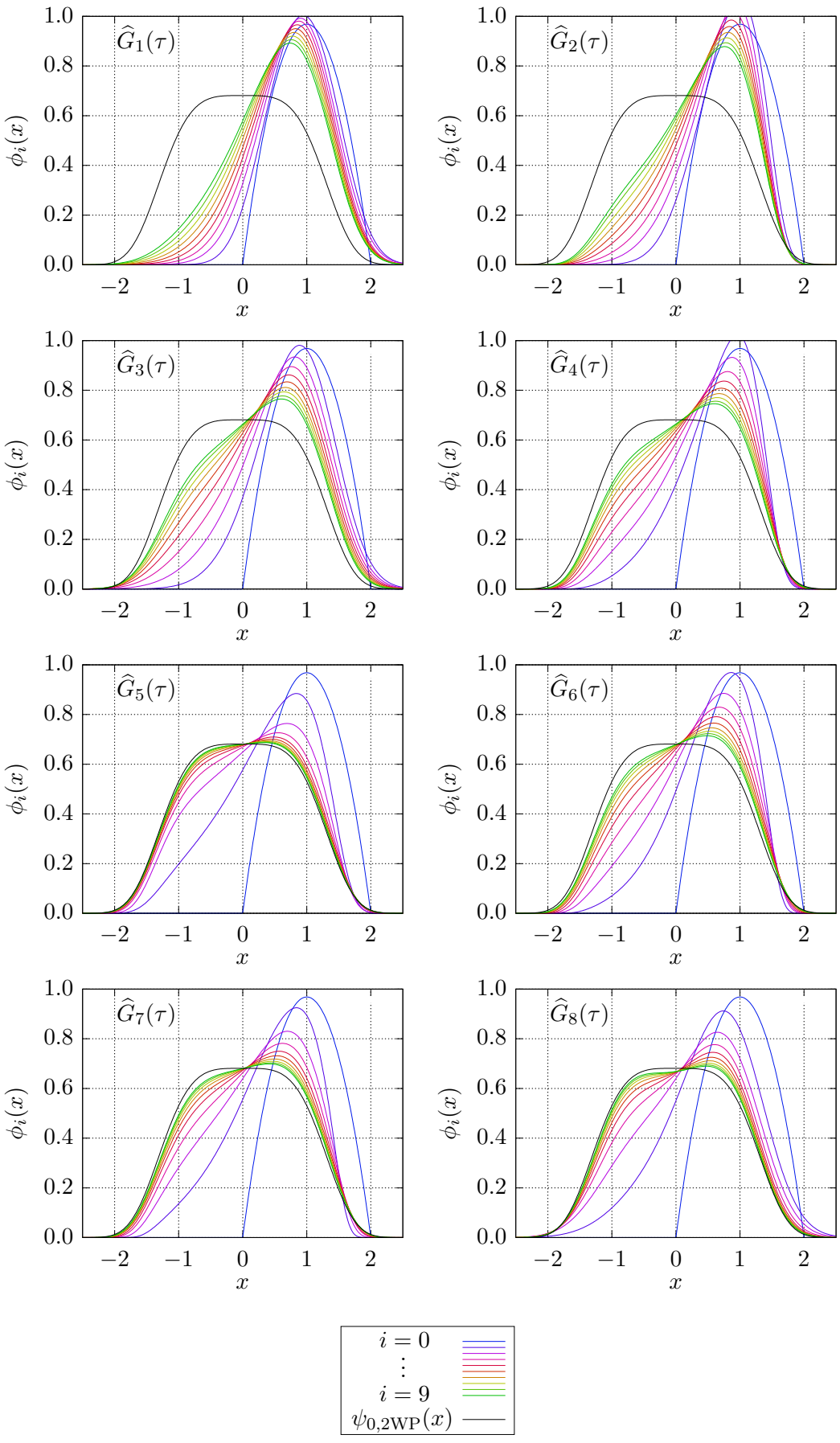

Figure 1.6: Progress of states $\phi_{i+1}(x) = \widehat{G}_j(\tau)\phi_i(x)$ for different operators $\widehat{G}_j(\tau)$ for 2WP.

2. Computational Methods

If the Hamiltonian $\widehat{H}$ has the form like in equation (1.2) with real-valued potential $V(\boldsymbol{x})$, the solution of the time-independent Schrödinger equation can be restricted to real-valued wave functions. Let be $\psi_{E,\alpha}(\boldsymbol{x})$ complex-valued solution of the time-independent Schrödinger equation (1.4) with energy E. Then the function $\psi^*_{E,\alpha}(\boldsymbol{x})$ is also solution

$$\begin{aligned}\left(\widehat{H}\psi_{E,\alpha}(\boldsymbol{x})\right)^* &= \left(E\psi_{E,\alpha}(\boldsymbol{x})\right)^* \\ \widehat{H}\psi^*_{E,\alpha}(\boldsymbol{x}) &= E\psi^*_{E,\alpha}(\boldsymbol{x})\,.\end{aligned}$$

Then we can replace 2 complex-valued solutions $\psi_{E,\alpha}(\boldsymbol{x})$ and $\psi^*_{E,\alpha}(\boldsymbol{x})$ with 2 real-valued solutions[1,2]

$$\frac{\psi_{E,\alpha}(\boldsymbol{x}) + \psi^*_{E,\alpha}(\boldsymbol{x})}{2}\,, \qquad \frac{\psi_{E,\alpha}(\boldsymbol{x}) - \psi^*_{E,\alpha}(\boldsymbol{x})}{2i}\,.$$

This is useful property, because we can restrain ourselves onto real-valued wave function without loss of generality.

The *Copenhagen interpretation* of quantum mechanics shows standard probabilistic interpretation of squared absolute value of wave function $|\psi(\boldsymbol{x})|^2$ as *probability density* $\rho(\boldsymbol{x})$

$$\mathrm{d}\,(\text{probability}) = |\psi(\boldsymbol{x})|^2\,\mathrm{d}V = \rho(\boldsymbol{x})\mathrm{d}V\,.$$

This allows to represent function $|\psi(\boldsymbol{x})|^2$ with randomly generated samples $\{\boldsymbol{x}_i\}$.[3] For some potentials the ground state wave function is not only real-valued, but also positive-valued function. This is not general rule. As a counterexample we can use any system with more than 2 fermions (with spin 1/2). The wave function of fermions is antisymmetric in any permutation of 2 particles. However if $\psi_0(\boldsymbol{x})$ is positive-valued function, we could ask if we can use not the function $\psi_0(\boldsymbol{x})^2$, but the function $\psi_0(\boldsymbol{x})$ as probability density.[4] And samples will represent the function $\psi_0(\boldsymbol{x})$ and not the function $\psi_0(\boldsymbol{x})^2$.

The function $\psi_0(\boldsymbol{x})$ can represent probability density iff

$$\int_{\mathbb{R}^N} \mathrm{d}\mathbb{R}^N\,\psi_0(\boldsymbol{x}) = I < +\infty\,. \tag{2.1}$$

To show rough justification that the integral (2.1) is finite, we will first focus on the 1D potential $V(x)$. For the potential $V(x)$ we require the condition[5]

$$\lim_{x\to\pm\infty} V(x) - E_0 = C_\pm > 0\,,$$

where E_0 is ground state energy. We can apply WKB approximation for region where $V(x) - E_0 < 0$ (classical motion)

$$\psi_0(x) \approx A_0 \frac{\mathrm{e}^{+i\int \mathrm{d}x\sqrt{2(E_0 - V(x))}}}{[2(E_0 - V(x))]^{1/4}} \tag{2.2}$$

[1] We need to renormalise new solutions.

[2] One can notice that if the solution $\psi_{E,\alpha}(\boldsymbol{x})$ is real-valued, we obtain pair $\psi_{E,\alpha}(\boldsymbol{x})$ and 0.

[3] This is for example used in some Monte Carlo methods.

[4] This probability density does not correspond to real probability of occurrence of particle in infinitesimal space $\mathrm{d}V$.

[5] The constant $C_\pm$ can be $+\infty$.

and for regions where $V(x) - E_0 > 0$ (quantum tunneling regions)

$$\psi_0(x) \approx \frac{A_+ \mathrm{e}^{+\int \mathrm{d}x \sqrt{2(V(x)-E_0)}} + A_- \mathrm{e}^{-\int \mathrm{d}x \sqrt{2(V(x)-E_0)}}}{[2(V(x)-E_0)]^{1/4}}\,. \tag{2.3}$$

The divergence of the integral I can be caused by 2 problems: infinite wave function at region of classical motion[6], or too slow decay of wave function into infinity $x \to \pm\infty$. For reasonable potential $V(x)$ the wave function (2.2) is finite and hence does not create infinity in integral I.[7] In quantum tunneling regions (2.3) there are 2 solution, one growing to infinity for $x \to \pm\infty$ and one decaying to zero for $x \to \pm\infty$. The growing term has constant $A_\pm$ equal to zero (otherwise the wave function could not be normalised). The condition (2.1) for finite $C_\pm$ guarantees at least exponential decay $\mathrm{e}^{\mp\sqrt{2C_\pm}x}$ in marginal regions, which is sufficient for integral I to be finite. The infinite $C_\pm$ guarantees even quicker decay.

Similar reasoning can be used for N-dimensional spherically symmetric potentials. The N-dimensional Schrödinger equation can be transformed into one-dimensional Schrödinger equation (more in Appendix A.3). For general case it is harder to obtain justification. Even though this is not rigorous justification, it gives some qualitative insight that it is possible for function $\psi_0(\boldsymbol{x})$ to represent probability density. But this can be overcame with introduction of positive and negative samples.

2.1 Calculation of Energy

When we are applying operator $\widehat{G}_i(\tau)$ on the wave function, we want to get closest to ground state as possible. Good indicator is energy of state $E = \frac{\langle\psi|\widehat{H}|\psi\rangle}{\langle\psi|\psi\rangle}$ (variational principle, equation (1.7)). It can be also used to set optimal parameter τ in one iteration. However the wave function[8] $\psi(\boldsymbol{x})$ is represented by n point-like samples $\{\boldsymbol{x}_i\}_{i=1}^n$, effectively represented by wave function

$$\psi(\boldsymbol{x}) \approx \frac{1}{n}\sum_{i=1}^{n} \delta_N(\boldsymbol{x} - \boldsymbol{x}_i)\,, \tag{2.4}$$

where $\delta_N(\cdot)$ is N-dimensional Dirac delta distribution. To evaluate energy E we need to evaluate three integrals: $\langle\psi|\psi\rangle$, $\langle\psi|\widehat{T}|\psi\rangle$ and $\langle\psi|\widehat{V}|\psi\rangle$.[9] Application of the kinetic energy $\widehat{T} = -\frac{1}{2}\Delta_N$ on the N-dimensional Dirac delta distribution $\delta_N(\boldsymbol{x}-\boldsymbol{x}_i)$ is not well-defined action. To overcome this problem there have been developed several different approaches.

2.1.1 Method A

This method is based on estimation of value of wave function and can be used to evaluate the norm $\langle\psi|\psi\rangle$ and the potential energy integral $\langle\psi|\widehat{V}|\psi\rangle$.

[6] The infinite value is not sufficient, it has to be infinite integral on finite interval.

[7] The finite wave function integral over classical motion interval I_C can be dominated as

$$\left|\int_{I_\mathrm{C}} \mathrm{d}x\, \psi(x)\right| \leq \int_{I_\mathrm{C}} \mathrm{d}x \max_{x\in I_\mathrm{C}}\{|\psi(x)|\} = \max_{x\in I_\mathrm{C}}\{|\psi(x)|\}\lambda(I_\mathrm{C}) < +\infty\,,$$

where $\lambda(I_\mathrm{C})$ is Lebesgue measure of the interval I_C (fancy word for *length*).

[8] We denote the wave function as $\psi(\boldsymbol{x})$ and not $\psi_0(\boldsymbol{x})$, because in following sections we will talk about energy evaluation on positive-valued function in general. Not only for the ground state.

[9] We need to remember that the samples are samples of function $\psi(\boldsymbol{x})$ not the function $\psi^2(\boldsymbol{x})$. This means that the function $\psi(\boldsymbol{x})$ is normalised and the integral $\langle\psi|\psi\rangle$ is not in general equal to 1.

In position representation the potential energy can be evaluated as

$$\langle\psi|\widehat{V}|\psi\rangle = \int_{\mathbb{R}^N} \mathrm{d}\boldsymbol{x}\, V(\boldsymbol{x})\psi(\boldsymbol{x})^2\,.$$

In standard Monte Carlo simulation for samples $\{\boldsymbol{x}_i\}_{i=1}^n$ of function $\psi(\boldsymbol{x})^2$ we could estimate the potential energy integral $\langle\psi|\widehat{V}|\psi\rangle$ as

$$\langle\psi|\widehat{V}|\psi\rangle \approx \frac{1}{n}\sum_{i=1}^{n} V(\boldsymbol{x}_i)\,.$$

However in case of samples of function $\psi(\boldsymbol{x})$ we need the value of the wave function $\psi(\boldsymbol{x}_i)$

$$\langle\psi|\widehat{V}|\psi\rangle \approx \frac{1}{n}\sum_{i=1}^{n} V(\boldsymbol{x}_i)\psi(\boldsymbol{x}_i)\,.$$

In Appendix A.2 we showed that $\psi(\boldsymbol{x}_i)$ can be estimated by $\widetilde{\psi}(\boldsymbol{x}_i)$ as (equation (A.11))

$$\widetilde{\psi}(\boldsymbol{x}_i) = \frac{1}{n}\frac{n(\boldsymbol{x}_i, r)N}{S_{N-1}r^N}\frac{1}{1+(V(\boldsymbol{x}_i)-E)\frac{r^2}{N+2}}\,, \tag{2.5}$$

where the radius of neighbourhood r was left as free parameter. In Figure 2.1 we demonstrate how to choose radius r optimally. The quantity $\langle\widetilde{\psi}(\boldsymbol{x}_i)\rangle$ is expected value of estimator $\widetilde{\psi}(\boldsymbol{x}_i)$. We want radius r to be as big as possible to get large $n(\boldsymbol{x}_i, r)$, because the relative error of estimate is approximately $1/\sqrt{n(\boldsymbol{x}_i, r)}$ (reddish band shows the error of $\langle\widetilde{\psi}(\boldsymbol{x}_i)\rangle$). On the other hand we want radius r to be as small as possible because the value $\psi(\boldsymbol{x})$ is changing from place to place and we are effectively calculating averaged wave function $\psi(\boldsymbol{x})$.[10]

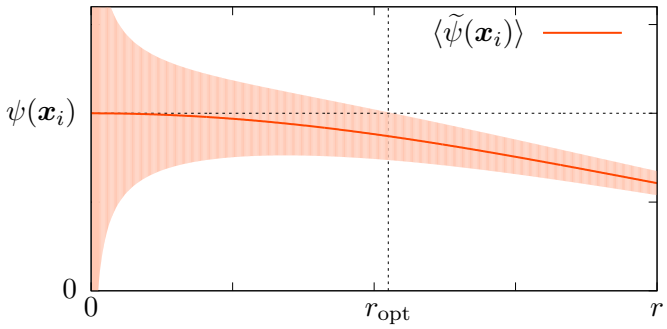

Figure 2.1: Choice of optimal radius r_{opt}.

We set some maximal number of samples $n_{\max}$ and find $n_{\max}$ closest samples, the furthest in radius $r_{\max}$. The number $n(\boldsymbol{x}_i, r)$ is approximately scaling as r^N

$$\frac{n(\boldsymbol{x}_i, r)}{n_{\max}} = \frac{r^N}{r_{\max}^N}\,.$$

The condition of optimal radius is relative error $1/\sqrt{n(\boldsymbol{x}_i, r)}$ equal to relative first correction

$$\frac{1}{\sqrt{n(\boldsymbol{x}_i, r_{\mathrm{opt}})}} = |V(\boldsymbol{x}_i) - E|\frac{r_{\mathrm{opt}}^2}{N+2}\,.$$

[10] This can be understood in term of Taylor series (A.9) in Appendix A.2, where residual term is rising with radius r.

From last two equations we can express the optimal radius r_{opt} as

$$r_{\text{opt}} = \left[\frac{(N+2) r_{\max}^{N/2}}{|V(\boldsymbol{x}_i) - E| n_{\max}^{1/2}} \right]^{\frac{2}{4+N}} . \tag{2.6}$$

We can see that for $V(\boldsymbol{x}_i) \approx E$ the optimal radius goes to infinity. We can expect that in regions where the potential energy $V(\boldsymbol{x})$ is further from value E we need smaller number of samples.

We define estimators of norm integral $\tilde{N}$, potential integral and calculated potential energy V_{cal} as

$$\begin{aligned} \tilde{N} &:= \frac{1}{n} \sum_{i=1}^{n} \tilde{\psi}(\boldsymbol{x}_i) , \\ \tilde{V} &:= \frac{1}{n} \sum_{i=1}^{n} V(\boldsymbol{x}_i) \tilde{\psi}(\boldsymbol{x}_i) , \\ V_{\text{cal}} &:= \frac{\tilde{V}}{\tilde{N}} . \end{aligned}$$

To demonstrate this method we sampled few analytic potentials (more in Appendix A.3): *gamma distribution function* and *Gaussian distribution function*.

In $N = 2$ dimensions we generated 1000 independent samples for gamma ($a = 2$, $b = 1$) and Gaussian distribution function ($a = 2$, $\sigma = 1$). The maximal number of samples was set $n_{\max} = 100$. In Figure 2.2 we plotted calculated and exact value of wave function $\psi(\boldsymbol{x}_i)$ with and without the correction (equation (2.5)). The samples are coloured according to number of samples in neighbourhood used to calculation n_{s}. This number is also important in view of that the estimated relative error is $1/\sqrt{n_{\text{s}}}$. The correction improved results, but the difference is not very noticeable.

We can also observe one important property. For gamma distribution the corresponding potential is Coulomb potential. Because it is unbound in origin we observe drop in number n_{s}. This is in agreement with equation (2.6). This can be seen in Figure 2.2 in top right plot. This means that the samples with the highest weight ($\psi(\boldsymbol{x}_i)$) have great error. On the other hand for Gaussian distribution the corresponding potential is (in origin) finite LHO and this behaviour is not present. The quadratic potential of LHO is also unbounded and this causes error for big radii, but these samples have small weight ($\psi(\boldsymbol{x}_i)$). In same Figure we can see calculated potential energy V_{cal} with estimated error compared to exact ratio $\frac{\langle V \rangle}{\langle \psi | \psi \rangle}$. Error was calculated from error of each sample $1/\sqrt{n_{\text{s}}}$. We can expect the error to be approximately $1/\sqrt{n_{\max}}$ or higher.

In $N = 3$ dimensions we generated 1000 samples for gamma ($a = 3$, $b = 1$) and Gaussian distribution function ($a = 3$, $\sigma = 1$). The maximal number of samples was set $n_{\max} = 100$. In Figure 2.3 we plotted analogous graphs to Figure 2.2. The correction strongly improved results in contrast to 2D case. In case of 3 dimensions we observe same problem with Coulomb potential as in case of 2 dimensions.

For 4-dimensional and 5-dimensional case we generated 1000 samples for gamma ($a = 4$, $b = 1$) and Gaussian distribution function ($a = 4$, $\sigma = 1$) with $n_{\max} = 100$. The graphs in Figure 2.4 are analogous to previous graphs. The correction helps to improve results, but they are scattered. However this seems does not effect the calculated potential energy. The samples are mostly under the precise value therefore they does not effect the calculated potential energy very much.

This method has 2 drawbacks: computational time rises as $\sim n^2$ with number of samples and this method does not provide calculation for the kinetic energy. Therefore there have been developed other methods.

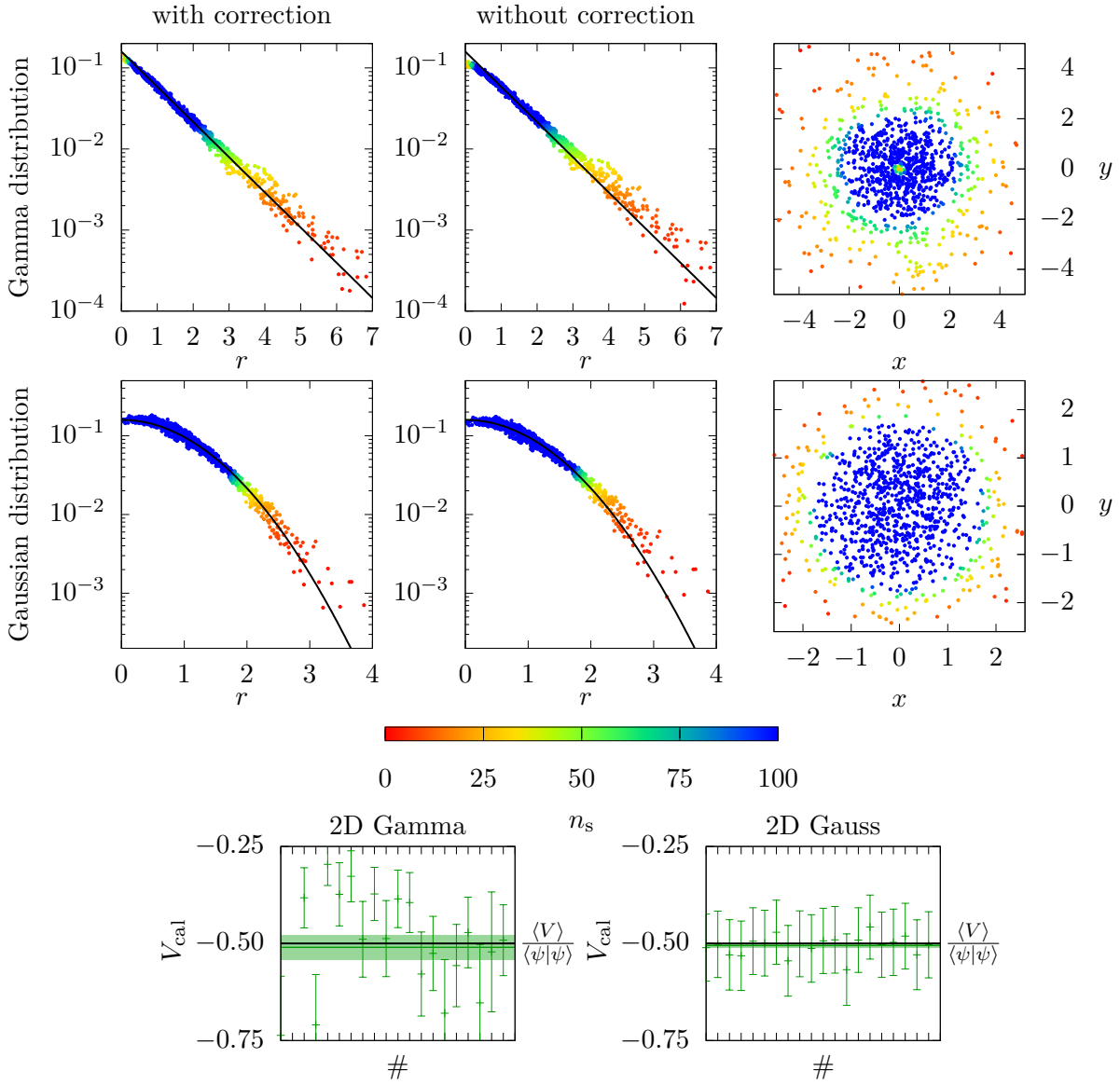

Figure 2.2: The dependance of calculated (coloured dots) and exact (black line) value of wave function $\psi(\boldsymbol{x}_i)$ on radius r with and without correction for gamma distribution (Coulomb potential) and Gaussian distribution (LHO), samples in 2D plane (2 right graphs) and calculated potential energy V_{cal} with estimated error compared to ratio $\frac{\langle V \rangle}{\langle \psi | \psi \rangle}$ for gamma and Gaussian distribution. The symbol # is run number. The average result with extimated error band is shown (green line and band).

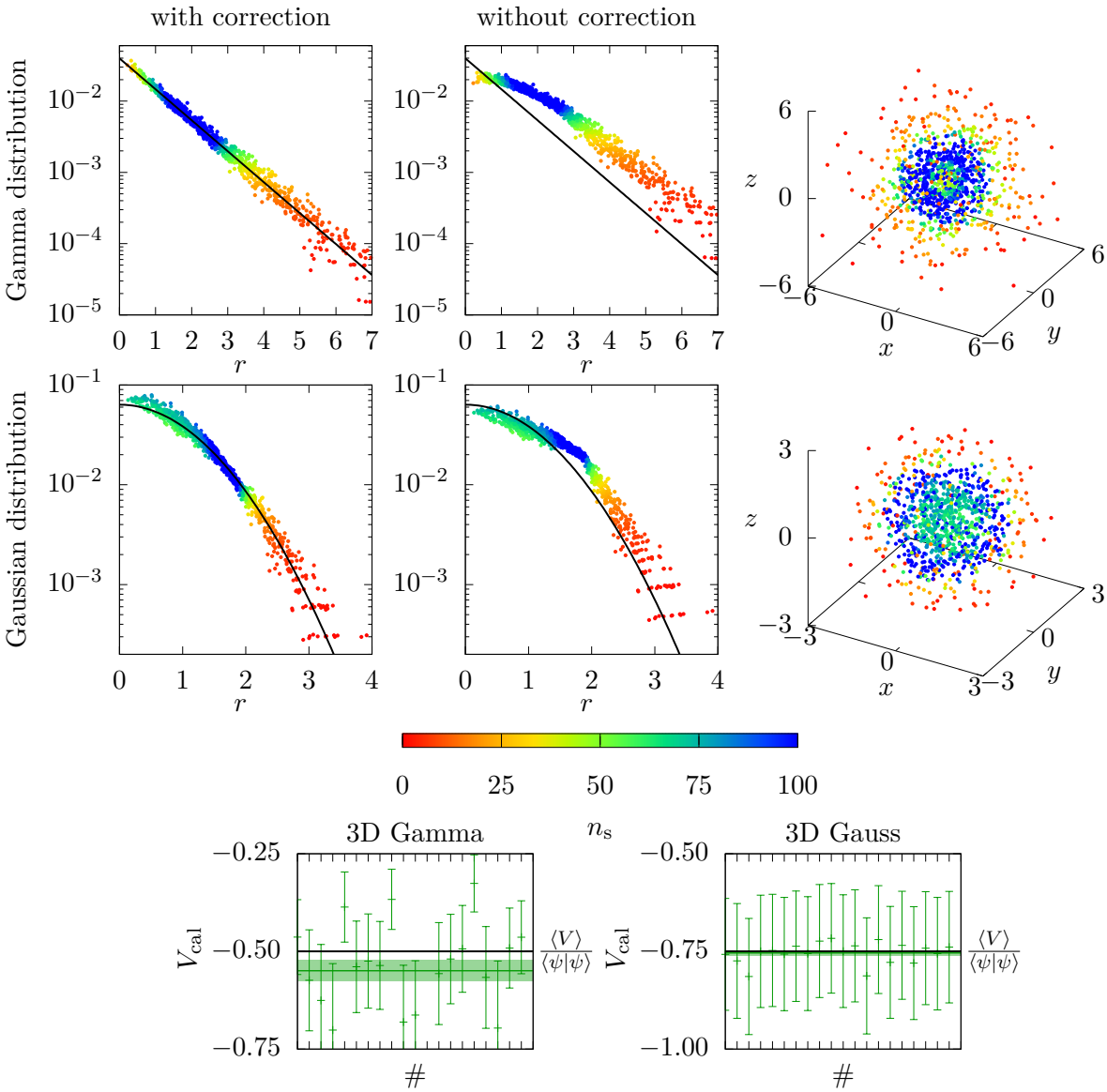

Figure 2.3: The dependance of calculated (coloured dots) and exact (black line) value of wave function $\psi(\boldsymbol{x}_i)$ on radius r with and without correction for gamma distribution (Coulomb potential) and Gaussian distribution (LHO), samples in 3D space (2 right graphs) and calculated potential energy V_{cal} with estimated error compared to ratio $\frac{\langle V \rangle}{\langle \psi | \psi \rangle}$ for gamma and Gaussian distribution.

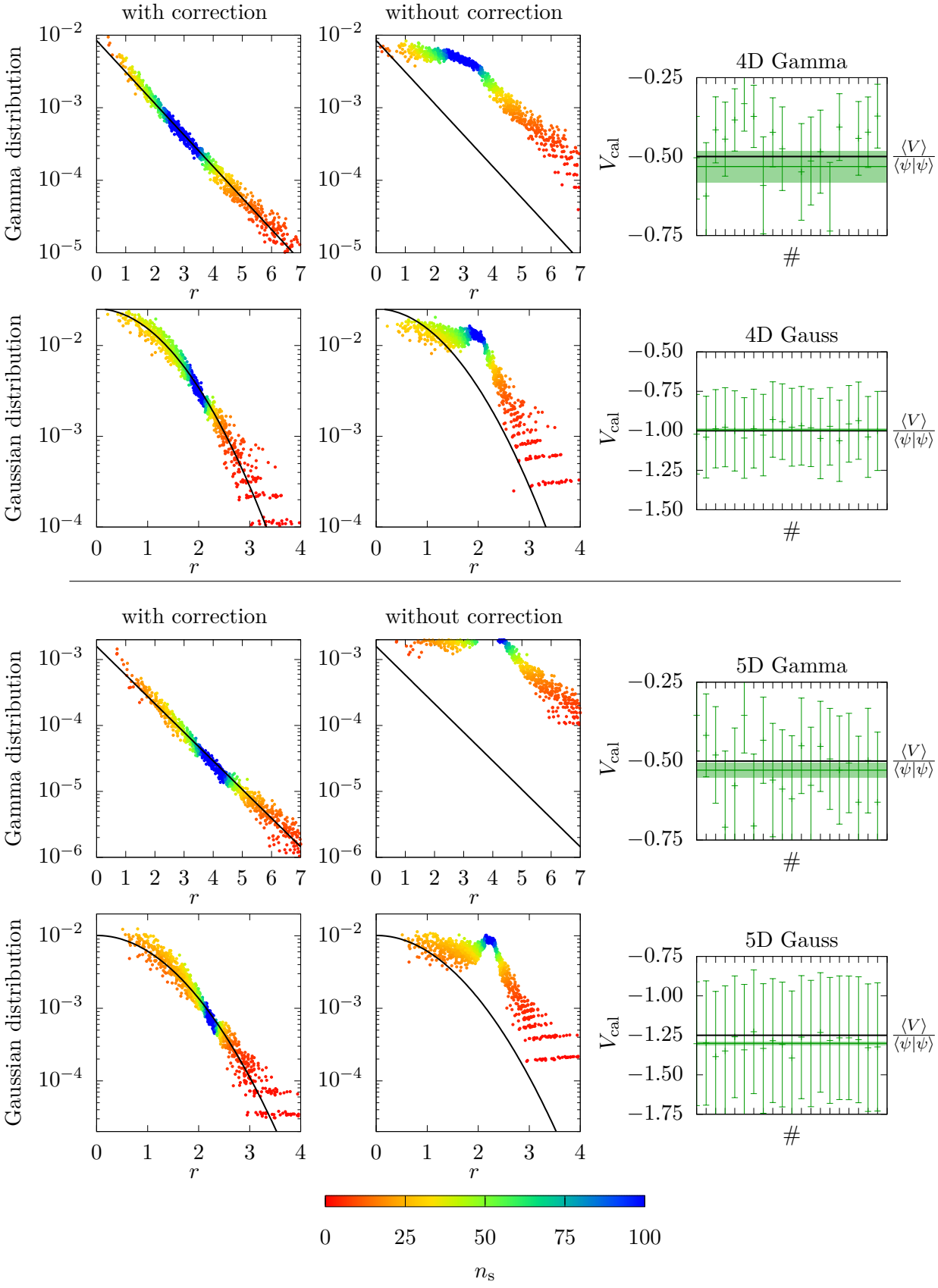

Figure 2.4: The dependance of calculated (coloured dots) and exact (black line) value of wave function $\psi(\boldsymbol{x}_i)$ on radius r with and without correction for gamma distribution (Coulomb potential) and Gaussian distribution (LHO) in 4D and 5D, the calculated potential energy V_{cal} with estimated error compared with exact value $\frac{\langle V\rangle}{\langle\psi|\psi\rangle}$.

2.1.2 Method B

The Method B employs the convolution of sampled wave function with heat kernel and can evaluate the norm $\langle\psi|\psi\rangle$, the kinetic energy integral $\langle\psi|\widehat{T}|\psi\rangle$ and the potential energy integral $\langle\psi|\widehat{V}|\psi\rangle$.

Kinetic Energy

Usually to calculate the kinetic energy we need the second derivative of wave function, but we represent the wave function with point-like objects: samples. Thus at first glance it looks hopelessly. But the operator $\mathrm{e}^{-\tau\widehat{T}}$ will help to overcome this obstacle.[11] The basic idea is as follows: the wave function represented by samples can be understood as linear combination of Dirac delta functions (equation (2.4)). Applying the operator $\mathrm{e}^{-\tau\widehat{T}}$ on the linear combination of Dirac delta functions we will get linear combination of Gaussian functions. We can calculate the kinetic energy of this linear combination and using the limit $\tau \to 0^+$ we can get the kinetic energy of the wave function $\psi(\boldsymbol{x})$.

The kinetic energy of the vector $\mathrm{e}^{-\tau\widehat{T}}|\psi\rangle$ can be formally calculated as

$$-\frac{\mathrm{d}}{\mathrm{d}\tau}\left(\mathrm{e}^{-\tau\widehat{T}}|\psi\rangle\right) = \widehat{T}\mathrm{e}^{-\tau\widehat{T}}|\psi\rangle\,.$$

This is justified in momentum representation as

$$-\frac{\mathrm{d}}{\mathrm{d}\tau}\langle\boldsymbol{p}|\mathrm{e}^{-\tau\widehat{T}}|\psi\rangle = -\frac{\mathrm{d}}{\mathrm{d}\tau}\mathrm{e}^{-\tau\frac{p^2}{2}}\langle\boldsymbol{p}|\psi\rangle = \frac{p^2}{2}\mathrm{e}^{-\tau\frac{p^2}{2}}\langle\boldsymbol{p}|\psi\rangle = \langle\boldsymbol{p}|\widehat{T}\mathrm{e}^{-\tau\widehat{T}}|\psi\rangle\,.$$

In position representation we get

$$\begin{aligned}\langle\boldsymbol{x}|\widehat{T}\mathrm{e}^{-\tau\widehat{T}}|\psi\rangle &= -\frac{\mathrm{d}}{\mathrm{d}\tau}\langle\boldsymbol{x}|\mathrm{e}^{-\tau\widehat{T}}|\psi\rangle = -\frac{\mathrm{d}}{\mathrm{d}\tau}\int_{\mathrm{R}^N}\mathrm{d}\boldsymbol{x}'\,\langle\boldsymbol{x}|\mathrm{e}^{-\tau\widehat{T}}|\boldsymbol{x}'\rangle\langle\boldsymbol{x}'|\psi\rangle \\ &\overset{\heartsuit}{=} \int_{\mathrm{R}^N}\mathrm{d}\boldsymbol{x}'\,\left(-\frac{\mathrm{d}}{\mathrm{d}\tau}\langle\boldsymbol{x}|\mathrm{e}^{-\tau\widehat{T}}|\boldsymbol{x}'\rangle\right) = \int_{\mathrm{R}^N}\mathrm{d}\boldsymbol{x}'\,\langle\boldsymbol{x}|\widehat{K}_0(\tau)|\boldsymbol{x}'\rangle\langle\boldsymbol{x}'|\psi\rangle\,,\end{aligned}$$

where in step $\heartsuit$ we used Lebesgue's *dominated convergence theorem*[12] to justify the

[11] The operator $\mathrm{e}^{-\tau\widehat{T}}$ is heat distribution propagator.

[12] The exchange is justified if the derivative of integrated function is dominated by some integrable function. If the function $\langle\boldsymbol{x}'|\psi\rangle$ is finite everywhere, we can write

$$\begin{aligned}\left|\frac{\mathrm{d}}{\mathrm{d}\tau}\left(\frac{\mathrm{e}^{-\frac{|\boldsymbol{x}-\boldsymbol{x}'|^2}{2\tau}}}{(2\pi\tau)^{N/2}}\psi(\boldsymbol{x}')\right)\right| &\le \left|\frac{N}{2\tau}\frac{1}{(2\pi\tau)^{N/2}}\mathrm{e}^{-\frac{|\boldsymbol{x}-\boldsymbol{x}'|^2}{2\tau}}\psi(\boldsymbol{x}')\right| + \left|\frac{|\boldsymbol{x}-\boldsymbol{x}'|^2}{2\tau^2}\frac{1}{(2\pi\tau)^{N/2}}\mathrm{e}^{-\frac{|\boldsymbol{x}-\boldsymbol{x}'|^2}{2\tau}}\psi(\boldsymbol{x}')\right| \\ &\le \max_{\boldsymbol{x}'\in\mathbb{R}^N}|\psi(\boldsymbol{x}')|\frac{1}{(2\pi\tau)^{N/2}}\left(\frac{N}{2\tau}+\frac{|\boldsymbol{x}-\boldsymbol{x}'|^2}{2\tau^2}\right)\mathrm{e}^{-\frac{|\boldsymbol{x}-\boldsymbol{x}'|^2}{2\tau}}\,.\end{aligned}$$

The dominating function is integrable

$$\int_{\mathbb{R}^N}\mathrm{d}\boldsymbol{x}'\,\left(\frac{N}{2\tau}+\frac{|\boldsymbol{x}-\boldsymbol{x}'|^2}{2\tau^2}\right)\mathrm{e}^{-\frac{|\boldsymbol{x}-\boldsymbol{x}'|^2}{2\tau}} \overset{\boldsymbol{t}=\boldsymbol{x}'-\boldsymbol{x}}{=\!=\!=} \int_{\mathbb{R}^N}\mathrm{d}\boldsymbol{t}\,\left(\frac{N}{2\tau}+\frac{t^2}{2\tau^2}\right)\mathrm{e}^{-\frac{t^2}{2\tau}} = \frac{N}{\tau}\left(2\pi\tau\right)^{N/2} < +\infty\,.$$

If the function $\langle\boldsymbol{x}'|\psi\rangle$ is infinite at some compact region C, we can imply

$$\psi(\boldsymbol{x}') \in L^2(\mathbb{R}^N) \implies \psi(\boldsymbol{x}') \in L^2(C) \implies \psi(\boldsymbol{x}') \in L^1(C)\,.$$

Therefore we can choose dominating integrable function $M\psi(\boldsymbol{x}')$, where

$$M = \max_{\boldsymbol{x}'\in C}\left|\frac{1}{(2\pi\tau)^{N/2}}\left(\frac{N}{2\tau}+\frac{|\boldsymbol{x}-\boldsymbol{x}'|^2}{2\tau^2}\right)\mathrm{e}^{-\frac{|\boldsymbol{x}-\boldsymbol{x}'|^2}{2\tau}}\right|\,.$$

interchange of derivative and integral. The matrix element $\langle \boldsymbol{x}|\widehat{K_0}(\tau)|\boldsymbol{x}'\rangle$ is

$$\langle \boldsymbol{x}|\widehat{K_0}(\tau)|\boldsymbol{x}'\rangle = \frac{\mathrm{e}^{-\frac{\Delta x^2}{2\tau}}}{(2\pi\tau)^{N/2}}\frac{1}{2\tau}\left(N - \frac{\Delta x^2}{\tau}\right),$$

where $\Delta x = |\boldsymbol{x} - \boldsymbol{x}'|$. Then in the limit $\tau \to 0^+$ we can write

$$\langle \psi|\widehat{T}|\psi\rangle = \lim_{\tau\to 0^+}\langle \psi|\widehat{T}\mathrm{e}^{-\tau\widehat{T}}|\psi\rangle = \lim_{\tau\to 0^+}\int_{\mathrm{R}^N}\mathrm{d}\boldsymbol{x}\int_{\mathrm{R}^N}\mathrm{d}\boldsymbol{x}'\,\langle\psi|\boldsymbol{x}\rangle\langle\boldsymbol{x}|\widehat{K_0}(\tau)|\boldsymbol{x}'\rangle\langle\boldsymbol{x}'|\psi\rangle\,. \quad (2.7)$$

For wave function $\psi(\boldsymbol{x})$ represented by samples $\{\boldsymbol{x}_i\}_{i=1}^n$ we can write estimator of kinetic energy as

$$\langle \psi|\widehat{T}|\psi\rangle \approx \lim_{\tau\to 0^+}\frac{1}{n^2}\sum_{i=1}^{n}\sum_{j=1}^{n}K_0(\tau,\Delta x_{ij})\,,$$

where we used more convenient notation $K_0(\tau,\Delta x_{ij}) = \langle \boldsymbol{x}_i|\widehat{K_0}(\tau)|\boldsymbol{x}_j\rangle$.

However we can notice that the operator $\widehat{K_0}(\tau)$ in power expansion of τ

$$\widehat{K_0}(\tau) = \widehat{T}\mathrm{e}^{-\tau\widehat{T}} = \widehat{T} - \tau\widehat{T}^2 + \frac{1}{2!}\tau^2\widehat{T}^3 - \frac{1}{3!}\tau^3\widehat{T}^4 + \dots$$

can be improved. In same matter as we could express $\langle \psi|\widehat{T}\mathrm{e}^{-\tau\widehat{T}}|\psi\rangle$, we can express any power $\langle \psi|\widehat{T}^n\mathrm{e}^{-\tau\widehat{T}}|\psi\rangle$ and make correction to operator $\widehat{K_0}(\tau)$. We define the higher order operators $\widehat{K_m}(\tau)$ as

$$\widehat{K_m}(\tau) := \widehat{T}\mathrm{e}^{-\tau\widehat{T}}T_m(\mathrm{e}^{\tau\widehat{T}})\,, \quad (2.8)$$

where $T_m(\cdot)$ is Taylor series of the m-th order in variable τ. In Appendix A.4 we calculated spacial matrix elements $\langle \boldsymbol{x}|\widehat{K_m}(\tau)|\boldsymbol{x}'\rangle$ for $m > 0$. Same procedure used before for $\widehat{K_0}(\tau)$ can be used to obtain more general form of equation (2.7)[13]

$$\langle \psi|\widehat{T}|\psi\rangle = \lim_{\tau\to 0^+}\int_{\mathrm{R}^N}\mathrm{d}\boldsymbol{x}\int_{\mathrm{R}^N}\mathrm{d}\boldsymbol{x}'\,\langle\psi|\boldsymbol{x}\rangle\langle\boldsymbol{x}|\widehat{K_m}(\tau)|\boldsymbol{x}'\rangle\langle\boldsymbol{x}'|\psi\rangle\,.$$

and estimator

$$\langle \psi|\widehat{T}|\psi\rangle \approx \lim_{\tau\to 0^+}\frac{1}{n^2}\sum_{i=1}^{n}\sum_{j=1}^{n}K_m(\tau,\Delta x_{ij})\,. \quad (2.9)$$

However the estimator (2.9) is biased and we would like to estimate the error of the estimator. In Appendix A.5 we showed that the estimator $\hat{\mathcal{T}}_1$ is unbiased (equation (A.19)) estimator of the integral $\langle \psi|\widehat{K_m}(\tau)|\psi\rangle$

$$\hat{\mathcal{T}}_1 := \frac{2}{n(n-1)}\sum_{\substack{i=1\\ j>i}}^{n}K_m(\tau,\Delta x_{ij})\,, \quad (2.10)$$

and the estimator $\hat{\mathscr{V}}_{\mathcal{T}_1}$ is unbiased estimator of the variance $\mathrm{Var}[\hat{\mathcal{T}}_1]$

$$\hat{\mathscr{V}}_{\mathcal{T}_1} := \frac{4}{n(n-1)(n-2)(3n-5)}\left[4\sum_{\substack{i=1\\ j>i}}^{n}\sum_{\substack{k=1\\ k\neq j}}^{n}K_m(\tau,\Delta x_{ij})K_m(\tau,\Delta x_{jk}) - \right.$$
$$\left. - \frac{n(n-1)(4n-5)}{2}(\hat{\mathcal{T}}_1)^2 - \sum_{\substack{i=1\\ j>i}}^{n}K_m^2(\tau,\Delta x_{ij})\right]. \quad (2.11)$$

[13]The justification for interchange of derivative and integral is similar. The dominating integrable function will have the form $P(\Delta x^2)\mathrm{e}^{-\frac{\Delta x^2}{2\tau}}$, where $P(\cdot)$ is polynomial.

Potential Energy and Norm

In same manner we can use this technique to find integral $\langle\psi|\psi\rangle$ and $\langle\psi|\widehat{V}|\psi\rangle$. We define the approximants of unit operator $\widehat{J}_m(\tau)$

$$\widehat{J}_m(\tau) := \mathrm{e}^{-\tau\widehat{T}} T_m(\mathrm{e}^{\tau\widehat{T}})\,, \tag{2.12}$$

and approximants of potential operator $\widehat{V}_m(\tau)$ as[14]

$$\widehat{V}_m(\tau) := \widehat{V}\mathrm{e}^{-\tau\widehat{T}} T_m(\mathrm{e}^{\tau\widehat{T}})\,.$$

In Appendix A.4 we calculated spacial matrix elements $\langle\boldsymbol{x}|\widehat{J}_m(\tau)|\boldsymbol{x}'\rangle$. The spacial matrix elements $\langle\boldsymbol{x}|\widehat{V}_m(\tau)|\boldsymbol{x}'\rangle$ are equal to

$$\langle\boldsymbol{x}|\widehat{V}_m(\tau)|\boldsymbol{x}'\rangle = V(\boldsymbol{x})\langle\boldsymbol{x}|\widehat{J}_m(\tau)|\boldsymbol{x}'\rangle\,.$$

We can generalise the formulas (2.10) and (2.11)

$$\begin{aligned}
\hat{\mathcal{X}}_1 :=& \frac{2}{n(n-1)} \sum_{\substack{i=1\\ j>i}}^{n} X_m(\tau, \Delta x_{ij})\,,\\
\hat{\mathscr{V}}_{\mathcal{X}_1} :=& \frac{4}{n(n-1)(n-2)(3n-5)} \left[4 \sum_{\substack{i=1\\ j>i}}^{n} \sum_{\substack{k=1\\ k\neq j}}^{n} X_m(\tau, \Delta x_{ij}) X_m(\tau, \Delta x_{jk}) - \right.\\
& \left. - \frac{n(n-1)(4n-5)}{2} (\hat{\mathcal{X}})^2 - \sum_{\substack{i=1\\ j>i}}^{n} X_m^2(\tau, \Delta x_{ij}) \right]\,,
\end{aligned}$$

where for $X \in \{J, T, V\}$ we introduce estimators $\hat{\mathcal{X}}_1 \in \{\hat{\mathcal{J}}_1, \hat{\mathcal{T}}_1, \hat{\mathcal{V}}_1\}$ and estimators of variance $\hat{\mathscr{V}}_{\mathcal{X}_1} \in \{\hat{\mathscr{V}}_{\mathcal{J}_1}, \hat{\mathscr{V}}_{\mathcal{T}_1}, \hat{\mathscr{V}}_{\mathcal{V}_1}\}$. The energy can be estimated as

$$\mathcal{H}_1 := \frac{\mathcal{T}_1 + \mathcal{V}_1}{\mathcal{J}_1}\,.$$

To demonstrate this method we will use analytic solvable system: Gaussian distribution function.

For $N = 2$ dimensional Gaussian function ($\sigma = 1$, equation (A.21)) we generated 4000 samples. In Figure 2.5 we plotted dependence of calculated integral $\langle\widehat{K}_m(\tau)\rangle$ (coloured, equation (2.10)) with estimated error (equation (2.11)) and exact values of integrals $\langle\widehat{K}_m(\tau)\rangle$ (black, equation (A.23)) for wide range of imaginary time τ.

For large τ the calculation is more precise, but the calculated value is further from value $\langle\psi|\widehat{T}|\psi\rangle$. For small τ the error is enormous. To choose optimal τ we propose following procedure: Set large τ and estimate integrals $\langle\psi|\widehat{K}_m(\tau)|\psi\rangle$ and $\langle\psi|\widehat{K}_{m+1}(\tau)|\psi\rangle$. Decrease τ until the estimates of $\langle\psi|\widehat{K}_m(\tau)|\psi\rangle$ and $\langle\psi|\widehat{K}_{m+1}(\tau)|\psi\rangle$ are within the estimated error.

This procedure was used to find optimal τ and calculate the norm $\langle\psi|\psi\rangle$, the kinetic energy integral $\langle\psi|\widehat{T}|\psi\rangle$ and the potential energy integral $\langle\psi|\widehat{V}|\psi\rangle$ (Figure 2.6).

[14] This definition is asymmetric, because the operators $\widehat{V}$ and $\widehat{T}$ are not commutative in general. One might want to define another approximants as $\mathrm{e}^{-\tau\widehat{T}} T_m(\mathrm{e}^{\tau\widehat{T}})\widehat{V}$. The difference between spacial matrix elements would be

$$V(\boldsymbol{x})\langle\boldsymbol{x}|\widehat{J}_m(\tau)|\boldsymbol{x}'\rangle \quad \text{vs.} \quad V(\boldsymbol{x}')\langle\boldsymbol{x}|\widehat{J}_m(\tau)|\boldsymbol{x}'\rangle\,.$$

But when the integral will be evaluated on samples and summed over pair of samples, the result will be same because the matrix elements $\langle\boldsymbol{x}|\widehat{J}_m(\tau)|\boldsymbol{x}'\rangle$ are symmetric in exchange of variables $\boldsymbol{x} \leftrightarrow \boldsymbol{x}'$.

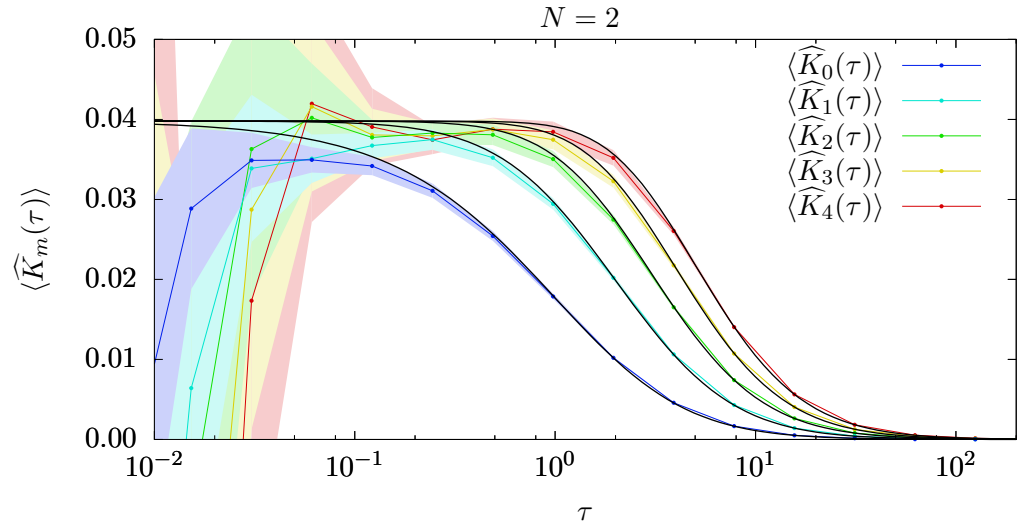

Figure 2.5: The τ-dependence of estimated (coloured with error band) and exact integrals $\langle\psi|\widehat{K}_m(\tau)|\psi\rangle$ for $N = 2$ (4000 samples).

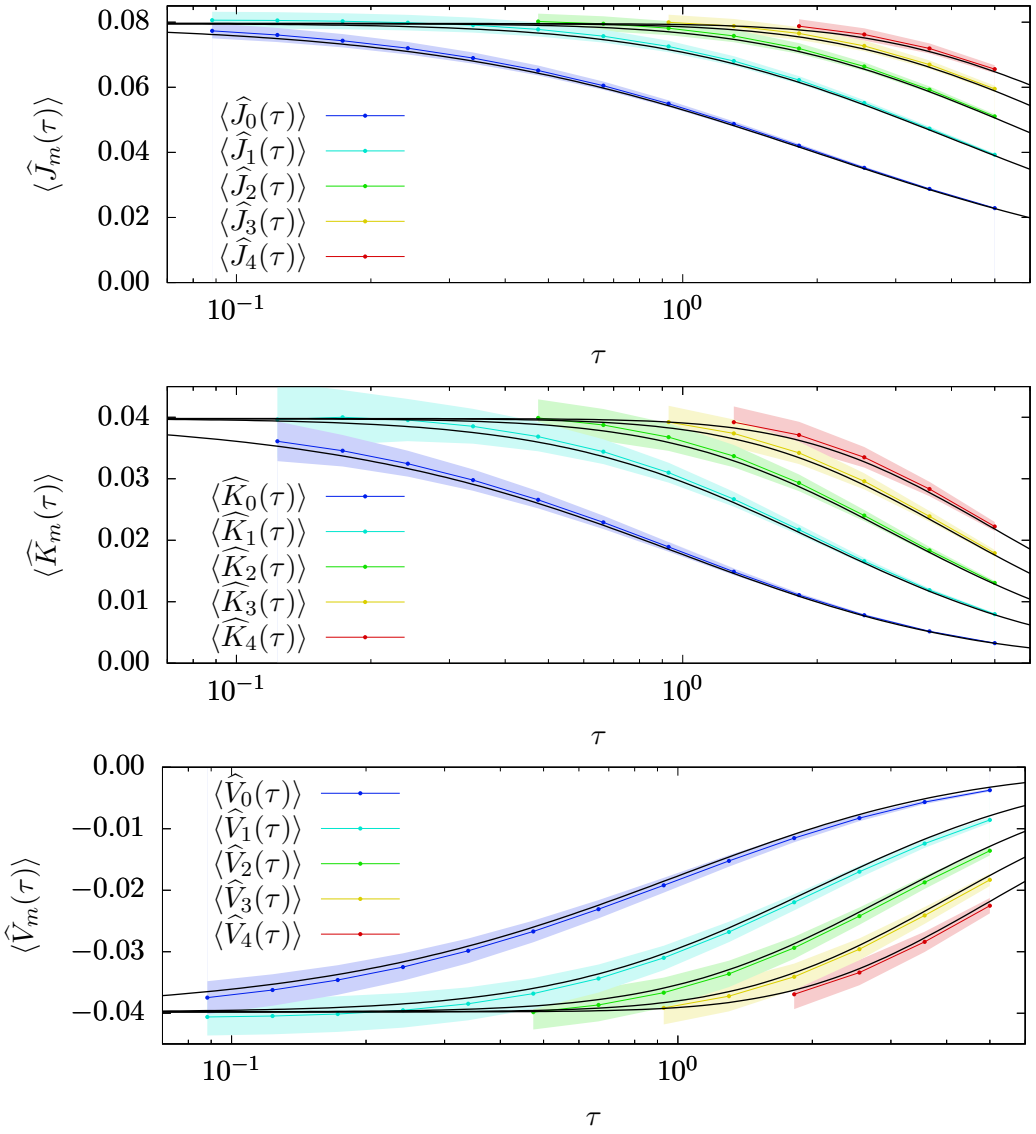

Figure 2.6: The choice of optimal τ and calculation of the norm $\langle\psi|\psi\rangle$, the kinetic energy integral $\langle\psi|\widehat{T}|\psi\rangle$ and the potential energy integral $\langle\psi|\widehat{V}|\psi\rangle$ for $N = 2$ (1000 samples).

We expect that when the calculated kinetic energy and real value are not within the error, then we need more samples of wave function for better representation of wave function.[15] Also when the sampled wave function and number of samples N does not change a lot, we need to find optimal τ only once.

However there is a catch. With n samples the estimators $\hat{\mathcal{X}}_1$ and $\hat{\mathscr{V}}_{\mathcal{X}_1}$ need approximately n^2 operations, because the estimators are evaluated on $n(n-1)/2$ pairs of samples. With rising number of samples the computational time rises unbearably. Also the pairs of samples are not independent, because each sample is in $(n-1)$ pairs. To solve this problem we need to generate independent pairs of samples. From n samples we have $n/2$ pairs of samples. The corresponding estimators are defined as

$$\begin{aligned}\hat{\mathcal{X}}_2 :=& \frac{1}{n}\sum_{i=1}^{n} X_m(\tau, \Delta x_i)\,,\\ \hat{\mathscr{V}}_{\mathcal{X}_2} :=& \frac{1}{n(n-1)}\sum_{i=1}^{n}\left[X_m(\tau,\Delta x_i) - \hat{\mathcal{X}}_2\right]^2\,,\end{aligned}$$

where for $X \in \{J, T, V\}$ we estimators estimators $\hat{\mathcal{X}}_2 \in \{\hat{\mathcal{J}}_2, \hat{\mathcal{T}}_2, \hat{\mathcal{V}}_2\}$ and estimators of variance $\hat{\mathscr{V}}_{\mathcal{X}_2} \in \{\hat{\mathscr{V}}_{\mathcal{J}_2}, \hat{\mathscr{V}}_{\mathcal{T}_2}, \hat{\mathscr{V}}_{\mathcal{V}_2}\}$.

We will not use all information from samples, but the estimators can be calculated quicker. For the same computational time the estimator $\hat{\mathcal{X}}_2$ from larger set of pairs of samples gives more precise value with smaller error. The energy can be estimated as

$$\mathcal{H}_2 := \frac{\mathcal{T}_2 + \mathcal{V}_2}{\mathcal{J}_2}\,.$$

In Appendix A.8 we discuss if and when does the energy defined as

$$\langle E\rangle := \frac{\langle\psi|\widehat{H}\widehat{J}_m(\tau)|\psi\rangle}{\langle\psi|\widehat{J}_m(\tau)|\psi\rangle}$$

have the lower bound and what is its relation to the ground state energy E_0.

For the ground state $|E_0\rangle$ the energy is equal to E_0 for any τ

$$\frac{\langle E_0|\widehat{H}\widehat{J}_m(\tau)|E_0\rangle}{\langle E_0|\widehat{J}_m(\tau)|E_0\rangle} = \frac{\langle E_0|E_0\widehat{J}_m(\tau)|E_0\rangle}{\langle E_0|\widehat{J}_m(\tau)|E_0\rangle} = E_0\,. \tag{2.13}$$

2.1.3 Method C

We define the averaged energy $\{H\}$ as[16]

$$\{H\} := \frac{\displaystyle\int_{\mathbb{R}^N} \mathrm{d}\boldsymbol{x}\,\widehat{H}\psi(\boldsymbol{x})}{\displaystyle\int_{\mathbb{R}^N}\mathrm{d}\boldsymbol{x}\,\psi(\boldsymbol{x})}\,.$$

[15] One may imagine wave function $N\cos^2(10x)\mathrm{e}^{-x^2}$. When the wave function is poorly sampled, the samples looks like samples of function $\frac{N}{2}\mathrm{e}^{-x^2}$. However the rapid changes in wave functions are more common for excited states.

[16] We can notice that the definition can be expressed as averaged local energy weighed by wave function

$$\frac{\displaystyle\int_{\mathbb{R}^N} \mathrm{d}\boldsymbol{x}\,\frac{\widehat{H}\psi(\boldsymbol{x})}{\psi(\boldsymbol{x})}\psi(\boldsymbol{x})}{\displaystyle\int_{\mathbb{R}^N}\mathrm{d}\boldsymbol{x}\,\psi(\boldsymbol{x})}\,.$$

For separable Hamiltonian from equation (1.2) we can write

$$\{H\} = \frac{\int_{\mathbb{R}^N} \mathrm{d}\boldsymbol{x} \left[-\frac{1}{2}\Delta_N + V(\boldsymbol{x})\right] \psi(\boldsymbol{x})}{\int_{\mathbb{R}^N} \mathrm{d}\boldsymbol{x}\, \psi(\boldsymbol{x})} = -\frac{1}{2} \frac{\int_{\mathbb{R}^N} \mathrm{d}\boldsymbol{x}\, \boldsymbol{\nabla} \cdot \boldsymbol{\nabla}\psi(\boldsymbol{x})}{\int_{\mathbb{R}^N} \mathrm{d}\boldsymbol{x}\, \psi(\boldsymbol{x})} + \frac{\int_{\mathbb{R}^N} \mathrm{d}\boldsymbol{x}\, V(\boldsymbol{x})\psi(\boldsymbol{x})}{\int_{\mathbb{R}^N} \mathrm{d}\boldsymbol{x}\, \psi(\boldsymbol{x})}$$

$$\overset{\heartsuit}{=} -\frac{1}{2} \frac{\int_{\partial(\mathbb{R}^N)} \boldsymbol{\nabla}\psi(\boldsymbol{x}) \cdot \mathrm{d}\boldsymbol{\Sigma}}{\int_{\mathbb{R}^N} \mathrm{d}\boldsymbol{x}\, \psi(\boldsymbol{x})} + \frac{\int_{\mathbb{R}^N} \mathrm{d}\boldsymbol{x}\, V(\boldsymbol{x})\psi(\boldsymbol{x})}{\int_{\mathbb{R}^N} \mathrm{d}\boldsymbol{x}\, \psi(\boldsymbol{x})} \overset{\spadesuit}{=} \frac{\int_{\mathbb{R}^N} \mathrm{d}\boldsymbol{x}\, V(\boldsymbol{x})\psi(\boldsymbol{x})}{\int_{\mathbb{R}^N} \mathrm{d}\boldsymbol{x}\, \psi(\boldsymbol{x})} =: \{V\}\,,$$

where in step $\heartsuit$ we used *Stokes' theorem*[17], in step $\spadesuit$ we used fact, that the wave function $\psi(\boldsymbol{x})$ vanishes to zero at boundary of space $\partial(\mathbb{R}^N)$ therefore the gradient $\boldsymbol{\nabla}\psi(\boldsymbol{x})$ vanishes to zero too. We defined averaged potential energy $\{V\}$, which is identical to $\{H\}$.

The averaged energy $\{H\}$ can be evaluated on samples as

$$\{\tilde{H}\} = \frac{1}{n} \sum_{i=1}^{n} V(\boldsymbol{x}_i)\,,$$

with estimate of error $\hat{\mathscr{V}}_{\{H\}}$

$$\hat{\mathscr{V}}_{\{H\}} = \frac{1}{n(n-1)} \sum_{i=1}^{n} \left[V(\boldsymbol{x}_i) - \{\tilde{H}\}\right]^2 .$$

In Appendix A.7 we showed that in the limit $\tau \to +\infty$ the Method B becomes the Method C in precise form and also in terms of estimators. Also in Appendix A.8 we showed that the averaged energy $\{H\}$ is non-variational energy and the infimum is $\min_{\boldsymbol{x}\in\mathbb{R}^N} \{V(\boldsymbol{x})\}$.

For the ground state $|E_0\rangle$ the averaged energy $\{H\}$ is equal to E_0

$$\{H\} = \frac{\int_{\mathbb{R}^N} \mathrm{d}\boldsymbol{x}\, \widehat{H}\psi_0(\boldsymbol{x})}{\int_{\mathbb{R}^N} \mathrm{d}\boldsymbol{x}\, \psi_0(\boldsymbol{x})} = \frac{\int_{\mathbb{R}^N} \mathrm{d}\boldsymbol{x}\, E_0\psi_0(\boldsymbol{x})}{\int_{\mathbb{R}^N} \mathrm{d}\boldsymbol{x}\, \psi_0(\boldsymbol{x})} = E_0\,.$$

2.1.4 Method D

This method (exponential decay method) uses change in number of samples in one iteration and does not need to handle the individual samples. We start with the operator $\widehat{G}_i(\tau)$ as the approximant of the operator $\mathrm{e}^{-\tau\widehat{H}}$.

$$\mathrm{e}^{-\tau\widehat{H}}|\psi\rangle = \widehat{G}_i(\tau)|\psi\rangle + O(\tau^n)\,.$$

We can write

$$\int_{\mathbb{R}^N} \mathrm{d}\boldsymbol{x}\, \langle\boldsymbol{x}|\mathrm{e}^{-\tau\widehat{H}}|\psi\rangle = \int_{\mathbb{R}^N} \mathrm{d}\boldsymbol{x}\, \langle\boldsymbol{x}|\widehat{G}_i(\tau)|\psi\rangle + O(\tau^n)\,.$$

When the state $|\psi\rangle$ is near the ground state $|E_0\rangle$ (or any eigenvector), then we can approximate $\widehat{H}|\psi\rangle \approx E|\psi\rangle$.

$$\int_{\mathbb{R}^N} \mathrm{d}\boldsymbol{x}\, \langle\boldsymbol{x}|\mathrm{e}^{-\tau\widehat{H}}|\psi\rangle \approx \mathrm{e}^{-\tau E} \int_{\mathbb{R}^N} \mathrm{d}\boldsymbol{x}\, \langle\boldsymbol{x}|\psi\rangle \approx \int_{\mathbb{R}^N} \mathrm{d}\boldsymbol{x}\, \langle\boldsymbol{x}|\widehat{G}_i(\tau)|\psi\rangle$$

[17] In this special case it is also called *divergence theorem* or *Gauss's theorem*.

We can express the energy as

$$E \approx \frac{1}{\tau} \ln \left(\frac{\int_{\mathbb{R}^N} \mathrm{d}\boldsymbol{x} \, \langle \boldsymbol{x} | \psi \rangle}{\int_{\mathbb{R}^N} \mathrm{d}\boldsymbol{x} \, \langle \boldsymbol{x} | \widehat{G}_i(\tau) | \psi \rangle} \right) .$$

We denote the number of samples in the j-th iteration as n_j. Then the estimator of energy $\tilde{E}$ can be expressed as

$$\tilde{E} = \frac{1}{\tau} \ln \left(\frac{n_j}{n_{j+1}} \right) .$$

However this method cannot be used in our case. In each iteration we chose optimal τ, where the energy has minimum. At this point the operator $\widehat{G}_i(\tau)$ already fails to approximate the exponential operator, because we do not observe exponential decay. Second disadvantage is dependence on the evolution of wave function. Also for small parameter τ the error is huge, for larger τ the relation is inaccurate.

2.2 Implementation of the Operators $\widehat{G}_i(\tau)$

The approximants $\widehat{G}_i(\tau)$ consist of two types of operators in sense of action on wave function: *multiplication with non-negative real-valued function* (operators $\mathrm{e}^{-\tau^{2i+1}\widehat{C}_i}$) and *convolution* (operator $\mathrm{e}^{-\tau\widehat{T}}$).

2.2.1 Multiplication

Let the $\{\boldsymbol{x}_i\}_{i=1}^n$ be initial set of samples of wave function $\psi(\boldsymbol{x})$ and we need samples of wave function

$$\langle \boldsymbol{x} | \widehat{F} | \psi \rangle = F(\boldsymbol{x}) \psi(\boldsymbol{x}) ,$$

where $F(\cdot)$ is non-negative real-valued function.

Implementation: Each sample $\boldsymbol{x}_i$ is duplicated $\lfloor F(\boldsymbol{x_i}) \rfloor$ times and we add extra duplicate with probability $(F(\boldsymbol{x_i}) - \lfloor F(\boldsymbol{x_i}) \rfloor)$.

The above mentioned procedure can be used to implement action of operators $\mathrm{e}^{-\tau^{2i+1}\widehat{C}_i}$.

2.2.2 Convolution

Let the $\{\boldsymbol{x}_i\}_{i=1}^n$ be initial set of samples of wave function $\psi(\boldsymbol{x})$ and we need samples of wave function

$$\langle \boldsymbol{x} | \mathrm{e}^{-\tau\widehat{T}} | \psi \rangle \overset{(A.8)}{=} \frac{1}{(2\pi\tau)^{N/2}} \int_{\mathbb{R}^N} \mathrm{d}\boldsymbol{y} \, \mathrm{e}^{-\frac{||\boldsymbol{x}-\boldsymbol{y}||^2}{2\tau}} \psi(\boldsymbol{y}) . \tag{2.14}$$

The samples can be understood as sum of Dirac delta distributions (equation (2.4)). Then the relation (2.14) becomes

$$\langle \boldsymbol{x} | \mathrm{e}^{-\tau\widehat{T}} | \psi \rangle \approx \frac{1}{n} \sum_{i=1}^{n} \frac{1}{(2\pi\tau)^{N/2}} \mathrm{e}^{-\frac{||\boldsymbol{x}-\boldsymbol{x}_i||^2}{2\tau}} .$$

Implementation: For each sample $\boldsymbol{x}_i$ we generate random vector $\boldsymbol{a}$ from N-dimensional Gaussian distribution $\rho_{\mathrm{G}}(\boldsymbol{a}; \sqrt{\tau})$

$$\rho_{\mathrm{G}}(\boldsymbol{a}; \sigma) = \frac{1}{(2\pi\sigma^2)^{N/2}} \mathrm{e}^{-\frac{||\boldsymbol{a}||^2}{2\sigma^2}} ,$$

and we add vector $\boldsymbol{a}$ to vector $\boldsymbol{x}_i$ to make new sample $\boldsymbol{x}'_i$

$$\boldsymbol{x}'_i = \boldsymbol{x}_i + \boldsymbol{a} .$$

2.3 Optimization

In our case we need a special type of optimization in one dimension. Usually the optimised function is differentiable, the derivative is easy to evaluate and problem is solved using *Newton's method*. However the derivative of energy with respect to the propagation imaginary time τ is difficult to evaluate. The effective algorithm, when we can only evaluate the function at points, is *golden-section search* [29].

2.3.1 Golden-section search

Let

- $I = (a, b)$ be given open interval,
- $F \in \mathscr{C}^0(I, \mathbb{R})$ be real-valued continuous function with one and only one local minimum

$$(\exists! c \in (a,b))(\exists \delta \in \mathbb{R})(\delta > 0)(\forall y \in P_\delta(c))(F(x) > F(c))\,,$$

where $P_\delta(c)$ is deleted δ-neighbourhood of the point c.

The search for the minimum is based on principle *divide et impera*. In one iteration we want to reduce the interval, where the minimum is located. Let (a_i, b_i) be interval in the i-th iteration and we know 2 values of the function $F(y)$ at endpoints a_i and b_i. The knowledge of the third value of the function does not help to reduce the interval. We need at least 4 values. Let $y_{i,1}$, $y_{i,2}$, $y_{i,3}$, $y_{i,4}$ be 4 points from interval (a_i, b_i)

$$a_i = y_{i,1} < y_{i,2} < y_{i,3} < y_{i,4} = b_i\,. \tag{2.15}$$

Also we would like to recycle values of the function from previous iteration, because it takes long computational time to evaluate one value. We restrict ourselves to proportional division. If we chose for next iteration subinterval $(a_{i+1}, b_{i+1}) = (y_{i,1}, y_{i,3})$, we obtain the following condition

$$\frac{y_{i,3} - y_{i,1}}{y_{i,4} - y_{i,1}} = \frac{y_{i+1,3} - y_{i+1,1}}{y_{i+1,4} - y_{i+1,1}} = \frac{y_{i,2} - y_{i,1}}{y_{i,3} - y_{i,1}}\,. \tag{2.16}$$

If we chose subinterval $(a_{i+1}, b_{i+1}) = (y_{i,2}, y_{i,4})$, the following condition arises

$$\frac{y_{i,4} - y_{i,2}}{y_{i,4} - y_{i,1}} = \frac{y_{i+1,4} - y_{i+1,2}}{y_{i+1,4} - y_{i+1,1}} = \frac{y_{i,4} - y_{i,3}}{y_{i,4} - y_{i,2}}\,. \tag{2.17}$$

It is convenient to introduce ratios Y_j as

$$Y_j = \frac{y_{i,j} - y_{i,1}}{y_{i,4} - y_{i,1}}\,.$$

From definition we get $Y_1 = 0$ and $Y_4 = 1$. Then the system of equations (2.16) and (2.17) in new variables reads

$$Y_3 = \frac{Y_2}{Y_3}\,, \qquad 1 - Y_2 = \frac{1 - Y_3}{1 - Y_2}\,.$$

We get 4 solutions

$$\begin{aligned} Y_2 &= 0\,, & Y_3 &= 0\,;\\ Y_2 &= 1\,, & Y_3 &= 1\,;\\ Y_2 &= -1 - \varphi\,, & Y_3 &= -1 - \varphi\,;\\ Y_2 &= 1 - \varphi\,, & Y_3 &= \varphi\,, \end{aligned}$$

where $\varphi := (\sqrt{5}-1)/2 \approx 0.618$. First three solutions are in conflict with condition (2.15). The only acceptable solution is division og the interval in the golden ratio[18].

Implementation:

1. Let $(a_0, b_0) = (a, b)$ be the initial interval.
2. Divide the interval (a_i, b_i) according to *golden ratio*

$$\begin{aligned} y_{i,0} &= a_i\,, \\ y_{i,0} &= a_i + (1-\varphi)(b_i - a_i)\,, \\ y_{i,0} &= a_i + \varphi(b_i - a_i)\,, \\ y_{i,0} &= b_i\,. \end{aligned}$$

3. If $i = 0$, evaluate function $F(y)$ at all 4 point $y_{0,j}$. If $i > 0$, evaluate function $F(y)$ at 1 new point ($y_{i,2}$ or $y_{i,3}$).
4. If $F(y_{i,2}) < F(y_{i,3})$, then $(a_{i+1}, b_{i+1}) = (y_{i,1}, y_{i,3})$, else $(a_{i+1}, b_{i+1}) = (y_{i,2}, y_{i,4})$.[19]
5. Return to the second step.

The spirit of the golden-section search method is captured in Figure 2.7. Depending on the value of the function at point $y_{i,3}$ we can see choice of new subinterval. For each case there is shown example functions $F_{\mathrm{A}}(y)$ and $F_{\mathrm{B}}(y)$. Golden-section in the next iteration is also shown.

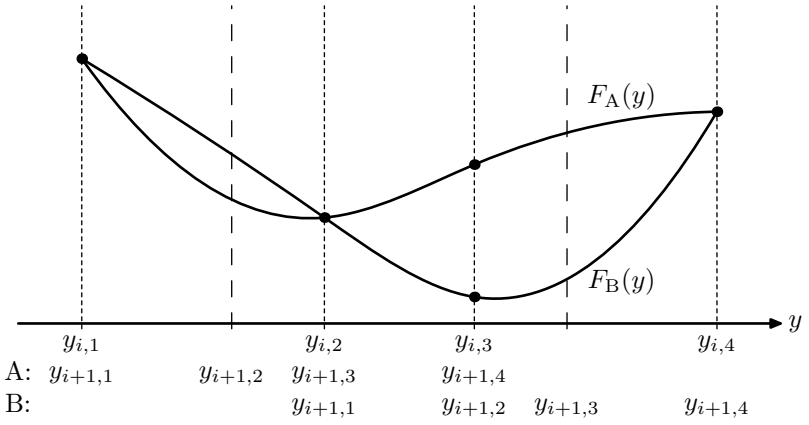

Figure 2.7: One iteration of the golden-section search.

[18] Origin of the name.

[19] In case of equality $F(y_{i,2}) = F(y_{i,3})$, the minimum lies in subinterval $(y_{i,2}, y_{i,3})$. However this practically does not happen and each choice of new interval (a_{i+1}, b_{i+1}) covers the subinterval $(y_{i,2}, y_{i,3})$.

3. Results and Discussion

To show the performance of proposed ITP methods, we choose systems with different difficulties: dimensionality, unbounded potential (Coulomb potential).

3.1 Harmonic Oscillator

The 6-dimensional LHO has well-behaving potential, but the challenge is dimensionality. The Hamiltonian $\widehat{H}$ for 6-dimensional LHO is

$$\widehat{H} = \underbrace{-\frac{1}{2}\Delta_6}_{\widehat{T}} \underbrace{+\frac{1}{2}r^2}_{\widehat{V}},$$

where Δ_6 is 6-dimensional Laplace operator and $r := ||\boldsymbol{x}||$ is norm of position $\boldsymbol{x} \in \mathbb{R}^6$. The operator $\widehat{C}_1$ is

$$\widehat{C}_1 = \boldsymbol{\nabla} V \cdot \boldsymbol{\nabla} V = r^2 .$$

The ground state[1] $\psi_0(\boldsymbol{x})$, energy E_0 and radial distribution function[2] $\rho_0(r)$ are known (more in Appendix A.3)

$$\psi_0(\boldsymbol{x}) = \frac{1}{(2\pi)^3} \mathrm{e}^{-\frac{r^2}{2}}, \qquad E_0 = 3, \qquad \rho_0(r) = \frac{1}{8} r^5 \mathrm{e}^{-\frac{r^2}{2}} .$$

For the initial wave function $\phi_0(\boldsymbol{x})$

$$\phi_0(\boldsymbol{x}) = \frac{1}{(2\pi\sigma^2)^3} \mathrm{e}^{-\frac{||\boldsymbol{x}-\boldsymbol{a_0}||^2}{2\sigma^2}}, \quad \sigma = \frac{6}{5}, \quad \boldsymbol{a_0} = \frac{1}{4}(1,1,1,1,1,1),$$

we evaluated integrals

$$\langle\phi_0|\phi_0\rangle = \frac{1}{(4\pi\sigma^2)^3}, \qquad \langle\phi_0|\widehat{T}|\phi_0\rangle = \frac{3}{2\sigma^2}\frac{1}{(4\pi\sigma^2)^3},$$
$$\langle\phi_0|\widehat{V}|\phi_0\rangle = \left(\frac{3\sigma^2}{3} + \frac{||\boldsymbol{a}_0||^2}{2}\right)\frac{1}{(4\pi\sigma^2)^3},$$

and initial energy

$$\frac{\langle\phi_0|\widehat{H}|\phi_0\rangle}{\langle\phi_0|\phi_0\rangle} = \frac{3}{2\sigma^2} + \frac{3\sigma^2}{2} + \frac{||\boldsymbol{a}_0||^2}{2} \approx 3.389 .$$

To choose optimal τ_O for Method B we generated 5,000,000 samples and calculated integrals $\langle\phi_0|\widehat{J}_m(\tau)|\phi_0\rangle$, $\langle\phi_0|\widehat{K}_m(\tau)|\phi_0\rangle$, $\langle\phi_0|\widehat{V}_m(\tau)|\phi_0\rangle$ (compare with Figure 2.6). The evaluated data are plotted in Figure 3.1. The optimal τ was set $\tau_\mathrm{O} = 1.7$ for approximation $m = 7$.

In bottom plots in Figure 3.1 we check whether and how are calculated integrals $\langle\phi_0|\widehat{J}_7(\tau_\mathrm{O})|\phi_0\rangle$, $\langle\phi_0|\widehat{K}_7(\tau_\mathrm{O})|\phi_0\rangle$, $\langle\phi_0|\widehat{V}_7(\tau_\mathrm{O})|\phi_0\rangle$ and $\langle\phi_0|\widehat{H}_7(\tau_\mathrm{O})|\phi_0\rangle$ biased. As we expected, the positive integrals ($\langle\phi_0|\widehat{J}_7(\tau_\mathrm{O})|\phi_0\rangle$, $\langle\phi_0|\widehat{K}_7(\tau_\mathrm{O})|\phi_0\rangle$) are underestimated and negative integral ($\langle\phi_0|\widehat{V}_7(\tau_\mathrm{O})|\phi_0\rangle$) overestimated. These biases cancel out a little bit in $\langle\phi_0|\widehat{H}_7(\tau_\mathrm{O})|\phi_0\rangle$, but the energy is overestimated. This is no surprise, because we know, that we get exact energy for eigenstates. Also for variational energy it is better to be overestimated.

[1] Mind the different normalization.

[2] One has to remember that the sampled function is $\psi_0(\boldsymbol{x})$ and not the function $|\psi_0(\boldsymbol{x})|^2$.

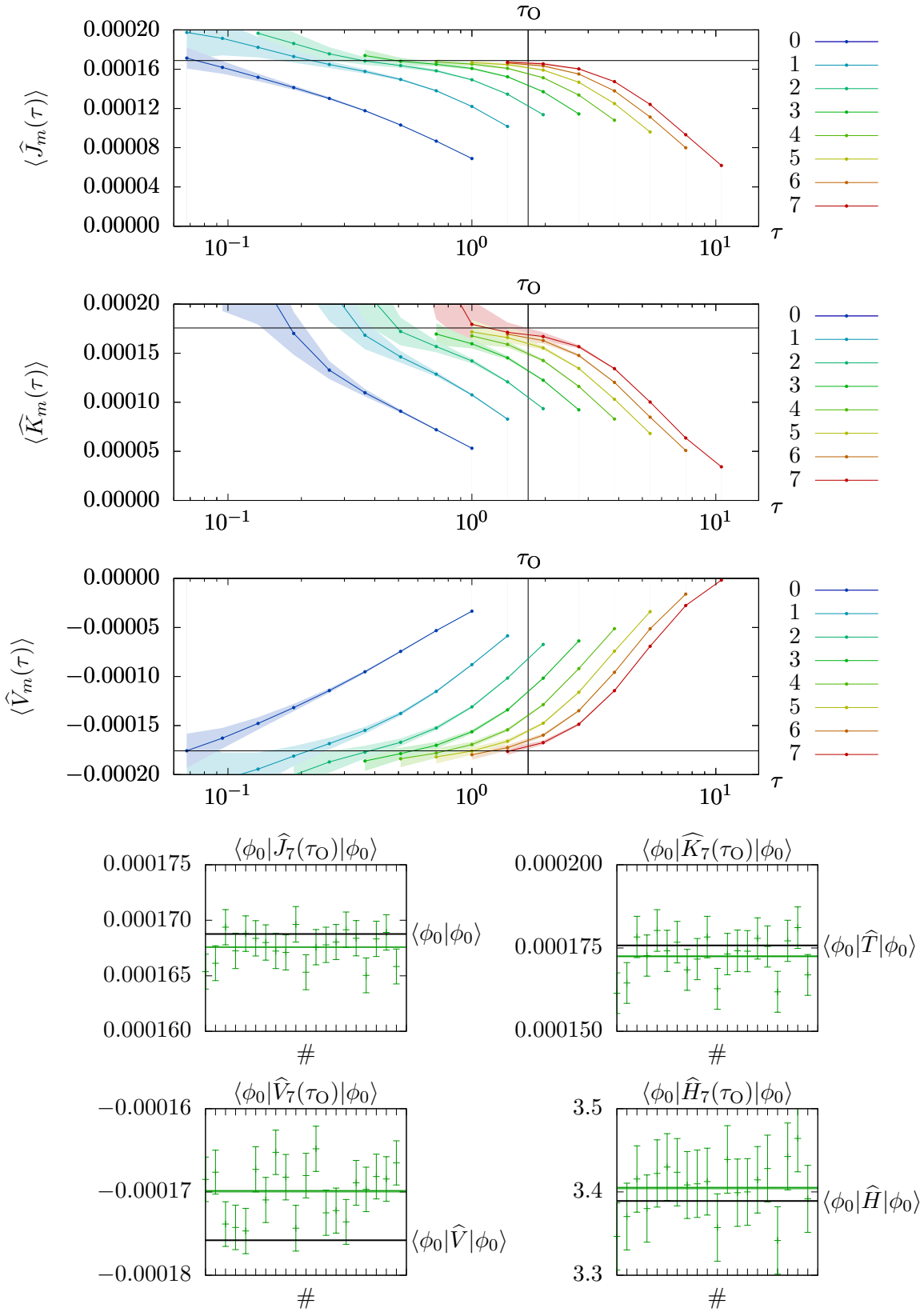

Figure 3.1: The choice of optimal $\tau_O = 1.7$ and the calculation of the norm $\langle \phi_0 | \phi_0 \rangle$, the kinetic energy integral $\langle \phi_0 | \widehat{T} | \phi_0 \rangle$ and the potential energy integral $\langle \phi_0 | \widehat{V} | \phi_0 \rangle$ for 6-dimensional LHO (5,000,000 samples, three upper plots). The chosen τ_O and exact values $\langle \phi_0 | \phi_0 \rangle$, $\langle \phi_0 | \widehat{T} | \phi_0 \rangle$ and $\langle \phi_0 | \widehat{V} | \phi_0 \rangle$ are marked with horizontal and vertical lines. The check for bias for calculated estimators $\langle \phi_0 | \widehat{J}_7(\tau_O) | \phi_0 \rangle$, $\langle \phi_0 | \widehat{K}_7(\tau_O) | \phi_0 \rangle$, $\langle \phi_0 | \widehat{V}_7(\tau_O) | \phi_0 \rangle$ and $\langle \phi_0 | \widehat{H}_7(\tau_O) | \phi_0 \rangle$ for 20 runs (four bottom plots).

The ITP method itself comes next. We sampled initial wave function $\phi_0(\boldsymbol{x})$. In each iteration we applied operator $\widehat{G}_8(\tau)$ on samples of function $\phi_i(\boldsymbol{x})$ (more in section 2.2). We calculated the energy $\langle E\rangle$ using the Method B. Using the golden-section search we optimised the energy $\langle E\rangle$ with respect to parameter τ until the energy difference was within errors of energy. For optimised parameter τ_i we sampled wave function $\phi_{i+1}(\boldsymbol{x})$ for next iteration

$$\phi_{i+1}(\boldsymbol{x}) = \widehat{G}_8(\tau_i)\phi_i(\boldsymbol{x})\,.$$

Along the ITP method we evaluated the averaged energy $\{H\}$ (Method C) and estimated virial-like ratio p (for LHO the precise value for the eigenstate is 1, more in 1.1) as[3]

$$p = \frac{\langle\phi_i|\widehat{V}_7(\tau_{\mathrm{O}})|\phi_i\rangle + \langle E\rangle\langle\phi_i|\widehat{J}_7(\tau_{\mathrm{O}})|\phi_i\rangle}{\langle\phi_i|\widehat{K}_7(\tau_{\mathrm{O}})|\phi_i\rangle}\,.$$

However the integrals in relation are biased, therefore we can expect biased ratio p.

The process of optimization is documented in Figure 3.3. We can observe few interesting behaviour: In one iteration the program rapidly improved the energy $\langle H\rangle$. In two iterations we got to ground state energy within the error. The energy $\langle H\rangle$ never undergoes the ground state energy within the error. The energy $\langle H\rangle$ gives the ground state energy with smaller systematic error compared with the averaged energy $\{H\}$. After first iteration the virial ratio p stops to improve and never reaches the exact value 1 within the error. This in agreement with theory, because virial theorem holds for eigenstates and we are effectively evaluating the ratio p on wave function $\widehat{J}_7(\tau_{\mathrm{O}})^{1/2}|\psi_0\rangle$. Therefore idea of calculating only one of the integrals $\langle\phi_0|\widehat{K}_7(\tau_{\mathrm{O}})|\phi_0\rangle$ or $\langle\phi_0|\widehat{V}_7(\tau_{\mathrm{O}})|\phi_0\rangle$ and estimate the energy using the virial theorem would lead to results with systematic error. The radial distribution function $\rho_{\phi_i}(r)$ improves significantly in the first iteration. In following iterations it is slowly approaching the ground state radial distribution function $\rho_0(r)$. For the 2nd and higher iterations the radial distribution functions $\rho_{\phi_i}(r)$ and the ground state radial distribution function $\rho_0(r)$ are indistinguishable from each other in the plot.

The ground state energy after 5 iterations was calculated as (3.0002 ± 0.0010), which is in good agreement with exact value $E_0 = 3$.

Because the ground state of LHO is known analytically, we can generate samples of the ground state $\psi_0(\boldsymbol{x})$. In Figure 3.2 we check bias of integrals. As expected the first three integrals are biased, but for the energy $\langle\psi_0|\widehat{H}_7(\tau_{\mathrm{O}})|\psi_0\rangle$ the ground state energy E_0 is within the errors (see equation (2.13)).

[3]One has to bear in mind that for ITP method we need to use offset potential $\tilde{V} = V - \langle E\rangle$, but for virial ratio we need homogeneous function.

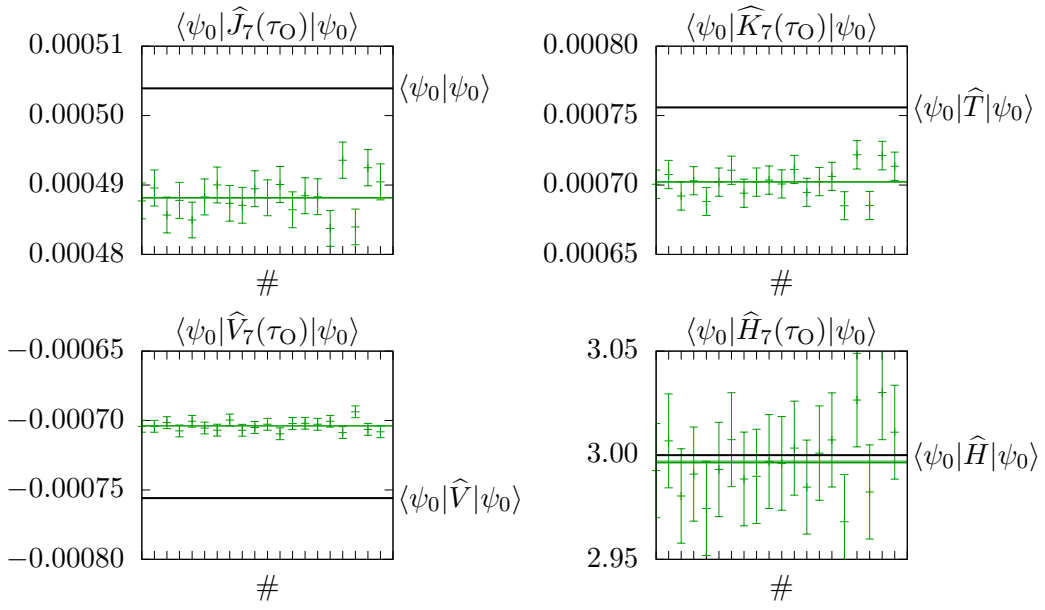

Figure 3.2: The check for bias for estimators $\langle\psi_0|\widehat{J}_7(\tau_O)|\psi_0\rangle$, $\langle\psi_0|\widehat{K}_7(\tau_O)|\psi_0\rangle$, $\langle\psi_0|\widehat{V}_7(\tau_O)|\psi_0\rangle$ and $\langle\psi_0|\widehat{H}_7(\tau_O)|\psi_0\rangle$ for 20 runs.

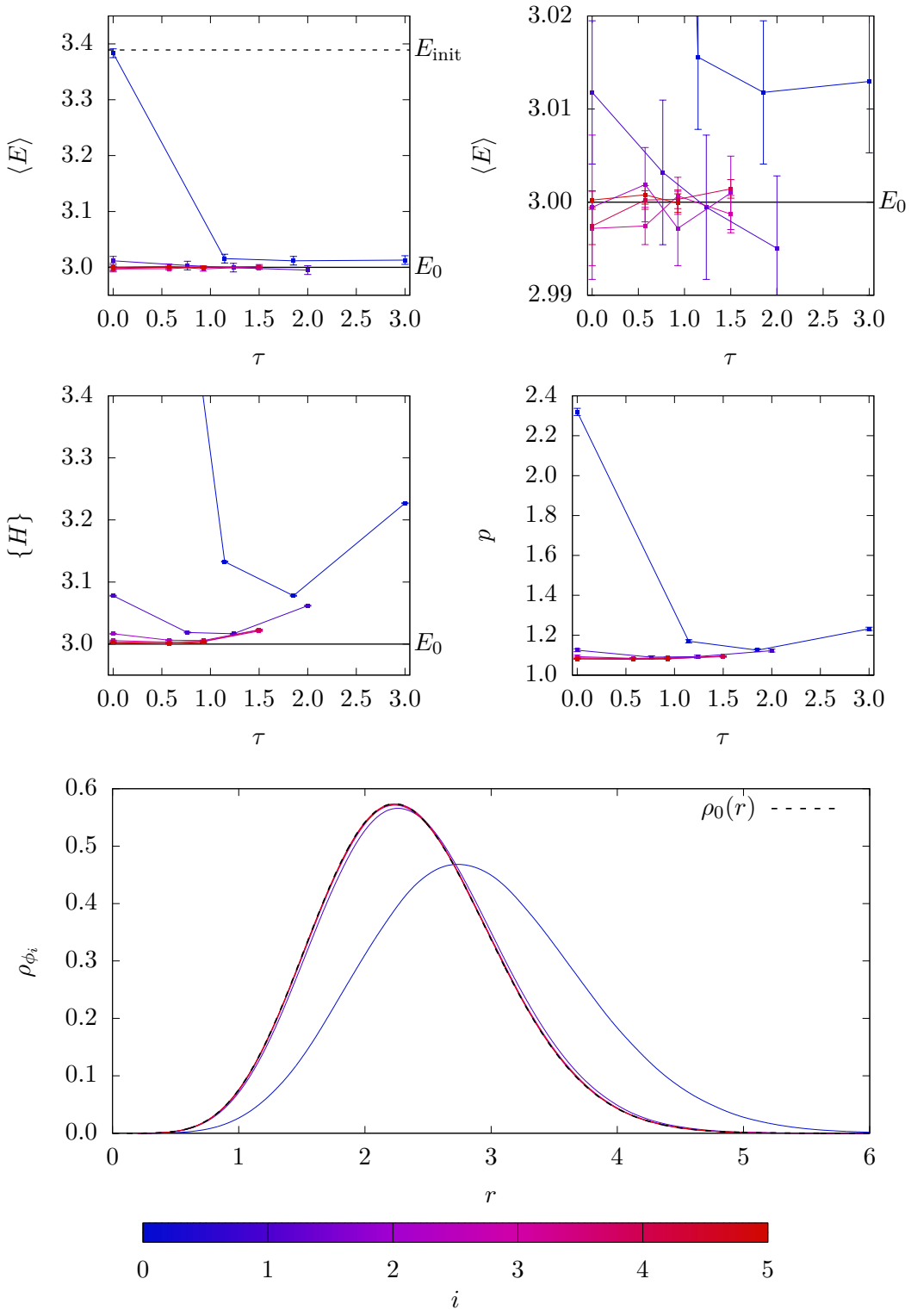

Figure 3.3: The ITP evolution of states $|\phi_{i+1}\rangle = \widehat{G}_8(\tau)|\phi_i\rangle$ in each iteration optimised energy $\langle E \rangle$ with respect to parameter τ (Method B, 2 upper plots). We evaluated along optimation the averaged energy $\{H\}$ (Method C) and the virial ratio p (exact value for any eigenstate is 1) (2 middle plots). The radial distribution function $\rho_{\phi_i}(r)$ after each iteration and the ground state radial distribution function $\rho_0(r)$ (bottom plot).

3.2 Anharmonic Oscillator

The harmonic oscillator is analytically solvable model and good first order approximation for various systems (e.g. molecular vibrations). However to obtain more precise results we need to include into potential higher than quadratic terms. To study performance of ITP method for such case we choose 3-dimensional octic potential with Hamiltonian

$$\widehat{H} = \underbrace{-\frac{1}{2}\Delta_3}_{\widehat{T}} \underbrace{+\sum_{i=1}^{8} \alpha_i r^i}_{\widehat{V}},$$

where Δ_3 is 3-dimensional Laplace operator, $r := ||\boldsymbol{x}||$ distance from the origin and α_i constants. The operator $\widehat{C}_1$ is

$$\widehat{C}_1 = \boldsymbol{\nabla} V \cdot \boldsymbol{\nabla} V = \left(\sum_{i=1}^{8} \alpha_i i r^{i-1} \right)^2 .$$

The coefficient was chosen from [30] as

$$\alpha_1 = -\frac{3}{2\sqrt{2}} \qquad \alpha_2 = \frac{25}{256} - \frac{5}{2\sqrt{2}} \qquad \alpha_3 = \frac{15}{64} - 3\sqrt{2} \qquad \alpha_4 = \frac{29}{64}$$
$$\alpha_5 = 1 \qquad \alpha_6 = 1 \qquad \alpha_7 = 1 \qquad \alpha_8 = 1$$

with known ground state $\psi_0(\boldsymbol{x})$, energy E_0 and radial distribution function $\rho_0(r)$

$$\psi_0(\boldsymbol{x}) = N \mathrm{e}^{-\frac{5}{16\sqrt{2}} r^2 - \frac{1}{4\sqrt{2}} r^3 - \frac{1}{4\sqrt{2}} r^4 - \frac{\sqrt{2}}{5} r^5}, \qquad E_0 = \frac{15}{16\sqrt{2}}, \qquad \rho_0(r) = 4\pi r^2 \psi_0(\boldsymbol{x}),$$

where $N \approx 0.23203$.[4] For the initial wave function $\phi_0(\boldsymbol{x})$

$$\phi_0(\boldsymbol{x}) = \frac{1}{(2\pi\sigma^2)^{3/2}} \mathrm{e}^{-\frac{||\boldsymbol{x}||^2}{2\sigma^2}},$$

we evaluated integrals

$$\langle \phi_0 | \phi_0 \rangle = \frac{1}{(4\pi\sigma^2)^{3/2}}, \qquad \langle \phi_0 | \widehat{T} | \phi_0 \rangle = \frac{3}{4\sigma^2} \frac{1}{(4\pi\sigma^2)^{3/2}},$$
$$\langle \phi_0 | \widehat{V} | \phi_0 \rangle = \frac{1}{(4\pi\sigma^2)^{3/2}} \sum_{i=1}^{8} \frac{2}{\pi^{1/2}} \alpha_i \sigma^i \Gamma\left(\frac{i+3}{2} \right),$$

and for optimal parameter $\sigma = 0.55237$ the initial energy

$$\frac{\langle \phi_0 | \widehat{H} | \phi_0 \rangle}{\langle \phi_0 | \phi_0 \rangle} = \frac{3}{4\sigma^2} + \sum_{i=1}^{8} \frac{2}{\pi^{1/2}} \alpha_i \sigma^i \Gamma\left(\frac{i+3}{2} \right) \approx 1.324 .$$

Following the same procedure we chose optimal parameter $\tau_{\mathrm{O}} = 0.6$ (3 upper plots in Figure 3.4) and checked for biases of calculated variables (4 bottom plots in Figure 3.4). Biases for $\langle \phi_0 | \widehat{J}_7(\tau_{\mathrm{O}}) | \phi_0 \rangle$ and $\langle \phi_0 | \widehat{K}_7(\tau_{\mathrm{O}}) | \phi_0 \rangle$ are same as before. However the values of $\langle \phi_0 | \widehat{V}_7(\tau_{\mathrm{O}}) | \phi_0 \rangle$ and $\langle \phi_0 | \widehat{H}_7(\tau_{\mathrm{O}}) | \phi_0 \rangle$ are underestimated.

Process of ITP method can be seen in Figure 3.5. We observe similar phenomena as before: The energy $\langle H \rangle$ gives results with smaller systematic error than the averaged energy $\{H\}$. The wave function rapidly converges to ground state and after few iterations the radial distribution function of generated samples $\rho_{\varphi_i}(r)$ and the ground state radial distribution function $\rho_0(r)$ overlap.

The ground state energy after 5 iterations was estimated as (0.6631 ± 0.0012). This in agreement with exact value $E_0 \approx 0.6629$.

[4] Evaluated numerically with the program *Mathematica* [15].

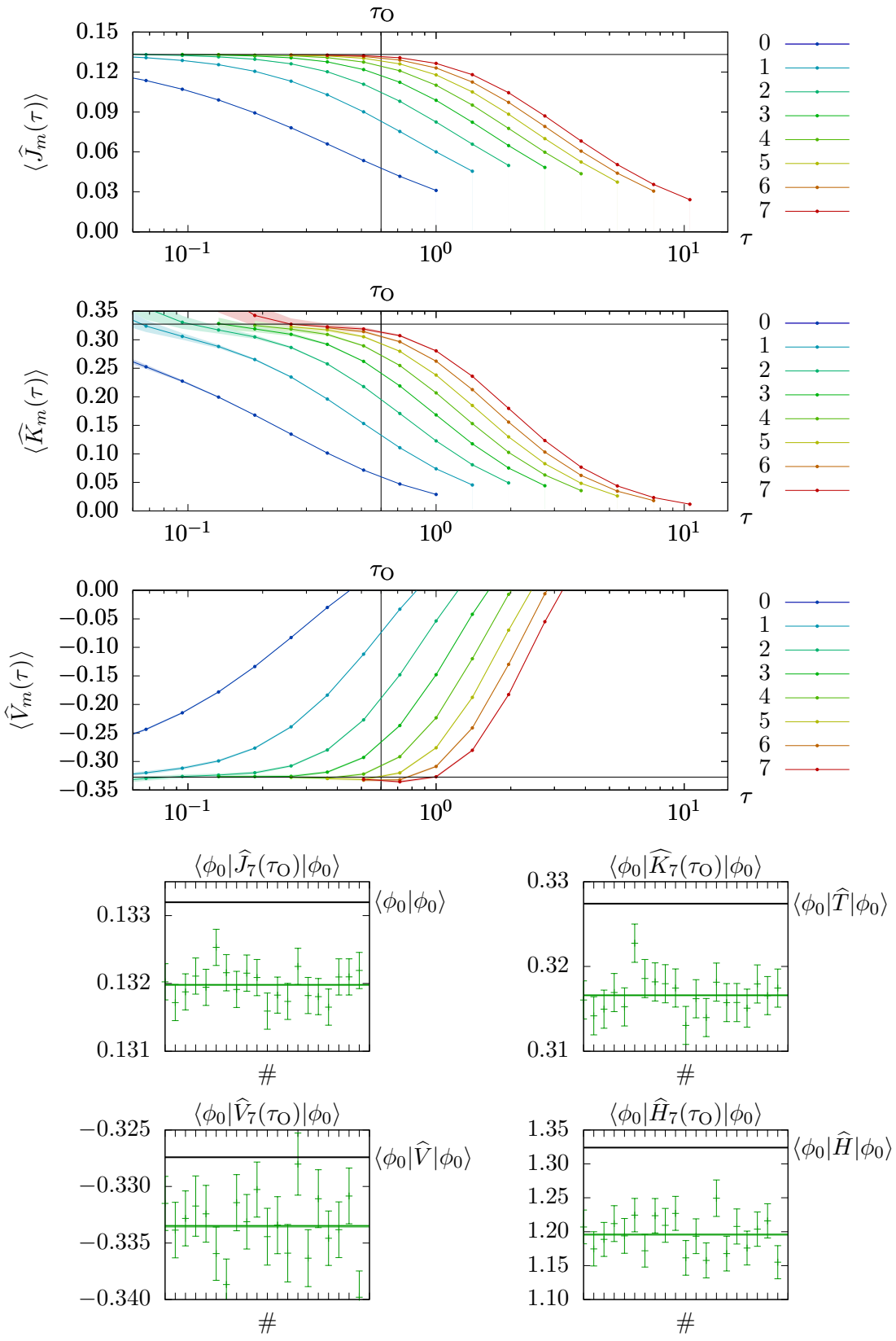

Figure 3.4: The choice of optimal $\tau_O = 0.6$ for 3-dimensional octic potential (5,000,000 samples) with marked precise values $\langle \phi_0 | \phi_0 \rangle$, $\langle \phi_0 | \widehat{T} | \phi_0 \rangle$ and $\langle \phi_0 | \widehat{V} | \phi_0 \rangle$ (three upper plots). The check for bias for calculated estimators $\langle \phi_0 | \widehat{J}_7(\tau_O) | \phi_0 \rangle$, $\langle \phi_0 | \widehat{K}_7(\tau_O) | \phi_0 \rangle$, $\langle \phi_0 | \widehat{V}_7(\tau_O) | \phi_0 \rangle$ and $\langle \phi_0 | \widehat{H}_7(\tau_O) | \phi_0 \rangle$ for 20 runs (four bottom plots).

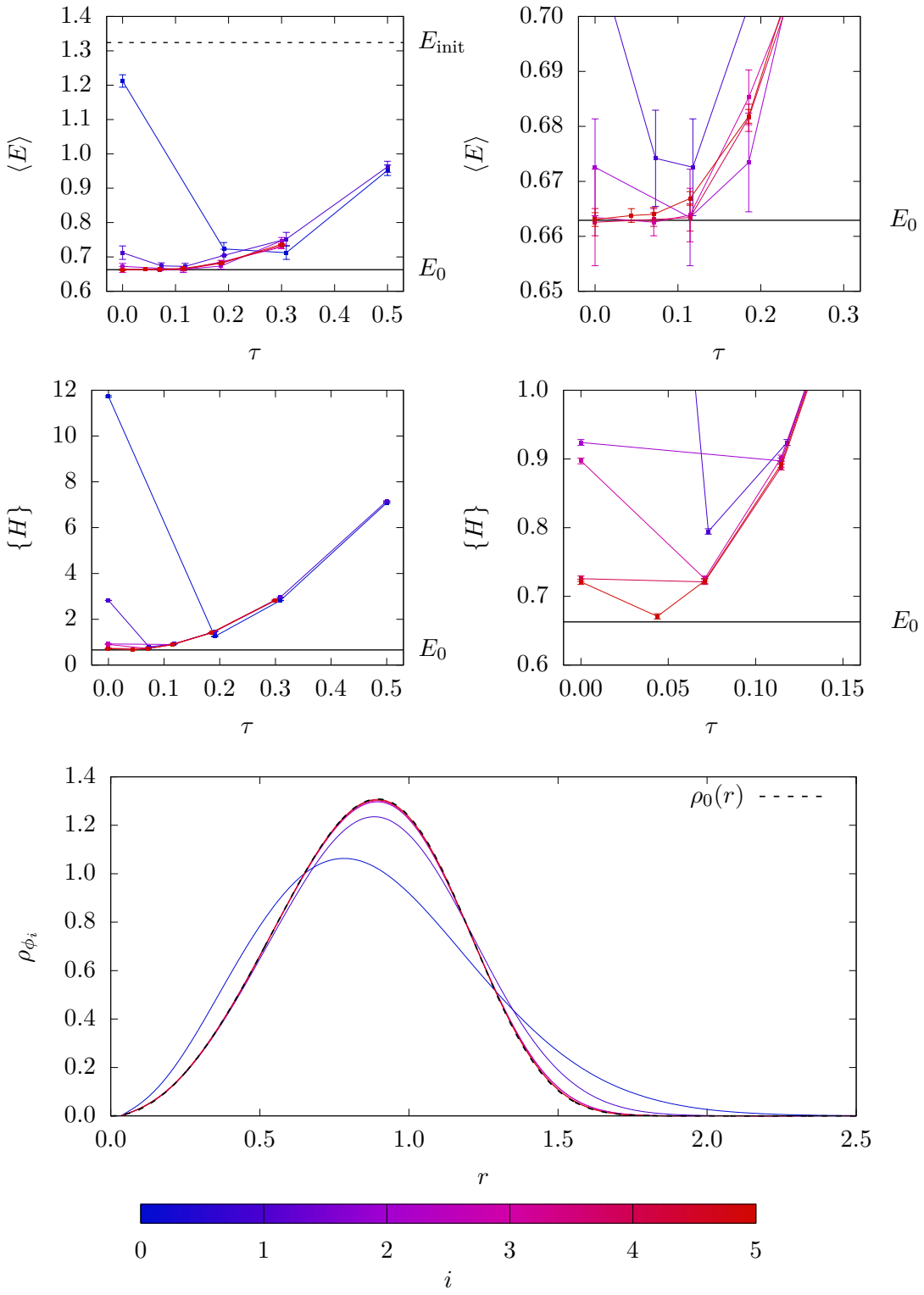

Figure 3.5: The ITP evolution of states $|\phi_{i+1}\rangle = \widehat{G}_8(\tau)|\phi_i\rangle$ in each iteration optimised with respect to energy $\langle E \rangle$ (Method B, 2 upper plots). We evaluated along optimation the averaged energy $\{H\}$ (Method C) (2 middle plots). The radial distribution function $\rho_{\phi_i}(r)$ after each iteration and the ground state radial distribution function $\rho_0(r)$ (bottom plot).

3.3 Hydrogen Atom

Compared to the example of the 6-dimensional LHO the hydrogen atom has lower dimensionality, but on the other hand comes with the difficulties caused by the Coulomb potential. The singularity in potential makes the 4th order approximant $\widehat{G}_8(\tau)$ the only reasonably usable operator for ITP method. The divergent part in $\mathrm{e}^{-\tau\widehat{V}}$ has to be suppressed by stronger zero in $\mathrm{e}^{-\tau^3\widehat{C}_1}$. Every operator $\mathrm{e}^{-\tau\widehat{V}}$ has to have neighbouring operator $\mathrm{e}^{-\tau\widehat{C}_1}$ and the operators $\mathrm{e}^{-\tau\widehat{V}}$ and $\mathrm{e}^{-\tau\widehat{C}_1}$ should not be the last one applied.

The Hamiltonian $\widehat{H}$ for hydrogen atom in atomic units is

$$\widehat{H} = \underbrace{-\frac{1}{2}\Delta_3}_{\widehat{T}} \underbrace{-\frac{1}{r}}_{\widehat{V}},$$

where Δ_3 is 3-dimensional Laplace operator and $r := ||\boldsymbol{x}||$ distance from the origin. The operator $\widehat{C}_1$ is (compare with Table 1.1)

$$\widehat{C}_1 = \boldsymbol{\nabla} V \cdot \boldsymbol{\nabla} V = \frac{1}{r^4}.$$

The ground state $\psi_0(\boldsymbol{x})$, energy E_0 and radial distribution function $\rho_0(r)$ are known (more see Appendix A.3)

$$\psi_0(\boldsymbol{x}) = \frac{1}{8\pi}\mathrm{e}^{-r}, \qquad E_0 = -\frac{1}{2}, \qquad \rho_0(r) = \frac{1}{2}r^2\mathrm{e}^{-r}.$$

For the initial wave function $\phi_0(\boldsymbol{x})$

$$\phi_0(\boldsymbol{x}) = \frac{1}{(2\pi\sigma^2)^{3/2}}\mathrm{e}^{-\frac{||\boldsymbol{x}-\boldsymbol{a_0}||^2}{2\sigma^2}}, \quad \sigma = \frac{6}{5}, \quad \boldsymbol{a_0} = \frac{1}{4}(1,1,1),$$

we evaluated integrals[5]

$$\langle\phi_0|\phi_0\rangle = \frac{1}{(4\pi\sigma^2)^{3/2}}, \quad \langle\phi_0|\widehat{T}|\phi_0\rangle = \frac{3}{4\sigma^2}\frac{1}{(4\pi\sigma^2)^{3/2}}, \quad \langle\phi_0|\widehat{V}|\phi_0\rangle \approx -0.0117055,$$

and the initial energy

$$\frac{\langle\phi_0|\widehat{H}|\phi_0\rangle}{\langle\phi_0|\phi_0\rangle} \approx -0.3802.$$

Following the same procedure as before we continue with the next step: search for the optimal τ_{O}. We generated 5,000,000 samples and estimated integrals $\langle\phi_0|\widehat{J}_m(\tau)|\phi_0\rangle$, $\langle\phi_0|\widehat{K}_m(\tau)|\phi_0\rangle$, $\langle\phi_0|\widehat{V}_m(\tau)|\phi_0\rangle$ (Figure 3.6). The optimal τ was chosen $\tau_{\mathrm{O}} = 2.3$ for approximation $m = 7$. In bottom plots we check for biases of estimators $\langle\phi_0|\widehat{J}_7(\tau_{\mathrm{O}})|\phi_0\rangle$, $\langle\phi_0|\widehat{K}_7(\tau_{\mathrm{O}})|\phi_0\rangle$, $\langle\phi_0|\widehat{V}_7(\tau_{\mathrm{O}})|\phi_0\rangle$ and $\langle\phi_0|\widehat{H}_7(\tau_{\mathrm{O}})|\phi_0\rangle$. We observe same biases as in case of 6-dimensional LHO.

In Figure 3.6 we can see the process of optimization. We observe few effects of unbounded Coulomb potential: The convergence is very slow and the optimal parameter τ in every iteration is shorter and shorter. The averaged energy $\{H\}$ starts at more negative energies[6] than E_0 and then the values overshoot the energy E_0 and converge to value ≈ -0.497. The virial ratio p stops improve and never reaches the exact value -2 (similar behaviour as in case of 6-dimensional linear oscillator). The radial distribution function $\rho_{\phi_i}(r)$ slowly approaches the ground state radial distribution function $\rho_0(r)$. Even though the calculated energy is equal to E_0 within the error, there is visible difference between radial distributions functions $\rho_{\phi_i}(r)$ and $\rho_0(r)$.

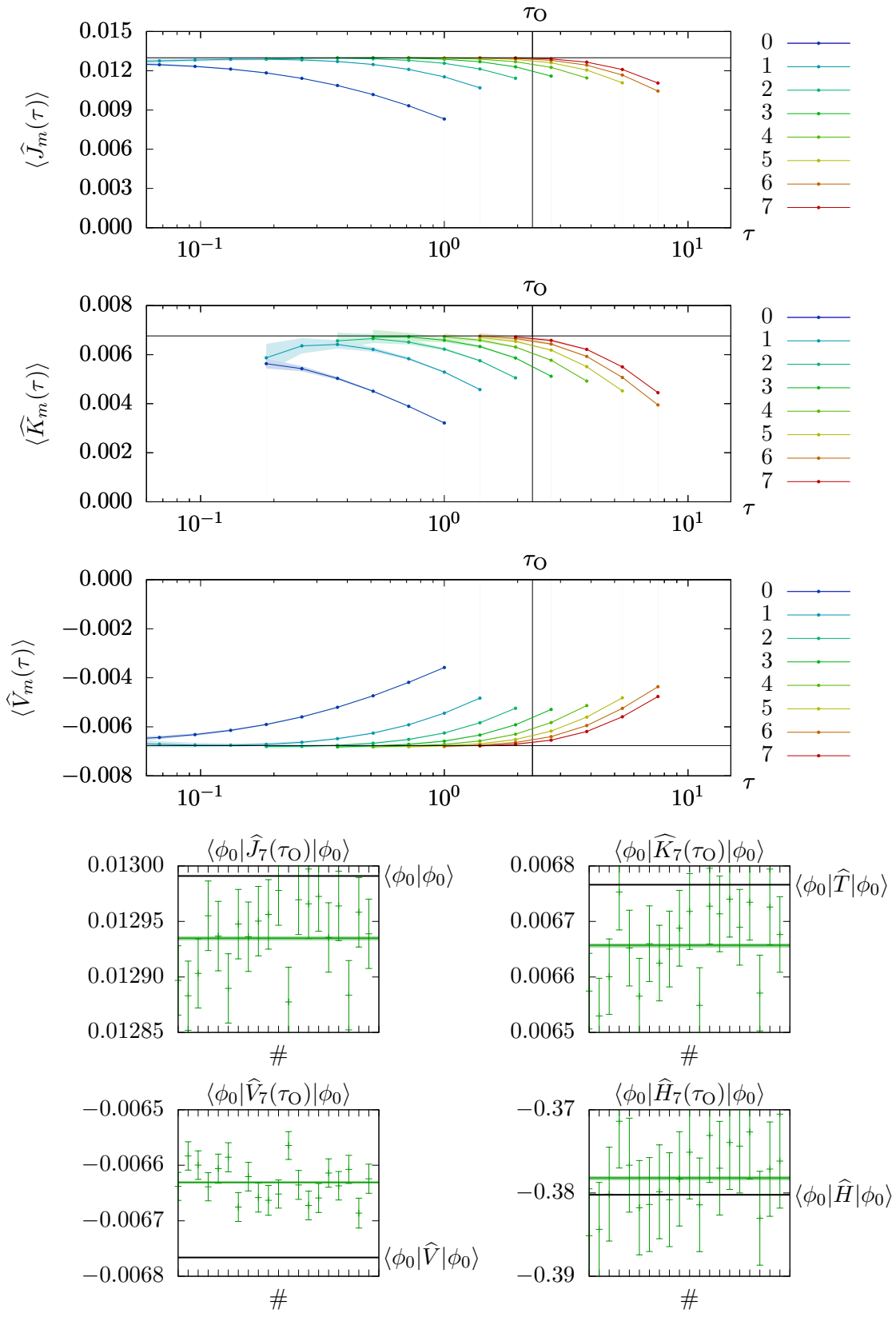

Figure 3.6: Optimization of τ and calculation of the integrals $\langle \phi_0 | \phi_0 \rangle$, $\langle \phi_0 | \widehat{T} | \phi_0 \rangle$ and $\langle \phi_0 | \widehat{V} | \phi_0 \rangle$ for hydrogen atom (5,000,000 samples, three upper plots). The chosen $\tau_O = 2.3$ and exact values $\langle \phi_0 | \phi_0 \rangle$, $\langle \phi_0 | \widehat{T} | \phi_0 \rangle$ and $\langle \phi_0 | \widehat{V} | \phi_0 \rangle$ are marked with lines. The check for biases of estimators $\langle \phi_0 | \widehat{J}_7(\tau_O) | \phi_0 \rangle$, $\langle \phi_0 | \widehat{K}_7(\tau_O) | \phi_0 \rangle$, $\langle \phi_0 | \widehat{V}_7(\tau_O) | \phi_0 \rangle$ and $\langle \phi_0 | \widehat{H}_7(\tau_O) | \phi_0 \rangle$ for 20 runs (four bottom plots).

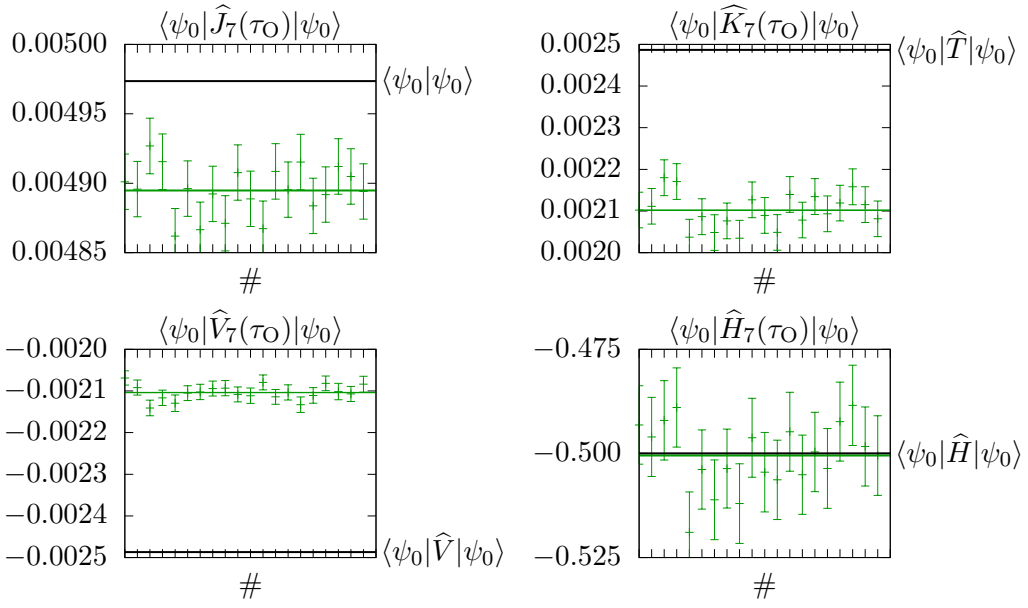

Figure 3.7: The check for biases of estimators $\langle\psi_0|\widehat{J}_7(\tau_O)|\psi_0\rangle$, $\langle\psi_0|\widehat{K}_7(\tau_O)|\psi_0\rangle$, $\langle\psi_0|\widehat{V}_7(\tau_O)|\psi_0\rangle$ and $\langle\psi_0|\widehat{H}_7(\tau_O)|\psi_0\rangle$ for 20 runs.

The ground state energy after 42 iterations was estimated as (-0.50005 ± 0.0007), which is in good agreement with exact value $E_0 = -0.5$.

For the hydrogen atom we can generate samples of the ground state $\psi_0(\boldsymbol{x})$. In Figure 3.7 we check for biases of integrals for the ground state. Same as for 6-dimensional linear oscillator first three integrals are biased and the energy $\langle\psi_0|\widehat{H}_7(\tau_O)|\psi_0\rangle$ is equal to E_0 within the error. This is in agreement with equation (2.13).

[5]The potential integral was evaluated numerically using the program *Mathematica* [15].

[6]This is in agreement with fact, that the averaged energy is bound by minimum of the potential: $-\infty$.

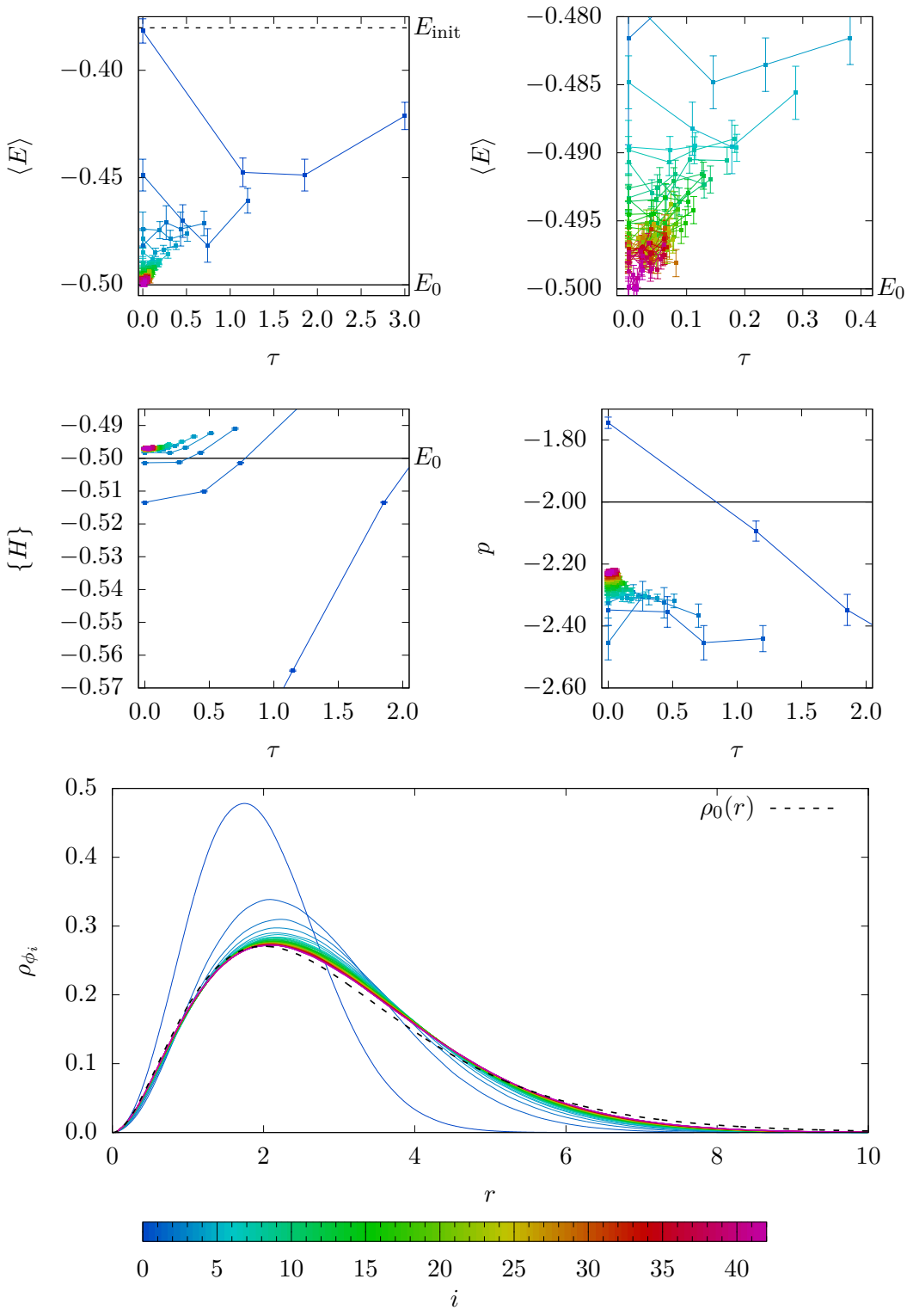

Figure 3.8: The ITP evolution of states $|\phi_{i+1}\rangle = \widehat{G}_8(\tau)|\phi_i\rangle$ in each iteration optimised with respect to energy $\langle E \rangle$ (Method B, 2 upper plots). We evaluated along optimation the averaged energy $\{H\}$ (Method C) and the virial ratio p (for any eigenstate is equal to -2) (2 middle plots). The radial distribution function $\rho_{\phi_i}(r)$ after each iteration and the ground state radial distribution function $\rho_0(r)$ (bottom plot).

Conclusions

In conclusion we would like to summerise achieved results. At first we computed approximants of the imaginary time propagation operator for different schemes and compared results with literature. To compare convergence of different approximants we simulated ITP method on 1D grid for linear harmonic potential and double-well potential. As expected higher order approximants showed quicker convergence.

We developed few method for energy calculation. The Method A showed that the first order correction strongly improves results. However worse time complexity $\sim n^2$ compared with other methods condemned the Method A to failure. The Method B provide more rigorous approach to energy calculation and the higher order methods provide lower error. Computed results are consistent with theoretical values. For ground state the Method B returns ground state energy. Also we can expect the calculated energy to be bounded by ground state energy. The Method C also returns correct energy for ground state, but is bounded by minimum of potential. We showed that the Method C is limit case of the Method B.

For potentials without singularities (6-dimensional harmonic oscillator and anharmonic oscillator) we observe quick convergence to ground state in few iteration for given error. Likewise higher dimensionality does not cause issues. The Method B provides more accurate results than the Method C. For singular potential (Coulomb potential) the ITP methods based on simpler VT-schemes are divergent and cannot be implemented. However the scheme $TVCTVCT$ can be used and is executable. Even though the convergence is slower, it can be improved by standard techniques for variance reduction in Monte Carlo methods [31].

We can conclude that this method comes with some difficulties, but it converges to ground state and can be easily implemented for massive parallel computations.

A. Appendices

A.1 The Matrix Elements of the Operator $\mathrm{e}^{-z\widehat{T}}$

In this thesis we often work with the operator $\mathrm{e}^{-z\widehat{T}}$, therefore we would like to explore its properties: well-definedness, analyticity and evaluation of the spatial matrix elements.

The subject of our interest is N-dimensional kinetic energy $\widehat{T} = \frac{1}{2}\widehat{\boldsymbol{p}}\cdot\widehat{\boldsymbol{p}} = -\frac{1}{2}\Delta_N$ and in general complex constant $z \in \mathbb{C}$. In general, if eigenvectors $|a\rangle$ of Hermitian operator $\widehat{A}$ form orthogonal basis, we can additionally define operator $f(\widehat{A})$ on eigenvectors $|a\rangle$ and in formalism of spectral decomposition define operator $f(\widehat{A})$ as follows[1]

$$\begin{aligned}\widehat{A}|a\rangle = a|a\rangle \implies f(\widehat{A})|a\rangle = f(a)|a\rangle\,,\\ \widehat{A} = \sum\!\!\!\!\!\!\int_a \mathrm{d}a\, a|a\rangle\langle a| \implies f(\widehat{A}) = \sum\!\!\!\!\!\!\int_a \mathrm{d}a\, f(a)|a\rangle\langle a|\,.\end{aligned}$$

Similarly, the operator $\mathrm{e}^{-z\widehat{T}}$ is defined at improper eigenvectors $|\boldsymbol{p}\rangle$ of momentum operator $\widehat{\boldsymbol{p}}$ as[2]

$$\widehat{\boldsymbol{p}}|\boldsymbol{p}\rangle = \boldsymbol{p}|\boldsymbol{p}\rangle \implies \mathrm{e}^{-z\widehat{T}}|\boldsymbol{p}\rangle = \mathrm{e}^{-z\frac{p^2}{2}}|\boldsymbol{p}\rangle\,. \tag{A.1}$$

The momentum matrix elements $\langle\boldsymbol{p}'|\mathrm{e}^{-z\widehat{T}}|\boldsymbol{p}\rangle$ are well-defined for any complex constant z

$$\langle\boldsymbol{p}'|\mathrm{e}^{-z\widehat{T}}|\boldsymbol{p}\rangle = \mathrm{e}^{-z\frac{p^2}{2}}\langle\boldsymbol{p}'|\boldsymbol{p}\rangle = \mathrm{e}^{-z\frac{p^2}{2}}\delta_N(\boldsymbol{p}'-\boldsymbol{p})\,,$$

where $\delta_N(\cdot)$ is N-dimensional Dirac delta distribution.

For the spatial matrix elements $\langle\boldsymbol{x}'|\mathrm{e}^{-z\widehat{T}}|\boldsymbol{x}\rangle$ it is more complicated. The spectral decomposition of the unit operator $\widehat{1}$ in terms of eigenvectors $|\boldsymbol{p}\rangle$ leads to

$$\begin{aligned}\langle\boldsymbol{x}'|\mathrm{e}^{-z\widehat{T}}|\boldsymbol{x}\rangle &= \langle\boldsymbol{x}'|\mathrm{e}^{-z\widehat{T}}\widehat{1}|\boldsymbol{x}\rangle = \int_{\mathbb{R}^N}\mathrm{d}\boldsymbol{p}\,\langle\boldsymbol{x}'|\mathrm{e}^{-z\widehat{T}}|\boldsymbol{p}\rangle\langle\boldsymbol{p}|\boldsymbol{x}\rangle \overset{(A.1)}{=} \int_{\mathbb{R}^N}\mathrm{d}\boldsymbol{p}\,\mathrm{e}^{-z\frac{p^2}{2}}\langle\boldsymbol{x}'|\boldsymbol{p}\rangle\langle\boldsymbol{p}|\boldsymbol{x}\rangle\\ &\overset{(1.3)}{=} \int_{\mathbb{R}^N}\mathrm{d}\boldsymbol{p}\,\frac{\mathrm{e}^{-z\frac{p^2}{2}}}{(2\pi)^N}\mathrm{e}^{i\boldsymbol{p}\cdot\Delta\boldsymbol{x}} \overset{(\heartsuit)}{=} \left(\int_{-\infty}^{+\infty}\mathrm{d}p_1\,\frac{\mathrm{e}^{-z\frac{p_1^2}{2}+ip_1\Delta x_1}}{2\pi}\right)\cdots\left(\int_{-\infty}^{+\infty}\mathrm{d}p_N\,\frac{\mathrm{e}^{-z\frac{p_N^2}{2}+ip_N\Delta x_N}}{2\pi}\right),\end{aligned}$$

where $\Delta\boldsymbol{x} := \boldsymbol{x}' - \boldsymbol{x}$. The step $(\heartsuit)$ is justified if each of the one-dimensional integrals is convergent in absolute value (*Fubini's theorem*).[3,4] Each one-dimensional integral is

[1] Only necessary condition for function $f(\cdot)$ is to be defined at eigenvalues.

[2] The symbol p^2 denotes $p^2 = \boldsymbol{p}\cdot\boldsymbol{p}$.

[3] *Fubini's theorem* (sometimes called *the Fubini-Tonelli theorem.*) Let

- $(X, \mathcal{M}_1, \mu_1)$ and $(Y, \mathcal{M}_2, \mu_2)$ be σ-finite measure spaces (this implies there is unique product measure for measure space $(X\times Y, \mathcal{M}_1\times\mathcal{M}_2, \mu)$),
- $f : \mathcal{M}_1\times\mathcal{M}_2 \to \mathbb{R}$ be measurable function,

and if any of three following integrals is finite

$$\int_X \mathrm{d}\mu_1\left(\int_Y \mathrm{d}\mu_2|f(x,y)|\right), \qquad \int_Y \mathrm{d}\mu_2\left(\int_X \mathrm{d}\mu_1|f(x,y)|\right), \qquad \int_{X\times Y}\mathrm{d}\mu|f(x,y)|\,,$$

then

$$\int_X \mathrm{d}\mu_1\left(\int_Y \mathrm{d}\mu_2 f(x,y)\right) = \int_Y \mathrm{d}\mu_2\left(\int_X \mathrm{d}\mu_1 f(x,y)\right) = \int_{X\times Y}\mathrm{d}\mu f(x,y)\,.$$

[4] To be clear and mathematically rigorous: in our case the measures μ_1, μ_2 and μ are the Lebesgue measures λ (which are σ-finite), the integrated function $f(\boldsymbol{x})$ is complex-valued function (not real-valued) and we should deal individually with integrals of real $f_{\mathrm{Re}}(\boldsymbol{x})$ and imaginary part $f_{\mathrm{Im}}(\boldsymbol{x})$,

convergent in absolute value for $\mathrm{Re}(z) > 0$

$$\int_{-\infty}^{+\infty} \mathrm{d}p \left| \frac{\mathrm{e}^{-z\frac{p^2}{2}+ip\Delta x}}{2\pi} \right| = \frac{1}{2\pi} \int_{-\infty}^{+\infty} \mathrm{d}p\, \mathrm{e}^{-\mathrm{Re}(z)\frac{p^2}{2}} \overset{\mathrm{Re}(z)>0}{=\!=\!=} \frac{1}{\sqrt{2\pi \mathrm{Re}(z)}} < +\infty\,. \tag{A.2}$$

For $\mathrm{Re}(z) \leq 0$ the integral (A.2) does not fulfil necessary condition for convergence: If the limit $\lim\limits_{p\to\pm\infty} f(p)$ exists, it has to be zero.[5]

$$\lim_{p\to\pm\infty} \mathrm{e}^{-\mathrm{Re}(z)\frac{p^2}{2}} = \begin{cases} 0 & \text{if } \mathrm{Re}(z) > 0; \\ 1 & \text{if } \mathrm{Re}(z) = 0; \\ +\infty & \text{if } \mathrm{Re}(z) < 0. \end{cases}$$

We will evaluate the one-dimensional integral by using basic tool of complex analysis: *Cauchy's integral theorem*[6]. First we will choose even part of integrated function (the odd one will cancel out) and replace with twice as big integral from 0 to $+\infty$ as follows

$$\frac{1}{2\pi} \int_{-\infty}^{+\infty} \mathrm{d}p\, \mathrm{e}^{-z\frac{p^2}{2}+ip\Delta x} = \frac{1}{2\pi} \int_{0}^{+\infty} \mathrm{d}p \underbrace{\mathrm{e}^{-z\frac{p^2}{2}} (\mathrm{e}^{ip\Delta x} + \mathrm{e}^{-ip\Delta x})}_{f_1(p)}\,. \tag{A.4}$$

Let $R > 0$ and choose closed contour γ as can be seen in Figure A.1. The complex constant $z = |z|\mathrm{e}^{i\varphi}$ has phase $\varphi \in (-\pi, +\pi\rangle$. Motivation behind this contour is to choose line γ_3 passing through the origin so, that constant in front of quadratic term in exponent will be purely real. This corresponds to substitution $p \to p\mathrm{e}^{-i\frac{\varphi}{2}}$. Construction of the line is shown in Figure A.1. Now it is useful to look at Cauchy integral of function $f_1(p)$ over the contour γ (function $f_1(p)$ is analytic in whole complex plane):

$$\int_0^R \mathrm{d}p\, f_1(p) + \int_{\gamma_2} \mathrm{d}p\, f_1(p) + \int_{\gamma_3} \mathrm{d}p\, f_1(p) = \oint_\gamma \mathrm{d}p\, f_1(p) \overset{(A.3)}{=} 0\,. \tag{A.5}$$

---

but convergent integral in absolute value implies convergent real and imaginary part of integral, thus convergent integral of function $f(\boldsymbol{x})$.

$$+\infty > \int_X \mathrm{d}\boldsymbol{x} |f(\boldsymbol{x})| \Longrightarrow \left\{ \begin{array}{l} +\infty > \int_X \mathrm{d}\boldsymbol{x} |f_{\mathrm{Re}}(\boldsymbol{x})| \implies +\infty > \left| \int_X \mathrm{d}\boldsymbol{x} f_{\mathrm{Re}}(\boldsymbol{x}) \right| \\ +\infty > \int_X \mathrm{d}\boldsymbol{x} |f_{\mathrm{Im}}(\boldsymbol{x})| \implies +\infty > \left| \int_X \mathrm{d}\boldsymbol{x} f_{\mathrm{Im}}(\boldsymbol{x}) \right| \end{array} \right\} \Longrightarrow +\infty > \left| \int_X \mathrm{d}\boldsymbol{x} f(\boldsymbol{x}) \right|\,.$$

[5]
$$\left(+\infty > \left| \int_{-\infty}^{+\infty} \mathrm{d}p\, f(p) \right| \right) \wedge \left(\exists \lim_{p\to\pm\infty} f(p) \right) \implies \left(\lim_{p\to\pm\infty} f(p) = 0 \right)$$

[6] *Cauchy's integral theorem.* Let

- $\Omega \subset \mathbb{C}$ be simply connected[7]open subset of the complex plane,
- $f(p)$ be analytic function on Ω,
- γ be closed path in Ω,

then

$$\oint_\gamma \mathrm{d}p\, f(p) = 0\,. \tag{A.3}$$

[7]The set is simply connected if 2 conditions are fulfilled:
1. Every two points of the set can be connected with continuous path from this set.
2. Every path between two fixed points can be continuously transformed into any other path between same two points.

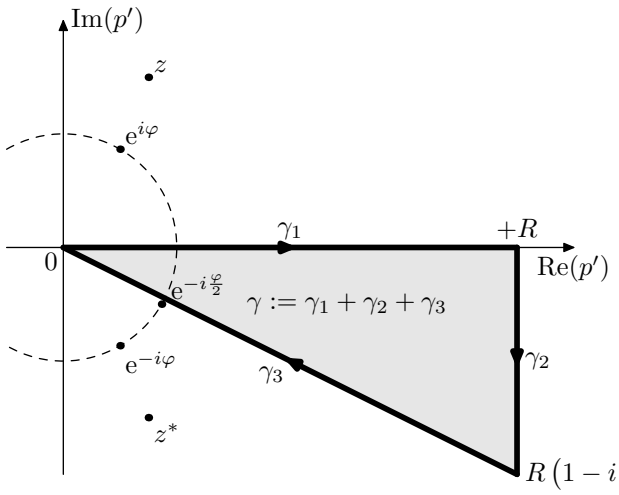

Figure A.1: The contour of integration γ in complex p-plane.

We are interested in the limit $R \to +\infty$. For $\varphi \in (-\frac{\pi}{2}, +\frac{\pi}{2})$ the integral over the contour γ_2 tends to zero in the limit.

$$\begin{aligned}
\lim_{R\to+\infty}\left|\int_{\gamma_2} \mathrm{d}p\, f_1(p)\right| &\le \lim_{R\to+\infty}\int_R^{R\left(1-i\tan\frac{\varphi}{2}\right)} \mathrm{d}p\, \left|\mathrm{e}^{-z\frac{p^2}{2}}\left(\mathrm{e}^{ip\Delta x}+\mathrm{e}^{-ip\Delta x}\right)\right| \\
&\overset{q=\frac{p-R}{iR}}{\le} \lim_{R\to+\infty}\int_0^{\tan\frac{\varphi}{2}} \mathrm{d}q\, R\left|\mathrm{e}^{-z\frac{R^2}{2}(1-iq)^2}\right|\left|\mathrm{e}^{iR\Delta x(1-iq)}+\mathrm{e}^{-iR\Delta x(1-iq)}\right| \\
&\le \lim_{R\to+\infty}\int_0^{\tan\frac{\varphi}{2}} \mathrm{d}q\, R\left|\mathrm{e}^{-|z|\frac{R^2}{2}(\cos\varphi+i\sin\varphi)(1-iq)^2}\right|\left(\mathrm{e}^{R\Delta xq}+\mathrm{e}^{-R\Delta xq}\right) \\
&= \lim_{R\to+\infty}\int_0^{\tan\frac{\varphi}{2}} \mathrm{d}q\, R\mathrm{e}^{-|z|\frac{R^2}{2}\left[\cos\varphi(1-q^2)+2q\sin\varphi\right]}\left(\mathrm{e}^{R\Delta xq}+\mathrm{e}^{-R\Delta xq}\right) \\
&\le \lim_{R\to+\infty}\left|\tan\frac{\varphi}{2}\right| R \max_{q\in\left\langle 0,\tan\frac{\varphi}{2}\right\rangle}\left\{\mathrm{e}^{-|z|\frac{R^2}{2}\left[\cos\varphi(1-q^2)+2q\sin\varphi\right]}\left(\mathrm{e}^{R\Delta xq}+\mathrm{e}^{-R\Delta xq}\right)\right\} \\
&\le \lim_{R\to+\infty}\left|\tan\frac{\varphi}{2}\right| R\mathrm{e}^{-|z|\frac{R^2}{2}\cos\varphi}\left(1+\mathrm{e}^{R\Delta x\left|\tan\frac{\varphi}{2}\right|}\right) \overset{\varphi\in\left(-\frac{\pi}{2},+\frac{\pi}{2}\right)}{=\!=\!=} 0
\end{aligned}$$

Also for $\varphi = \pm\frac{\pi}{2}$ and $|z| > 0$.

$$\begin{aligned}
&\lim_{R\to+\infty}\left|\int_{\gamma_2} \mathrm{d}p\, f_1(p)\right| \overset{q=\frac{p-R}{iR}}{\le} \lim_{R\to+\infty}\int_0^{\pm1} \mathrm{d}q\, R\left|\mathrm{e}^{-z\frac{R^2}{2}(1-iq)^2}\left(\mathrm{e}^{iR\Delta x(1-iq)}+\mathrm{e}^{-iR\Delta x(1-iq)}\right)\right| \\
&\le \lim_{R\to+\infty}\left(\int_0^{\pm1} \mathrm{d}q\, R\left|\mathrm{e}^{-z\frac{R^2}{2}(1-iq)^2+iR\Delta x(1-iq)}\right|+\int_0^{\pm1} \mathrm{d}q\, R\left|\mathrm{e}^{-z\frac{R^2}{2}(1-iq)^2-iR\Delta x(1-iq)}\right|\right) \\
&= \lim_{R\to+\infty}\left(\int_0^{\pm1} \mathrm{d}q\, R\mathrm{e}^{(\mp|z|R^2+R\Delta x)q}+\int_0^{\pm1} \mathrm{d}q\, R\mathrm{e}^{(\mp|z|R^2-R\Delta x)q}\right) \\
&= \lim_{R\to+\infty}\left(\frac{1-\mathrm{e}^{-|z|R^2\pm R\Delta x}}{\pm|z|R-\Delta x}+\frac{1-\mathrm{e}^{-|z|R^2\mp R\Delta x}}{\pm|z|R+\Delta x}\right) \overset{|z|>0}{=\!=} 0
\end{aligned}$$

From equation (A.5) in limit $R \to +\infty$ we get

$$\begin{aligned}
\lim_{R\to+\infty}\int_0^R \mathrm{d}p\, f_1(p) &= \lim_{R\to+\infty}\int_0^{R\left(1-i\tan\frac{\varphi}{2}\right)} \mathrm{d}p\, f_1(p) \\
&\overset{p=p'\mathrm{e}^{-i\frac{\varphi}{2}}}{=\!=\!=} \lim_{R\to+\infty}\mathrm{e}^{-i\frac{\varphi}{2}}\int_0^{\frac{R}{\cos\frac{\varphi}{2}}} \mathrm{d}p'\, f\left(p'\mathrm{e}^{-i\frac{\varphi}{2}}\right).
\end{aligned}$$

We undo the symmetrization from step (A.4) and rearrange quadratic term in exponent.

$$\begin{aligned}\frac{1}{2\pi}\int_{-\infty}^{+\infty}\mathrm{d}p\,\mathrm{e}^{-z\frac{p^2}{2}+ip\Delta x} &= \frac{\mathrm{e}^{-i\frac{\varphi}{2}}}{2\pi}\int_{-\infty}^{+\infty}\mathrm{d}p'\,\mathrm{e}^{-|z|\frac{p'^2}{2}+ip'\Delta x\mathrm{e}^{-i\frac{\varphi}{2}}} \\ &= \frac{\mathrm{e}^{-i\frac{\varphi}{2}}}{2\pi}\int_{-\infty}^{+\infty}\mathrm{d}p'\,\underbrace{\mathrm{e}^{-\frac{|z|}{2}\left(p'-i\Delta x\mathrm{e}^{-i\frac{\varphi}{2}}\right)^2-\frac{\Delta x^2}{2z}}}_{f_2(p')}\end{aligned} \tag{A.6}$$

Now we will need to use integral in complex plane again. Let $R>0$ and choose rectangular contour γ as in Figure A.2. One horizontal line is passing through origin, the other one through point $i\Delta x\mathrm{e}^{-i\frac{\varphi}{2}}$ (compare with (A.6)).

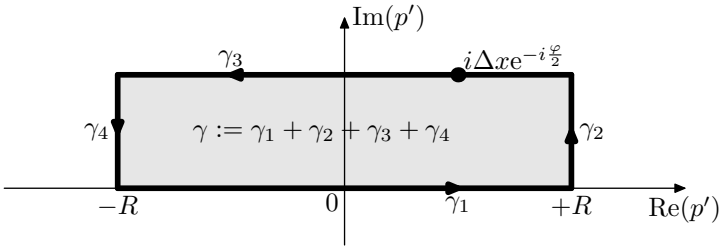

Figure A.2: The contour of integration γ in complex p'-plane.

Cauchy integral of function $f_2(p')$ over the contour γ gives (function $f_2(p')$ is analytic in whole complex plane)

$$\int_{-R}^{R}\mathrm{d}p'\,f_2(p')+\int_{\gamma_2}\mathrm{d}p'\,f_2(p')+\int_{\gamma_3}\mathrm{d}p'\,f_2(p')+\int_{\gamma_4}\mathrm{d}p'\,f_2(p')=\oint_{\gamma}\mathrm{d}p'\,f_2(p')\overset{\text{(A.3)}}{=}0\,. \tag{A.7}$$

Again we are interested in the limit $R\to+\infty$. The integrals over the contours γ_2 and γ_4 go to zero in the limit.

$$\begin{aligned}\lim_{R\to+\infty}\left|\int_{\gamma_{2/4}}\mathrm{d}p'\,f_2(p')\right| &\le \lim_{R\to+\infty}\int_{\gamma_{2/4}}\mathrm{d}p'\,\left|f_2(p')\right| \\ &\overset{p'=\pm R+iq}{=\!=\!=} \lim_{R\to+\infty}\int_0^{\Delta x}\mathrm{d}q\,\mathrm{e}^{-\frac{|z|}{2}(R^2-q^2)\pm R\Delta x\sin\frac{\varphi}{2}-q\Delta x\cos\frac{\varphi}{2}} \\ &\le \lim_{R\to+\infty}\Delta x\mathrm{e}^{-\frac{|z|}{2}(R^2-\Delta x^2)\pm R\Delta x\sin\frac{\varphi}{2}}=0\end{aligned}$$

From equation (A.7) and (A.6) in limit $R\to+\infty$ we get

$$\frac{1}{2\pi}\int_{-\infty}^{+\infty}\mathrm{d}p\,\mathrm{e}^{-z\frac{p^2}{2}+ip\Delta x}=\frac{\mathrm{e}^{-i\frac{\varphi}{2}}}{2\pi}\mathrm{e}^{-\frac{\Delta x^2}{2z}}\underbrace{\int_{-\infty}^{+\infty}\mathrm{d}p'\,\mathrm{e}^{-\frac{|z|}{2}p'^2}}_{\sqrt{\frac{2\pi}{|z|}}}=\frac{1}{\sqrt{2\pi z}}\mathrm{e}^{-\frac{\Delta x^2}{2z}}\,.$$

Inserting into N-dimensional integral we get

$$\langle\boldsymbol{x}'|\mathrm{e}^{-z\widehat{T}}|\boldsymbol{x}\rangle=\frac{1}{(2\pi z)^{N/2}}\mathrm{e}^{-\frac{\Delta x^2}{2z}}\,, \tag{A.8}$$

where $\Delta x^2=\boldsymbol{\Delta x}\cdot\boldsymbol{\Delta x}$.

We can conclude a few properties. In limit $|z|\to 0$ we get N-dimensional Dirac delta distribution $\delta_N(\boldsymbol{\Delta x})$. For $\mathrm{Re}(z)>0$ the formula (A.8) is justified in sense of Lebesgue integral and is well-defined. For $\mathrm{Re}(z)=0$ the matrix element (A.8) doesn't converge and is ill-defined, but can be evaluated in sense of Cauchy principal value. For

$\mathrm{Re}(z) < 0$ the matrix element is ill-defined and can't be fixed. The matrix element is analytic in terms of z. Therefore we could only evaluate the matrix element for $z \in \mathbb{R}^+$ and uniquely analytically continue the formula into half-plane $\mathrm{Re}(z) > 0$ and obtain same result. However we can analytically continue the formula for whole complex plane. In fact, the second root in formula causes analytic continuation into Riemann surface over 2 complex sheets. In sense of analytic continuation we can assign for the matrix elements value (A.8) evem for $\mathrm{Re}(z) < 0$. However the spatial matrix elements for $\mathrm{Re}(z) < 0$ cause problems like infinities or instabilities because of reasons mentioned above. Our result is in agreement with [24].

A.2 Estimate of the Value of Wave Function

We want to estimate the value of wave function $\psi(\boldsymbol{a})$ at $\boldsymbol{a}$ from n samples. It can be can be estimated using density of samples in neighbourhood. The straightforward estimate is

$$\psi(\boldsymbol{a}) \approx \frac{1}{n} \frac{n(\boldsymbol{a}, r)}{\mathcal{V}(r)} ,$$

where $n(\boldsymbol{a}, r)$ is number of samples in N-dimensional sphere $S(\boldsymbol{a}, r)$ with center $\boldsymbol{a}$, radius r and volume $\mathcal{V}(r)$.

Let's assume that the wave function can be expressed as Taylor series in N dimensions at point $\boldsymbol{a}$ as[8]

$$\psi(\boldsymbol{x}) = \psi(\boldsymbol{a}) + \partial_i \psi(\boldsymbol{a})(\boldsymbol{x} - \boldsymbol{a})_i + \frac{1}{2} \partial_{ij} \psi(\boldsymbol{a})(\boldsymbol{x} - \boldsymbol{a})_i (\boldsymbol{x} - \boldsymbol{a})_j + \cdots , \tag{A.9}$$

where $\partial_{ij\ldots}$ are partial derivatives with respect to x_i, x_j, ... and $(\boldsymbol{v})_i$ is the i-th coordinate of vector $\boldsymbol{v}$. The average number of samples $\langle n(\boldsymbol{a}, r) \rangle$ in sphere $S(\boldsymbol{a}, r)$ is

$$\langle n(\boldsymbol{a}, r) \rangle = n \int_{S(\boldsymbol{a},r)} \mathrm{d}\boldsymbol{x}\, \psi(\boldsymbol{x}) \overset{\boldsymbol{x} \to \boldsymbol{x} + \boldsymbol{a}}{=\!=\!=} n \int_{S(\boldsymbol{0},r)} \mathrm{d}\boldsymbol{x}\, \psi(\boldsymbol{x} + \boldsymbol{a}) .$$

Using the Taylor series (A.9) we get

$$\langle n(\boldsymbol{a}, r) \rangle = n \int_{S(\boldsymbol{0},r)} \mathrm{d}\boldsymbol{x} \left[\psi(\boldsymbol{a}) + \partial_i \psi(\boldsymbol{a})(\boldsymbol{x})_i + \frac{1}{2} \partial_{ij} \psi(\boldsymbol{a})(\boldsymbol{x})_i (\boldsymbol{x})_j + \cdots \right] \tag{A.10}$$

The integral breaks down into simple following integrals

$$\begin{aligned}
&\int_{S(\boldsymbol{0},r)} \mathrm{d}\boldsymbol{x} = \int_\Omega \mathrm{d}\Omega \int_0^r \mathrm{d}\rho\, \rho^{N-1} = S_{N-1} \frac{r^N}{N} = \mathcal{V}(r) , \\
&\int_{S(\boldsymbol{0},r)} \mathrm{d}\boldsymbol{x}\, x_i \overset{x_i \to -x_i}{=\!=\!=} -\int_{S(\boldsymbol{0},r)} \mathrm{d}\boldsymbol{x}\, x_i = 0 , \\
&\int_{S(\boldsymbol{0},r)} \mathrm{d}\boldsymbol{x}\, x_i x_j \overset{x_i \to -x_i}{=\!=\!=} -\int_{S(\boldsymbol{0},r)} \mathrm{d}\boldsymbol{x}\, x_i x_j = 0 , \quad \text{for } i \neq j , \\
&\int_{S(\boldsymbol{0},r)} \mathrm{d}\boldsymbol{x}\, x_i^2 = \frac{1}{N} \int_{S(\boldsymbol{0},r)} \mathrm{d}\boldsymbol{x}\, \boldsymbol{x} \cdot \boldsymbol{x} = \frac{1}{N} \int_\Omega \mathrm{d}\Omega \int_0^r \mathrm{d}\rho\, \rho^{N+1} = S_{N-1} \frac{r^{N+2}}{N(N+2)} , \\
&\int_{S(\boldsymbol{0},r)} \mathrm{d}\boldsymbol{x}\, x_i x_j x_k \overset{x_i \to -x_i}{=\!=\!=} -\int_{S(\boldsymbol{0},r)} \mathrm{d}\boldsymbol{x}\, x_i x_j x_k = 0 , \quad \text{for } i \neq j \neq k , \\
&\int_{S(\boldsymbol{0},r)} \mathrm{d}\boldsymbol{x}\, x_i x_j^2 \overset{x_i \to -x_i}{=\!=\!=} -\int_{S(\boldsymbol{0},r)} \mathrm{d}\boldsymbol{x}\, x_i x_j^2 = 0 , \quad \text{for } i \neq j , \\
&\int_{S(\boldsymbol{0},r)} \mathrm{d}\boldsymbol{x}\, x_i^3 \overset{x_i \to -x_i}{=\!=\!=} -\int_{S(\boldsymbol{0},r)} \mathrm{d}\boldsymbol{x}\, x_i^3 = 0 .
\end{aligned}$$

[8] We used Einstein summation convention.

Inserting into (A.10) we get

$$\langle n(\boldsymbol{a},r)\rangle = n\left[\psi(\boldsymbol{a})S_{N-1}\frac{r^N}{N} + \frac{1}{2}\Delta_N\psi(\boldsymbol{a})S_{N-1}\frac{r^{N+2}}{N(N+2)} + O(r^{N+4})\right].$$

Let assume that the wave function $\psi(\boldsymbol{x})$ is ground state.[9] Then from the time-independent Schrödinger equation (1.4) for Hamiltonian (1.2) we can write

$$\frac{1}{2}\Delta_N\psi(\boldsymbol{x}) = (V(\boldsymbol{x}) - E)\psi(\boldsymbol{x})\,.$$

So we obtain the estimation with correction as

$$\psi(\boldsymbol{a}) \approx \frac{1}{n}\frac{n(\boldsymbol{a},r)}{\mathcal{V}(r)}\frac{1}{1 + (V(\boldsymbol{a}) - E)\frac{r^2}{N+2}}\,, \tag{A.11}$$

where $\mathcal{V}(r) = S_{N-1}\frac{r^N}{N}$.

A.3 Analytically Solvable Potentials

In this appendix we will review some solvable potentials, which can serve as good test potentials. First we start with N-dimensional spherically symmetrical potential $V(r)$. We are looking for spherically symmetrical wave function $\psi(\boldsymbol{r})$. The Laplace operator Δ_N can be written in spherical coordinates as

$$\Delta_N f = \frac{1}{r^{N-1}}\frac{\partial}{\partial r}\left(r^{N-1}\frac{\partial f}{\partial r}\right) + \frac{1}{r^2}\Delta_{S^{N-1}}f\,,$$

where $\Delta_{S^{N-1}}$ is *Laplace-Beltrami operator* on the $(N-1)$-dimensional sphere. Applying all changes to the time-independent Schrödinger equation (1.4) for Hamiltonian (1.2) we get[10]

$$-\frac{1}{2r^{N-1}}\frac{\mathrm{d}}{\mathrm{d}r}\left(r^{N-1}\frac{\mathrm{d}\psi}{\mathrm{d}r}\right) + (V(r) - E)\,\psi(r) = 0\,.$$

Using substitution $\psi(r) = R(r)r^m$ for $m = -\frac{N-1}{2}$ we obtain one-dimensional Schrödinger equation with changed potential[11]

$$-\frac{1}{2}\frac{\mathrm{d}^2R}{\mathrm{d}r^2} + \left[V(r) + \frac{(N-1)(N-3)}{8}\frac{1}{r^2} - E\right]R(r) = 0\,. \tag{A.12}$$

Now we can enter known spherically symmetrical wave function $\psi(r)$ and obtain the corresponding potential $V(r)$. The input function will be radial distribution $\rho(r)$, which will be in following relation to $\psi(r)$

$$\mathrm{d}p = \rho(r)\mathrm{d}r = \psi(r)\mathrm{d}r\int_\Omega \mathrm{d}\Omega r^{N-1} = \psi(r)r^{N-1}S_{N-1}\mathrm{d}r\,, \tag{A.13}$$

where Ω is spatial angle on $(N-1)$-dimensional unit sphere, S_{N-1} surface of $(N-1)$-dimensional unit sphere. The function S_{N-1} can be expressed as

$$S_{N-1} = \frac{2\pi^{N/2}}{\Gamma\left(\frac{N}{2}\right)}\,.$$

From (A.13) we get

$$\psi(r) = \frac{\rho(r)}{r^{N-1}S_{N-1}}\,. \tag{A.14}$$

[9] The wave function in simulation is near the ground state and we are doing estimation, so this should be minor effect.

[10] The functions are function of one variable hence the partial derivatives become derivatives.

[11] The parameter m was chosen so that we can get rid of the first derivative.

Gamma Distribution Function

For gamma distribution function $\rho_\Gamma(r;a,b)$ for $a>0$ and $b>0$

$$\rho_\Gamma(r;a,b)=\frac{r^{a-1}\mathrm{e}^{-r/b}}{\Gamma(a)b^a}\quad\overset{(A.14)}{\Longrightarrow}\quad\psi(r)=\frac{r^{a-N}\mathrm{e}^{-r/b}}{\Gamma(a)b^aS_{N-1}}\quad\Longrightarrow\quad R(r)=\frac{r^{a-\frac{N+1}{2}}\mathrm{e}^{-r/b}}{\Gamma(a)b^aS_{N-1}}$$

after substitution to (A.12) we get

$$V(r)-E=\frac{1}{2}(a-2)(a-N)\frac{1}{r^2}-\frac{1}{b}\left(a-\frac{N+1}{2}\right)\frac{1}{r}+\frac{1}{2b^2}\,.$$

Especially for $a=N$ we get N-dimensional Coulomb potential

$$V(r)-E=-\frac{N-1}{2b}\frac{1}{r}+\frac{1}{2b^2}\,.$$

Gaussian Distribution Function

For Gaussian distribution function $\rho_G(r;a,\sigma)$ for $a>0$ and $\sigma>0$

$$\rho_G(r;a,\sigma)=\frac{2r^{a-1}\mathrm{e}^{-r^2/2\sigma^2}}{\Gamma\left(\frac{a}{2}\right)2^{a/2}\sigma^a}\overset{(A.14)}{\Longrightarrow}\psi(r)=\frac{2r^{a-N}\mathrm{e}^{-r^2/2\sigma^2}}{\Gamma\left(\frac{a}{2}\right)2^{a/2}\sigma^aS_{N-1}}\Longrightarrow R(r)=\frac{2r^{a-\frac{N+1}{2}}\mathrm{e}^{-r^2/2\sigma^2}}{\Gamma\left(\frac{a}{2}\right)2^{a/2}\sigma^aS_{N-1}}$$

after substitution to (A.12) we get

$$V(r)-E=\frac{1}{2}(a-2)(a-N)\frac{1}{r^2}+\frac{1}{2\sigma^4}r^2+\frac{1}{2\sigma^2}(N-2a)\,.$$

Especially for $a=N$ we get N-dimensional LHO

$$V(r)-E=\frac{1}{2\sigma^4}r^2-\frac{N}{2\sigma^2}\,.$$

Let $E=0$. Then the integrals $\langle\psi|\psi\rangle$, $\langle\psi|\widehat{T}|\psi\rangle$ and $\langle\psi|\widehat{V}|\psi\rangle$ are shown in Table A.1.

	$\langle\psi\vert\psi\rangle$	$\langle\psi\vert\widehat{T}\vert\psi\rangle$	$\langle\psi\vert\widehat{V}\vert\psi\rangle$
gamma	$\dfrac{\Gamma(\frac{N}{2})}{2^{N+1}\Gamma(N)\pi^{N/2}b^N}$	$\dfrac{1}{2b^2}\dfrac{\Gamma(\frac{N}{2})}{2^{N+1}\Gamma(N)\pi^{N/2}b^N}$	$-\dfrac{1}{2b^2}\dfrac{\Gamma(\frac{N}{2})}{2^{N+1}\Gamma(N)\pi^{N/2}b^N}$
Gauss	$\dfrac{1}{(4\pi\sigma^2)^{N/2}}$	$\dfrac{N}{4\sigma^2}\dfrac{1}{(4\pi\sigma^2)^{N/2}}$	$-\dfrac{N}{4\sigma^2}\dfrac{1}{(4\pi\sigma^2)^{N/2}}$

Table A.1: Integrals $\langle\psi|\psi\rangle$, $\langle\psi|\widehat{T}|\psi\rangle$ and $\langle\psi|\widehat{V}|\psi\rangle$ for gamma and Gaussian distributions.

A.4 Approximants of the Kinetic Energy and the Unit Operator

To evaluate matrix elements of operators $\widehat{K}_i(\tau)$ it is useful to define operator $\widehat{M}_i(\tau):=\widehat{T}^i\mathrm{e}^{-\tau\widehat{T}}$. For spatial matrix elements $\langle\boldsymbol{x}'|\widehat{M}_i(\tau)|\boldsymbol{x}\rangle$ we can write

$$\langle\boldsymbol{x}'|\widehat{M}_{i+1}(\tau)|\boldsymbol{x}\rangle=-\frac{\mathrm{d}}{\mathrm{d}\tau}\langle\boldsymbol{x}'|\widehat{M}_i(\tau)|\boldsymbol{x}\rangle\,.\tag{A.15}$$

Starting with $\widehat{M}_0 = \mathrm{e}^{-\tau\widehat{T}}$ from (A.8) we can write

$$
\begin{aligned}
\langle \boldsymbol{x}'|\widehat{M}_0(\tau)|\boldsymbol{x}\rangle &= \frac{\mathrm{e}^{-\frac{\Delta x^2}{2\tau}}}{(2\pi\tau)^{N/2}}\,,\\
\langle \boldsymbol{x}'|\widehat{M}_1(\tau)|\boldsymbol{x}\rangle &= \frac{\mathrm{e}^{-\frac{\Delta x^2}{2\tau}}}{(2\pi\tau)^{N/2}}\frac{1}{2\tau}\left[N-\frac{\Delta x^2}{\tau}\right]\,,\\
\langle \boldsymbol{x}'|\widehat{M}_2(\tau)|\boldsymbol{x}\rangle &= \frac{\mathrm{e}^{-\frac{\Delta x^2}{4\tau^2}}}{(2\pi\tau)^{N/2}}\frac{1}{4\tau^2}\left[N(N+2)-2(N+2)\frac{\Delta x^2}{\tau}+\frac{\Delta x^4}{\tau^2}\right]\,,\\
\langle \boldsymbol{x}'|\widehat{M}_3(\tau)|\boldsymbol{x}\rangle &= \frac{\mathrm{e}^{-\frac{\Delta x^2}{4\tau^2}}}{(2\pi\tau)^{N/2}}\frac{1}{8\tau^3}\left[N(N+2)(N+4)-3(N+2)(N+4)\frac{\Delta x^2}{\tau}+\right.\\
&\qquad \left.+3(N+4)\frac{\Delta x^4}{\tau^2}-\frac{\Delta x^6}{\tau^3}\right]\,,\\
&\ \ \vdots\\
\langle \boldsymbol{x}'|\widehat{M}_i(\tau)|\boldsymbol{x}\rangle &= \frac{\mathrm{e}^{-\frac{\Delta x^2}{4\tau^2}}}{(2\pi\tau)^{N/2}}\frac{1}{2^i\tau^i}\left[\binom{i}{0}\frac{[N+2(i-1)]!!}{(N-2)!!}-\binom{i}{1}\frac{[N+2(i-1)]!!}{N!!}\frac{\Delta x^2}{\tau}+\right.\\
&\qquad \left.+\binom{i}{2}\frac{[N+2(i-1)]!!}{(N+2)!!}\left(\frac{\Delta x^2}{\tau}\right)^2+\cdots+(-1)^i\binom{i}{i}\left(\frac{\Delta x^2}{\tau}\right)^i\right]\,.
\end{aligned}
$$

From definition (2.8) we can write for matrix elements $\langle \boldsymbol{x}'|\widehat{K}_m(\tau)|\boldsymbol{x}\rangle$

$$
\langle \boldsymbol{x}'|\widehat{K}_m(\tau)|\boldsymbol{x}\rangle = \sum_{i=0}^{m}\frac{\tau^i}{i!}\langle \boldsymbol{x}'|\widehat{M}_{i+1}(\tau)|\boldsymbol{x}\rangle\,. \tag{A.16}
$$

We calculated first few matrix elements $\langle \boldsymbol{x}'|\widehat{K}_m(\tau)|\boldsymbol{x}\rangle$ as

$$\begin{aligned}
\langle \boldsymbol{x}'|\widehat{K}_0(\tau)|\boldsymbol{x}\rangle &= \frac{\mathrm{e}^{-\frac{\Delta x^2}{2\tau}}}{(2\pi\tau)^{N/2}}\frac{1}{2\tau}\left[N-\frac{\Delta x^2}{\tau}\right],\\
\langle \boldsymbol{x}'|\widehat{K}_1(\tau)|\boldsymbol{x}\rangle &= \frac{\mathrm{e}^{-\frac{\Delta x^2}{2\tau}}}{(2\pi\tau)^{N/2}}\frac{1}{2\tau}\left[\frac{N(N+4)}{2}-\frac{(2N+6)\Delta x^2}{2\tau}+\frac{\Delta x^4}{2\tau^2}\right],\\
\langle \boldsymbol{x}'|\widehat{K}_2(\tau)|\boldsymbol{x}\rangle &= \frac{\mathrm{e}^{-\frac{\Delta x^2}{2\tau}}}{(2\pi\tau)^{N/2}}\frac{1}{2\tau}\left[\frac{N(N+4)(N+6)}{8}-\frac{(N+6)(3N+8)\Delta x^2}{8\tau}+\right.\\
&\quad \left.+\frac{(3N+16)\Delta x^4}{8\tau^2}-\frac{\Delta x^6}{8\tau^3}\right],\\
\langle \boldsymbol{x}'|\widehat{K}_3(\tau)|\boldsymbol{x}\rangle &= \frac{\mathrm{e}^{-\frac{\Delta x^2}{2\tau}}}{(2\pi\tau)^{N/2}}\frac{1}{2\tau}\left[\frac{N(N+4)(N+6)(N+8)}{48}-\right.\\
&\quad -\frac{(N+6)(N+8)(4N+10)\Delta x^2}{48\tau}+\frac{(N+8)(4N+20)\Delta x^4}{32\tau^2}-\\
&\quad \left.-\frac{(4N+30)\Delta x^6}{48\tau^3}+\frac{\Delta x^8}{48\tau^4}\right],\\
\langle \boldsymbol{x}'|\widehat{K}_4(\tau)|\boldsymbol{x}\rangle &= \frac{\mathrm{e}^{-\frac{\Delta x^2}{2\tau}}}{(2\pi\tau)^{N/2}}\frac{1}{2\tau}\left[\frac{N(N+4)(N+6)(N+8)(N+10)}{384}-\right.\\
&\quad -\frac{(N+6)(N+8)(N+10)(5N+12)\Delta x^2}{384\tau}+\\
&\quad +\frac{(N+8)(N+10)(5N+24)\Delta x^4}{192\tau^2}-\\
&\quad \left.-\frac{(N+10)(5N+36)\Delta x^6}{192\tau^3}+\frac{(5N+48)\Delta x^8}{384\tau^4}-\frac{\Delta x^{10}}{384\tau^5}\right].
\end{aligned}$$

From definition (2.12) we can write for matrix elements $\langle \boldsymbol{x}'|\widehat{K}_m(\tau)|\boldsymbol{x}\rangle$

$$\langle \boldsymbol{x}'|\widehat{J}_m(\tau)|\boldsymbol{x}\rangle = \sum_{i=0}^{m}\frac{\tau^i}{i!}\langle \boldsymbol{x}'|\widehat{M}_i(\tau)|\boldsymbol{x}\rangle\,. \tag{A.17}$$

We calculated first few matrix elements $\langle \boldsymbol{x}'|\widehat{J}_m(\tau)|\boldsymbol{x}\rangle$ as

$$\begin{aligned}
\langle \boldsymbol{x}'|\widehat{J}_0(\tau)|\boldsymbol{x}\rangle &= \frac{\mathrm{e}^{-\frac{\Delta x^2}{2\tau}}}{(2\pi\tau)^{N/2}}\,,\\
\langle \boldsymbol{x}'|\widehat{J}_1(\tau)|\boldsymbol{x}\rangle &= \frac{\mathrm{e}^{-\frac{\Delta x^2}{2\tau}}}{(2\pi\tau)^{N/2}}\left[\frac{(N+2)}{2}-\frac{\Delta x^2}{2\tau}\right],\\
\langle \boldsymbol{x}'|\widehat{J}_2(\tau)|\boldsymbol{x}\rangle &= \frac{\mathrm{e}^{-\frac{\Delta x^2}{2\tau}}}{(2\pi\tau)^{N/2}}\left[\frac{(N+2)(N+4)}{8}-\frac{(N+4)\Delta x^2}{4\tau}+\frac{\Delta x^4}{8\tau^2}\right],\\
\langle \boldsymbol{x}'|\widehat{J}_3(\tau)|\boldsymbol{x}\rangle &= \frac{\mathrm{e}^{-\frac{\Delta x^2}{2\tau}}}{(2\pi\tau)^{N/2}}\left[\frac{(N+2)(N+4)(N+6)}{48}-\frac{(N+4)(N+6)\Delta x^2}{16\tau}+\right.\\
&\quad\left.+\frac{(N+6)\Delta x^4}{16\tau^2}-\frac{\Delta x^6}{48\tau^3}\right],\\
\langle \boldsymbol{x}'|\widehat{J}_4(\tau)|\boldsymbol{x}\rangle &= \frac{\mathrm{e}^{-\frac{\Delta x^2}{2\tau}}}{(2\pi\tau)^{N/2}}\left[\frac{(N+2)(N+4)(N+6)(N+8)}{384}-\right.\\
&\quad-\frac{(N+4)(N+6)(N+8)\Delta x^2}{96\tau}+\frac{(N+6)(N+8)\Delta x^4}{64\tau^2}-\\
&\quad\left.-\frac{(N+8)\Delta x^6}{96\tau^3}+\frac{\Delta x^8}{384\tau^4}\right].\\
&\vdots\\
\langle \boldsymbol{x}'|\widehat{J}_m(\tau)|\boldsymbol{x}\rangle &= \frac{\mathrm{e}^{-\frac{\Delta x^2}{2\tau}}}{(2\pi\tau)^{N/2}}\frac{1}{(2m)!!}\left[\binom{m}{0}\frac{(N+2m)!!}{N!!}-\binom{m}{1}\frac{(N+2m)!!}{(N+2)!!}\frac{\Delta x^2}{\tau}+\right.\\
&\quad\left.+\binom{m}{2}\frac{(N+2m)!!}{(N+4)!!}\left(\frac{\Delta x^2}{\tau}\right)^2+\cdots+(-1)^m\binom{m}{m}\left(\frac{\Delta x^2}{\tau}\right)^m\right].
\end{aligned}$$

A.5 Estimators of the Kinetic Energy

We start from the biased estimator $\hat{\mathcal{T}}_0$ from (2.9)

$$\hat{\mathcal{T}}_0 := \frac{1}{n^2}\sum_{i=1}^{n}\sum_{j=1}^{n} K_m(\tau,\Delta x_{ij})\,. \tag{A.18}$$

The expected value $\mathrm{E}\left[K_m(\tau,\Delta x_{ij})\right]$ is

$$\mathrm{E}[K_m(\tau,\Delta x_{ij})] = \begin{cases} \displaystyle\int_{\mathrm{R}^N\times\mathrm{R}^N} \mathrm{d}\boldsymbol{x}\mathrm{d}\boldsymbol{y}\, K_m(\tau,|\boldsymbol{x}-\boldsymbol{y}|)\phi(\boldsymbol{x})\phi(\boldsymbol{y}) & \text{if } i\neq j;\\ K_m(\tau,0) & \text{if } i=j. \end{cases} \tag{A.19}$$

Then the expected value of estimator $\hat{\mathcal{T}}_0$ is

$$\mathrm{E}[\hat{\mathcal{T}}_0] = \frac{n-1}{n} I_{1,m}(\tau) + \frac{1}{n} K_m(\tau,0)\,,$$

where for the convenience we denote $I_{1,m}(\tau) := \displaystyle\int_{\mathrm{R}^N\times\mathrm{R}^N} \mathrm{d}\boldsymbol{x}\mathrm{d}\boldsymbol{y}\, K_m(\tau,|\boldsymbol{x}-\boldsymbol{y}|)\phi(\boldsymbol{x})\phi(\boldsymbol{y})$. To avoid duplicity and biased terms in estimator $\hat{\mathcal{T}}_0$ in (A.18) we suggest new estimator

$$\hat{\mathcal{T}}_1 := \frac{2}{n(n-1)}\sum_{\substack{i=1\\ j>i}}^{n} K_m(\tau,\Delta x_{ij})\,,$$

with expected value

$$\mathrm{E}[\hat{\mathcal{T}}_1] = I_{1,m}(\tau)\,.$$

The variance of new estimator $\hat{\mathcal{T}}_1$ is

$$\mathrm{Var}[\hat{\mathcal{T}}_1] = \mathrm{E}[(\hat{\mathcal{T}}_1 - \mathrm{E}[\hat{\mathcal{T}}_1])^2] = \frac{2}{n(n-1)}\left[I_{2,m}(\tau) + \frac{4}{3}(n-2)I_{3,m}(\tau) - \frac{1}{3}(4n-5)I_{1,m}^2(\tau)\right], \tag{A.20}$$

where we denote

$$I_{2,m}(\tau) = \int_{\mathrm{R}^N\times\mathrm{R}^N} \mathrm{d}\boldsymbol{x}\mathrm{d}\boldsymbol{y}\; K_m^2(\tau, |\boldsymbol{x}-\boldsymbol{y}|)\phi(\boldsymbol{x})\phi(\boldsymbol{y})\,,$$
$$I_{3,m}(\tau) = \int_{\mathrm{R}^N\times\mathrm{R}^N\times\mathrm{R}^N} \mathrm{d}\boldsymbol{x}\mathrm{d}\boldsymbol{y}\mathrm{d}\boldsymbol{z}\; K_m(\tau, |\boldsymbol{x}-\boldsymbol{y}|)K_m(\tau, |\boldsymbol{y}-\boldsymbol{z}|)\phi(\boldsymbol{x})\phi(\boldsymbol{y})\phi(\boldsymbol{z})\,.$$

To estimate the error (square root of the variance) of estimator $\hat{\mathcal{T}}_1$ from samples we need to find expected value of product $K_m(\tau, \Delta x_{ij})K_m(\tau, \Delta x_{kl})$. The value depends on difference of indices i, j, k and l, so we created scheme in Figure A.3 where we distinguish different cases with color. We get

$$\mathrm{E}[K_m(\tau, \Delta x_{ij})K_m(\tau, \Delta x_{kl})] = \begin{cases} I_{2,m}(\tau) & \text{for } \blacksquare; \\ I_{3,m}(\tau) & \text{for } \blacksquare; \\ I_{1,m}^2(\tau) & \text{for } \blacksquare. \end{cases}$$

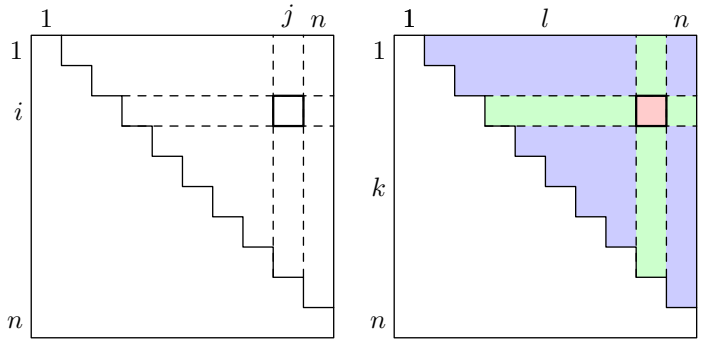

Figure A.3: Color scheme for indices i, j, k and l.

The total number of quadruple indices is $\left[\frac{n(n-1)}{2}\right]^2 = n^2(n-1)^2/4$. The number of different types of quadruples are

$$\#(\blacksquare) = \frac{1}{2}n(n-1)\,,\quad \#(\blacksquare) = \frac{1}{3}n(n-1)(n-2)\,,\quad \#(\blacksquare) = \frac{1}{24}n(n-1)(n-2)(3n-5)\,.$$

The leading terms in variance (A.20) are terms $I_{3,m}(\tau)$ and $I_{1,m}^2(\tau)$. The number of corresponding quadruples rises as $\sim n^3$ and $\sim n^4$ respectively. To avoid long computation time we provide three estimators $\hat{\mathcal{S}}_1$, $\hat{\mathcal{S}}_2$ and $\hat{\mathcal{S}}_3$, which can be computed in $\sim n^2$ steps.

$$\hat{\mathcal{S}}_1 := \frac{2}{n(n-1)}\sum_{\substack{i=1\\j>i}}^{n} K_m^2(\tau, \Delta x_{ij})$$
$$\hat{\mathcal{S}}_2 := (\hat{\mathcal{T}})^2$$
$$\hat{\mathcal{S}}_3 := \frac{2}{n(n-1)(n-2)}\sum_{\substack{i=1\\j>i}}^{n} K_m(\tau, \Delta x_{ij})\Big(\sum_{\substack{k=1\\k\neq j}}^{n} K_m(\tau, \Delta x_{jk})\Big)$$

The expected values of estimators are

$$\begin{aligned}
&\mathrm{E}[\hat{\mathcal{S}}_1] := I_2\,,\\
&\mathrm{E}[\hat{\mathcal{S}}_2] := \frac{2}{n(n-1)}\left[I_{2,m}(\tau) + \frac{4}{3}(n-2)I_{3,m}(\tau) + \frac{1}{6}(n-2)(3n-5)I^2_{1,m}(\tau)\right]\,,\\
&\mathrm{E}[\hat{\mathcal{S}}_3] := I_{3,m}(\tau) + \frac{1}{n-2}I_{2,m}(\tau)\,.
\end{aligned}$$

Using linear combination of estimators $\hat{\mathcal{S}}_1$, $\hat{\mathcal{S}}_2$ and $\hat{\mathcal{S}}_3$ we can match the expected value of new estimator to be equal to $\mathrm{Var}[\hat{\mathcal{T}}]$ in (A.20) as

$$\begin{aligned}
\hat{\mathscr{V}}_{\mathcal{T}_1} :=& \frac{4}{n(n-1)(n-2)(3n-5)}\left[4\sum_{\substack{i=1\\j>i}}^{n}\sum_{\substack{k=1\\k\neq j}}^{n} K_m(\tau,\Delta x_{ij})K_m(\tau,\Delta x_{jk}) - \right.\\
&\left. - \frac{n(n-1)(4n-5)}{2}(\hat{\mathcal{T}}_1)^2 - \sum_{\substack{i=1\\j>i}}^{n} K^2_m(\tau,\Delta x_{ij})\right]\,.
\end{aligned}$$

It is important to note, that the estimator $\hat{\mathscr{V}}_{\mathcal{T}_1}$ is not guaranteed to be non-negative.

A.6 Gaussian Wave Function

Let the wave function be normalised N-dimensional Gaussian function

$$\langle \boldsymbol{x}|\psi\rangle = \frac{1}{(2\pi\sigma^2)^{N/2}}\mathrm{e}^{-\frac{|\boldsymbol{x}|^2}{2\sigma^2}}\,. \tag{A.21}$$

Then we can analytically calculate $\mathrm{e}^{-\tau\widehat{T}}|\psi\rangle$ as

$$\begin{aligned}
\langle \boldsymbol{x}|\mathrm{e}^{-\tau\widehat{T}}|\psi\rangle &= \int_{\mathbb{R}^N}\mathrm{d}\boldsymbol{x}'\,\langle \boldsymbol{x}|\mathrm{e}^{-\tau\widehat{T}}|\boldsymbol{x}'\rangle\langle \boldsymbol{x}'|\psi\rangle \overset{(A.8)}{=} \frac{1}{(4\pi^2\tau\sigma^2)^{N/2}}\int_{\mathbb{R}^N}\mathrm{d}\boldsymbol{x}'\,\mathrm{e}^{-\frac{|\boldsymbol{x}'-\boldsymbol{x}|^2}{2\tau}-\frac{|\boldsymbol{x}'|^2}{2\sigma^2}}\\
&= \frac{1}{(2\pi\tau)^{N/2}(2\pi\sigma^2)^{N/2}}\int_{\mathbb{R}^N}\mathrm{d}\boldsymbol{x}'\,\mathrm{e}^{-\frac{\sigma^2+\tau}{2\sigma^2\tau}\left|\boldsymbol{x}'-\boldsymbol{x}\frac{\sigma^2}{\sigma^2+\tau}\right|^2-\frac{|\boldsymbol{x}|^2}{2(\sigma^2+\tau)}}\\
&\overset{\boldsymbol{x}'\to\boldsymbol{x}'+\boldsymbol{x}\frac{\sigma^2}{\sigma^2+\tau}}{=\!=\!=\!=\!=\!=\!=\!=\!=} \frac{1}{[2\pi(\sigma^2+\tau)]^{N/2}}\mathrm{e}^{-\frac{|\boldsymbol{x}|^2}{2(\sigma^2+\tau)}}\,.
\end{aligned} \tag{A.22}$$

Also we can calculate the matrix element $\langle\psi|\widehat{M}_0(\tau)|\psi\rangle$ as

$$\begin{aligned}
\langle\psi|\widehat{M}_0(\tau)|\psi\rangle &= \int_{\mathbb{R}^N}\mathrm{d}\boldsymbol{x}\,\langle\psi|\boldsymbol{x}\rangle\langle\boldsymbol{x}|\mathrm{e}^{-\tau\widehat{T}}|\psi\rangle\\
&\overset{(A.21)}{\underset{(A.22)}{=}} \frac{1}{(2\pi\sigma^2)^{N/2}}\frac{1}{[2\pi(\sigma^2+\tau)]^{N/2}}\int_{\mathbb{R}^N}\mathrm{d}\boldsymbol{x}\,\mathrm{e}^{-\frac{|\boldsymbol{x}|^2(2\sigma^2+\tau)}{2\sigma^2(\sigma^2+\tau)}} = \frac{1}{[2\pi(2\sigma^2+\tau)]^{N/2}}\,.
\end{aligned}$$

Using the definition (A.15) and Lebesgue's dominated convergence theorem[12] we can interchange derivative and integral and easily calculate all higher matrix elements

[12]The dominating integrable function will have the form $P(\Delta x^2)\mathrm{e}^{-A\Delta x^2}$, where $P(\cdot)$ is polynomial.

$\langle\psi|\widehat{M}_i(\tau)|\psi\rangle$ as

$$\begin{aligned}
\langle\psi|\widehat{M}_1(\tau)|\psi\rangle &= -\frac{\mathrm{d}}{\mathrm{d}\tau}\langle\psi|\widehat{M}_0(\tau)|\psi\rangle = \frac{N}{2}\frac{1}{(2\pi)^{N/2}}\frac{1}{(2\sigma^2+\tau)^{N/2+1}}\,,\\
\langle\psi|\widehat{M}_2(\tau)|\psi\rangle &= \frac{N}{2}\left(\frac{N}{2}+1\right)\frac{1}{(2\pi)^{N/2}}\frac{1}{(2\sigma^2+\tau)^{N/2+2}}\,,\\
&\vdots\\
\langle\psi|\widehat{M}_i(\tau)|\psi\rangle &= \frac{\left(\frac{N}{2}+i-1\right)!}{\left(\frac{N}{2}-1\right)!}\frac{1}{(2\pi)^{N/2}}\frac{1}{(2\sigma^2+\tau)^{N/2+i}}\,.
\end{aligned}$$

From matrix elements $\langle\psi|\widehat{M}_i(\tau)|\psi\rangle$ we can using the equation (A.16) find the matrix elements $\langle\psi|\widehat{K}_m(\tau)|\psi\rangle$ as follows

$$\begin{aligned}
\langle\psi|\widehat{K}_0(\tau)|\psi\rangle &= \frac{N}{2}\frac{1}{(2\pi)^{N/2}}\frac{1}{(2\sigma^2+\tau)^{N/2+1}}\,,\\
\langle\psi|\widehat{K}_1(\tau)|\psi\rangle &= \frac{N}{2}\frac{1}{(2\pi)^{N/2}}\frac{1}{(2\sigma^2+\tau)^{N/2+1}}\left[1+\frac{\tau(\frac{N}{2}+1)}{2\sigma^2+\tau}\right]\,,\\
\langle\psi|\widehat{K}_2(\tau)|\psi\rangle &= \frac{N}{2}\frac{1}{(2\pi)^{N/2}}\frac{1}{(2\sigma^2+\tau)^{N/2+1}}\left[1+\frac{\tau(\frac{N}{2}+1)}{2\sigma^2+\tau}+\frac{\tau^2(\frac{N}{2}+1)(\frac{N}{2}+2)}{2(2\sigma^2+\tau)^2}\right]\,,\\
&\vdots\\
\langle\psi|\widehat{K}_m(\tau)|\psi\rangle &= \frac{N}{2}\frac{1}{(2\pi)^{N/2}}\frac{1}{(2\sigma^2+\tau)^{N/2+1}}\,T_{m,x}\left[\frac{1}{\left(1-x\frac{\tau}{2\sigma^2+\tau}\right)^{N/2+1}}\right]\Bigg|_{x=1}\,, \qquad \text{(A.23)}
\end{aligned}$$

where $T_{m,x}\left[\cdot\right]\big|_{x=1}$ is Taylor series of the m-th order in variable x evaluated for $x=1$. In the limit $m\to+\infty$ we can write

$$\begin{aligned}
\lim_{m\to+\infty}\langle\psi|\widehat{K}_m(\tau)|\psi\rangle &= \frac{N}{2}\frac{1}{(2\pi)^{N/2}}\frac{1}{(2\sigma^2+\tau)^{N/2+1}}\left[\frac{1}{\left(1-\frac{\tau}{2\sigma^2+\tau}\right)^{N/2+1}}\right]\\
&= \frac{N}{2}\frac{1}{(2\pi)^{N/2}}\frac{1}{(2\sigma^2)^{N/2+1}}\,,
\end{aligned}$$

which is correct kinetic energy $\langle\psi|\widehat{T}|\psi\rangle$ (compare with Table A.1). We get the correct kinetic energy from every $\langle\psi|\widehat{K}_m(\tau)|\psi\rangle$ in the limit $\tau\to 0^+$.

We can also calculate matrix elements $\langle\psi|\widehat{J}_i(\tau)|\psi\rangle$ using the equation (A.17) as follows

$$\begin{aligned}
\langle\psi|\widehat{J}_0(\tau)|\psi\rangle &= \frac{1}{(2\pi)^{N/2}}\frac{1}{(2\sigma^2+\tau)^{N/2}}\,,\\
\langle\psi|\widehat{J}_1(\tau)|\psi\rangle &= \frac{1}{(2\pi)^{N/2}}\frac{1}{(2\sigma^2+\tau)^{N/2}}\left[1+\frac{\tau(\frac{N}{2})}{2\sigma^2+\tau}\right]\,,\\
\langle\psi|\widehat{J}_2(\tau)|\psi\rangle &= \frac{1}{(2\pi)^{N/2}}\frac{1}{(2\sigma^2+\tau)^{N/2}}\left[1+\frac{\tau(\frac{N}{2})}{2\sigma^2+\tau}+\frac{\tau^2(\frac{N}{2})(\frac{N}{2}+1)}{2(2\sigma^2+\tau)^2}\right]\,,\\
&\vdots\\
\langle\psi|\widehat{J}_m(\tau)|\psi\rangle &= \frac{1}{(2\pi)^{N/2}}\frac{1}{(2\sigma^2+\tau)^{N/2}}\,T_{m,x}\left[\frac{1}{\left(1-x\frac{\tau}{2\sigma^2+\tau}\right)^{N/2}}\right]\Bigg|_{x=1}\,.
\end{aligned}$$

In the limit $m \to +\infty$ we get (compare with Table A.1)

$$\lim_{m\to+\infty} \langle\psi|\widehat{J}_m(\tau)|\psi\rangle = \frac{1}{(2\pi)^{N/2}} \frac{1}{(2\sigma^2+\tau)^{N/2}} \left[\frac{1}{\left(1-\frac{\tau}{2\sigma^2+\tau}\right)^{N/2}}\right] = \frac{1}{(4\pi\sigma^2)^{N/2}}\,.$$

The matrix elements $\langle\psi|\widehat{V}_m(\tau)|\psi\rangle$ have been also calculated using the technique of derivative by parameter τ and linear combination. The resulting elements are

$$\langle\psi|\widehat{V}_m(\tau)|\psi\rangle = -\langle\psi|\widehat{K}_m(\tau)|\psi\rangle\,.$$

A.7 Relation Between Methods B and C

In this Appendix we will show that in the limit $t \to +\infty$ the Method B becomes the Method C. For simplicity we begin with $m = 0$. We are interested in the limit

$$\lim_{\tau\to+\infty} \frac{\langle\psi|\widehat{H}\mathrm{e}^{-\tau\widehat{T}}|\psi\rangle}{\langle\psi|\mathrm{e}^{-\tau\widehat{T}}|\psi\rangle}\,.$$

The numerator and denominator both go to zero in the limit. The most important is the leading term. It is convenient to work with the operator $\mathrm{e}^{-\tau\widehat{T}}$ in eigenbasis of improper eigenvectors $|\boldsymbol{p}\rangle$.

$$\lim_{\tau\to+\infty} \frac{\langle\psi|\widehat{H}\mathrm{e}^{-\tau\widehat{T}}|\psi\rangle}{\langle\psi|\mathrm{e}^{-\tau\widehat{T}}|\psi\rangle} = \lim_{\tau\to+\infty} \frac{\displaystyle\int_{\mathbb{R}^N} \mathrm{d}\boldsymbol{p}\,\langle\psi|\widehat{H}|\boldsymbol{p}\rangle\langle\boldsymbol{p}|\mathrm{e}^{-\tau\widehat{T}}|\psi\rangle}{\displaystyle\int_{\mathbb{R}^N} \mathrm{d}\boldsymbol{p}\,\langle\psi|\boldsymbol{p}\rangle\langle\boldsymbol{p}|\mathrm{e}^{-\tau\widehat{T}}|\psi\rangle} =$$

$$= \lim_{\tau\to+\infty} \frac{\displaystyle\int_{\mathbb{R}^N} \mathrm{d}\boldsymbol{p}\,\langle\psi|\widehat{H}|\boldsymbol{p}\rangle \left(\frac{\tau}{2\pi}\right)^{N/2} \mathrm{e}^{-\tau\frac{p^2}{2}}\langle\boldsymbol{p}|\psi\rangle}{\displaystyle\int_{\mathbb{R}^N} \mathrm{d}\boldsymbol{p}\,\langle\psi|\boldsymbol{p}\rangle \left(\frac{\tau}{2\pi}\right)^{N/2} \mathrm{e}^{-\tau\frac{p^2}{2}}\langle\boldsymbol{p}|\psi\rangle} =$$

In the limit $\tau \to +\infty$ the sequence of functions $\left(\frac{\tau}{2\pi}\right)^{N/2} \mathrm{e}^{-\tau\frac{p^2}{2}}$ becomes the N-dimensional Dirac delta distribution $\delta_N(\boldsymbol{p})$.[13]

$$= \frac{\displaystyle\int_{\mathbb{R}^N} \mathrm{d}\boldsymbol{p}\,\langle\psi|\widehat{H}|\boldsymbol{p}\rangle\delta_N(\boldsymbol{p})\langle\boldsymbol{p}|\psi\rangle}{\displaystyle\int_{\mathbb{R}^N} \mathrm{d}\boldsymbol{p}\,\langle\psi|\boldsymbol{p}\rangle\delta_N(\boldsymbol{p})\langle\boldsymbol{p}|\psi\rangle} = \frac{\langle\psi|\widehat{H}|\boldsymbol{p}=\boldsymbol{0}\rangle\cancel{\langle\boldsymbol{p}=\boldsymbol{0}|\psi\rangle}}{\langle\psi|\boldsymbol{p}=\boldsymbol{0}\rangle\cancel{\langle\boldsymbol{p}=\boldsymbol{0}|\psi\rangle}} = \frac{\langle\psi|\widehat{H}|\boldsymbol{p}=\boldsymbol{0}\rangle}{\langle\psi|\boldsymbol{p}=\boldsymbol{0}\rangle} =$$

We assume that the wave function $|\psi\rangle$ in position representation has the form of real-valued function $\psi(\boldsymbol{x})$. Expressing the matrix elements in terms of spatial elements we get

$$= \frac{\displaystyle\int_{\mathbb{R}^N} \mathrm{d}\boldsymbol{x}\,\langle\psi|\widehat{H}|\boldsymbol{x}\rangle\langle\boldsymbol{x}|\boldsymbol{p}=\boldsymbol{0}\rangle}{\displaystyle\int_{\mathbb{R}^N} \mathrm{d}\boldsymbol{x}\,\langle\psi|\boldsymbol{x}\rangle\langle\boldsymbol{x}|\boldsymbol{p}=\boldsymbol{0}\rangle} = \frac{\displaystyle\int_{\mathbb{R}^N} \mathrm{d}\boldsymbol{x}\,\widehat{H}\psi(\boldsymbol{x})}{\displaystyle\int_{\mathbb{R}^N} \mathrm{d}\boldsymbol{x}\,\psi(\boldsymbol{x})} = \{H\}\,.$$

[13] This can be understood at lower level as follows: The function $\mathrm{e}^{-\tau\frac{p^2}{2}}$ in the limit $\tau \to +\infty$ suppresses matrix elements for all values $\boldsymbol{p}$ except for $\boldsymbol{p} = \boldsymbol{0}$.

Following the same procedure for any m we obtain same result

$$\lim_{\tau\to+\infty}\frac{\langle\psi|\widehat{H}\mathrm{e}^{-\tau\widehat{T}}T_m(\mathrm{e}^{\tau\widehat{T}})|\psi\rangle}{\langle\psi|\mathrm{e}^{-\tau\widehat{T}}T_m(\mathrm{e}^{\tau\widehat{T}})|\psi\rangle}=\frac{\displaystyle\int_{\mathbb{R}^N}\mathrm{d}\boldsymbol{p}\,\langle\psi|\widehat{H}|\boldsymbol{p}\rangle\delta_N(\boldsymbol{p})T_m(\mathrm{e}^{\tau\frac{p^2}{2}})\langle\boldsymbol{p}|\psi\rangle}{\displaystyle\int_{\mathbb{R}^N}\mathrm{d}\boldsymbol{p}\,\langle\psi|\boldsymbol{p}\rangle\delta_N(\boldsymbol{p})T_m(\mathrm{e}^{\tau\frac{p^2}{2}})\langle\boldsymbol{p}|\psi\rangle}\overset{\heartsuit}{=}\{H\}\,,$$

where in step $\heartsuit$ we used that $T_m(\mathrm{e}^{\tau\frac{p^2}{2}})\Big|_{\boldsymbol{p}=\boldsymbol{0}}=1$.

This results holds also for estimators.

$$\begin{aligned}\lim_{\tau\to+\infty}\frac{\mathcal{T}_2+\mathcal{V}_2}{\mathcal{J}_2}&=\lim_{\tau\to+\infty}\frac{\displaystyle\sum_{i=1}^{n}\langle\boldsymbol{x}_i|\widehat{K}_m(\tau)|\boldsymbol{x}_i'\rangle+\langle\boldsymbol{x}_i|\widehat{V}_m(\tau)|\boldsymbol{x}_i'\rangle}{\displaystyle\sum_{i=1}^{n}\langle\boldsymbol{x}_i|\widehat{J}_m(\tau)|\boldsymbol{x}_i'\rangle}\\&=\lim_{\tau\to+\infty}\frac{\displaystyle\sum_{i=1}^{n}\frac{\mathrm{e}^{-\frac{\Delta x_i^2}{2\tau}}}{(2\pi\tau)^{N/2}}\frac{(N+2m)!!}{(2m)!!N!!}\left[\frac{1}{2\tau}\frac{N}{N+2}+V(\boldsymbol{x}_i)+O\left(\frac{1}{\tau}\right)\right]}{\displaystyle\sum_{i=1}^{n}\frac{\mathrm{e}^{-\frac{\Delta x_i^2}{2\tau}}}{(2\pi\tau)^{N/2}}\frac{(N+2m)!!}{(2m)!!N!!}\left(1+O\left(\frac{1}{\tau}\right)\right)}\\&=\frac{1}{n}\sum_{i=1}^{n}V(\boldsymbol{x}_i)=\{\tilde{H}\}\,,\end{aligned}$$

where we used the leading terms in spacial matrix elements from Appendix A.4. We can notice, that in the limit $\tau\to+\infty$ the kinetic term is insignificant with respect to the potential term as in $\{H\}$.

A.8 Variational Principle and Estimators of Energy

The estimators of energy can be sometimes used as variational energy, in sense that their lower bound is ground state energy E_0 or higher. In that case they can be used as the upper bound for this energy and can be used as indicator in case of optimization. To find lower bound of estimators, we use variational principle. In extreme the value of estimator is fixed in respect to small perturbation $|\delta\psi\rangle$ in wave function $|\psi\rangle$.

Method B

To find the lower bound for the Method B, we look at the ratio $H(\tau)$

$$H(\tau)=\frac{\langle\psi|\widehat{H}\widehat{J}_m(\tau)|\psi\rangle}{\langle\psi|\widehat{J}_m(\tau)|\psi\rangle}$$

for fixed τ. We expand the variation $\delta H(\tau)$. The second and higher order terms (like $\langle\delta\psi|\delta\psi\rangle$) are omitted. We assume real-valued perturbation $\langle\boldsymbol{x}|\delta\psi\rangle$. This implies that all matrix elements are real $\langle|\cdot|\rangle^*=\langle|\cdot|\rangle$.

$$\begin{aligned}\delta H(\tau)&=\frac{\langle\psi+\delta\psi|\widehat{H}\widehat{J}_m(\tau)|\psi+\delta\psi\rangle}{\langle\psi+\delta\psi|\widehat{J}_m(\tau)|\psi+\delta\psi\rangle}-\frac{\langle\psi|\widehat{H}\widehat{J}_m(\tau)|\psi\rangle}{\langle\psi|\widehat{J}_m(\tau)|\psi\rangle}\\&=\frac{\langle\psi|\widehat{H}\widehat{J}_m(\tau)|\psi\rangle+\langle\delta\psi|\widehat{H}\widehat{J}_m(\tau)+\widehat{J}_m(\tau)\widehat{H}|\psi\rangle}{\langle\psi|\widehat{J}_m(\tau)|\psi\rangle+2\langle\delta\psi|\widehat{J}_m(\tau)|\psi\rangle}-\frac{\langle\psi|\widehat{H}\widehat{J}_m(\tau)|\psi\rangle}{\langle\psi|\widehat{J}_m(\tau)|\psi\rangle}\\&=\frac{\langle\delta\psi|\widehat{H}\widehat{J}_m(\tau)+\widehat{J}_m(\tau)\widehat{H}-2H(\tau)\widehat{J}_m(\tau)|\psi\rangle}{(\langle\psi|\widehat{J}_m(\tau)|\psi\rangle+2\langle\delta\psi|\widehat{J}_m(\tau)|\psi\rangle)}\end{aligned}\tag{A.24}$$

The necessary condition for variational extreme is $\delta H(\tau) = 0$ for all $|\delta\psi\rangle$. From equation (A.24) we can see that, this is fulfilled iff

$$\frac{1}{2}\left(\widehat{H}\widehat{J}_m(\tau) + \widehat{J}_m(\tau)\widehat{H}\right)|\psi\rangle = H(\tau)\widehat{J}_m(\tau)|\psi\rangle\,. \tag{A.25}$$

In other words the extremes of the ratio $H(\tau)$ are eigenvalues of operator $\frac{1}{2}\left(\widehat{J}_m^{-1}(\tau)\widehat{H}\widehat{J}_m(\tau) + \widehat{H}\right)$.[14] For separable Hamiltonian $\widehat{H}$ from equation (1.2) we can write

$$\frac{1}{2}\left(\widehat{J}_m^{-1}(\tau)\widehat{H}\widehat{J}_m(\tau) + \widehat{H}\right) = \widehat{T} + \frac{1}{2}\left(\widehat{J}_m^{-1}(\tau)\widehat{V}\widehat{J}_m(\tau) + \widehat{V}\right)\,.$$

For $\tau = 0$ we get eigenvalues of Hamiltonian and the lower bound is ground state energy E_0

$$\widehat{J}_m(0) = \widehat{1} \qquad \Longrightarrow \qquad \widehat{H}|\psi\rangle = H(0)|\psi\rangle \qquad \Longrightarrow \qquad \min\{H(0)\} = E_0\,.$$

For $\tau > 0$ it is hard in general to solve the equation (A.25). For 1-dimensional LHO for $\tau > 0$ and $m = 0$ the ground state is

$$\langle x|\psi_0\rangle = \frac{1}{(2\pi\sigma^2)^{1/2}}\mathrm{e}^{-\frac{x^2}{2\sigma^2}}\,, \qquad \sigma^2 = \frac{1}{2}\left(\sqrt{4-\tau^2} - \tau\right)\,,$$

with energy

$$H(\tau) = \frac{1}{4}(4-\tau^2)^{1/2}\,.$$

For small $\tau \ll 1$ the lower bound changes in the second order

$$H(\tau) = \frac{1}{2} - \frac{\tau^2}{16} + O(\tau^4))\,.$$

However we can see that for $\tau \geq \sqrt{2}$ we don't have the ground state.

In general we can expect that for small τ the ratio $H(\tau)$ has lower bound, which is equal to ground state energy E_0 to the second order. Also we expect that for higher m, the operators $\widehat{J}_m(\tau)$ are better approximation of the unit operator $\widehat{1}$ and therefore the lower bound of the ratio $H(\tau)$ is equal to ground state energy E_0 to the higher order.

Method C

For the Method C, we look at the averaged energy $\{H\} = \{V\}$.

$$\{V\} = \frac{\displaystyle\int_{\mathbb{R}^N} \mathrm{d}\boldsymbol{x}\, V(\boldsymbol{x})\psi(\boldsymbol{x})}{\displaystyle\int_{\mathbb{R}^N} \mathrm{d}\boldsymbol{x}\, \psi(\boldsymbol{x})}$$

We variate the averaged energy $\delta\{V\}$ with perturbation $\langle\boldsymbol{x}|\delta\psi\rangle$.

$$\delta\{V\} = \frac{\displaystyle\int_{\mathbb{R}^N} \mathrm{d}\boldsymbol{x}\, \langle\boldsymbol{x}|\widehat{V}|\psi+\delta\psi\rangle}{\displaystyle\int_{\mathbb{R}^N} \mathrm{d}\boldsymbol{x}\, \langle\boldsymbol{x}|\psi+\delta\psi\rangle} - \frac{\displaystyle\int_{\mathbb{R}^N} \mathrm{d}\boldsymbol{x}\, \langle\boldsymbol{x}|\widehat{V}|\psi\rangle}{\displaystyle\int_{\mathbb{R}^N} \mathrm{d}\boldsymbol{x}\, \langle\boldsymbol{x}|\psi\rangle} = \frac{\displaystyle\int_{\mathbb{R}^N} \mathrm{d}\boldsymbol{x}\, \langle\boldsymbol{x}|\widehat{V} - \{V\}|\delta\psi\rangle}{\displaystyle\int_{\mathbb{R}^N} \mathrm{d}\boldsymbol{x}\, \langle\boldsymbol{x}|\psi+\delta\psi\rangle}$$

The necessary condition for variational extreme is $\delta\{V\} = 0$ for all $\langle\boldsymbol{x}|\delta\psi\rangle$. This happens iff the averaged energy is eigenvalue of the potential

$$\widehat{V}|\boldsymbol{x}\rangle = \{V\}|\boldsymbol{x}\rangle\,.$$

[14] One has to remember, that the operator $\widehat{J}_m^{-1}(\tau)$ for $\tau > 0$ is not well-defined and we are talking about formal solution. The original condition is equation (A.25).

The eigenvectors of the potential $\widehat{V}$ are improper eigenvectors $|\boldsymbol{x}\rangle$, therefore the infimum for $\{V\}$ is

$$\inf\{\{V\}\} = \min_{\boldsymbol{x}\in\mathbb{R}^N}\{V(\boldsymbol{x})\}\ .$$

One may argue that the vector $|x\rangle$ is improper therefore we will never reach the lower bound, but we can construct the sequence of proper vectors

$$\psi_\sigma(\boldsymbol{x}) = \frac{1}{(2\pi\sigma^2)^{N/2}}\mathrm{e}^{-\frac{||\boldsymbol{x}-\boldsymbol{x}_{\min}||^2}{2\sigma^2}}\ ,$$

where $\boldsymbol{x}_{\min}$ is position of the potential minimum. In the limit $\sigma \to 0^+$ the sequence will lead the averaged energy $\{V\}$ to value $\min_{\boldsymbol{x}\in\mathbb{R}^N}\{V(\boldsymbol{x})\}$.

Bibliography

[1] I. N. Levine, "Quantum chemistry 5th ed," 1991.

[2] S. A. Chin and E. Krotscheck, "Fourth-order algorithms for solving the imaginary time Gross-Pitaevskii equation in a rotating anisotropic trap," *Physical Review E*, 2005.

[3] L. Lehtovaara, J. Toivanen, and J. Eloranta, "Solution of time-independent Schrödinger equation by the imaginary time propagation method," *Journal of Computational Physics*, vol. 221, pp. 148–157, Jan. 2007.

[4] P. J. J. Luukko and E. Räsänen, "Imaginary time propagation code for large-scale two-dimensional eigenvalue problems in magnetic fields," *Computer Physics Communications*, 2013.

[5] P. Bader, S. Blanes, and F. Casas, "Solving the Schrödinger eigenvalue problem by the imaginary time propagation technique using splitting methods with complex coefficients," *The Journal of Chemical Physics*, vol. 139, no. 12, p. 124117, 2013.

[6] S. A. Chin, "Symplectic integrators from composite operator factorizations," *Physics Letters A*, vol. 226, no. 6, pp. 344–348, 1997.

[7] S. Blanes, F. Casas, and J. Ros, "Processing symplectic methods for near-integrable Hamiltonian systems," *Celestial Mechanics and Dynamical Astronomy*, vol. 77, pp. 17–36, Jul. 2000.

[8] J. Laskar and P. Robutel, "High order symplectic integrators for perturbed Hamiltonian systems," *Celestial Mechanics and Dynamical Astronomy*, vol. 80, no. 1, pp. 39–62, 2001.

[9] I. Omelyan, I. Mryglod, and R. Folk, "Construction of high-order force-gradient algorithms for integration of motion in classical and quantum systems," *Physical Review E*, vol. 66, no. 2, p. 026701, Aug. 2002.

[10] J. E. Chambers, "Symplectic integrators with complex time steps," *The Astronomical Journal*, vol. 126, pp. 1119–1126, Aug. 2003.

[11] X.-P. Li and J. Q. Broughton, "High-order correction to the Trotter expansion for use in computer simulation," *The Journal of Chemical Physics*, vol. 86, pp. 5094–5100, May 1987.

[12] S. A. Chin, "Quantum statistical calculations and symplectic corrector algorithms," *Physical Review E*, vol. 69, no. 4, p. 046118, Apr. 2004.

[13] P. Behroozi, "Analytical imaginary time propagation at a single point," 2008. [Online]. Available: http://large.stanford.edu/courses/2008/ph372/behroozi2/

[14] R. E. Zillich, J. M. Mayrhofer, and S. A. Chin, "Extrapolated high-order propagators for path integral Monte Carlo simulations," *The Journal of Chemical Physics*, vol. 132, no. 4, pp. 044 103–044 103, Jan. 2010.

[15] W. R. Inc., "Mathematica, Version 11.0.1.0," champaign, IL, 2017.

[16] J. Squire, J. Burby, and H. Qin, "VEST: Abstract vector calculus simplification in Mathematica," *Computer Physics Communications*, vol. 185, pp. 128–135, Jan. 2014.

[17] J. W. Helton, M. de Oliveira, M. Stankus, and R. L. Miller. NCAlgebra – Version 4.0.6. [Online]. Available: http://math.ucsd.edu/~ncalg

[18] Q. Sheng, "Solving linear partial differential equations by exponential splitting," *IMA Journal of Numerical Analysis*, vol. 9, no. 2, pp. 199–212, 1989.

[19] M. Suzuki, "General theory of fractal path integrals with applications to many-body theories and statistical physics," *Journal of Mathematical Physics*, vol. 32, no. 2, pp. 400–407, 1991.

[20] D. Goldman and T. J. Kaper, "N th-order operator splitting schemes and nonreversible systems," *SIAM Journal on Numerical Analysis*, vol. 33, no. 1, pp. 349–367, 1996.

[21] E. Hansen and A. Ostermann, "High order splitting methods for analytic semigroups exist," *BIT Numerical Mathematics*, vol. 49, no. 3, p. 527, Sep. 2009. [Online]. Available: http://dx.doi.org/10.1007/s10543-009-0236-x

[22] H. Yoshida, "Construction of higher order symplectic integrators," *Physics Letters A*, vol. 150, pp. 262–268, Nov. 1990.

[23] N. Hatano and M. Suzuki, "Finding exponential product formulas of higher orders," *Quantum annealing and other optimization methods*, pp. 37–68, Jan. 2005. [Online]. Available: http://dx.doi.org/10.1007/11526216_2

[24] F. Castella, P. Chartier, S. Descombes, and G. Vilmart, "Splitting methods with complex times for parabolic equations," *BIT Numerical Mathematics*, vol. 49, no. 3, p. 487, Sep. 2009. [Online]. Available: http://dx.doi.org/10.1007/s10543-009-0235-y

[25] S. Blanes, F. Casas, P. Chartier, and A. Murua, "Optimized high-order splitting methods for some classes of parabolic equations," *Mathematics of Computation*, 2013.

[26] S. A. Chin and J. Geiser, "Multi-product operator splitting as a general method of solving autonomous and nonautonomous equations," *IMA Journal of Numerical Analysis*, vol. 31, no. 4, pp. 1552–1577, 2011.

[27] S. A. Chin, "Structure of positive decompositions of exponential operators," *Physical Review E*, vol. 71, no. 1, p. 016703, 2005.

[28] M. Aichinger and E. Krotscheck, "A fast configuration space method for solving local Kohn–Sham equations," *Computational Materials Science*, vol. 34, no. 2, pp. 188–212, 2005.

[29] R. Brent, "A new algorithm for minimizing a function of several variables without calculating derivatives," *Algorithms for minimization without derivatives*, pp. 200–248, 1976.

[30] D. Brandon, N. Saad, and S.-H. Dong, "On some polynomial potentials in d-dimensions," *Journal of Mathematical Physics*, vol. 54, no. 8, pp. 082 106–082 106, Aug. 2013.

[31] M. H. Kalos and P. A. Whitlock, *Monte Carlo methods*. John Wiley & Sons, 2008.